Proceedings of the
Annual Stability Conference
Structural Stability Research Council
Toronto, Canada, March 25-28, 2014

On the Relevance of Local-Distortional Interaction Effects in the Behavior and Design of Cold-Formed Steel Columns

A.D. Martins[1], P.B. Dinis[1], D. Camotim[1], P. Providência[2]

Abstract

The paper reports the results of a numerical (ABAQUS shell finite element analysis) investigation on the relevance of web-triggered local-distortional interaction on the ultimate strength of a large number of cold-formed steel fixed-ended (plain) lipped channel, zed, hat and rack columns. These results concern columns with various geometries (cross-section dimensions and unrestrained length) and yield stresses, ensuring a wide variety of combined ratios between the (i) distortional and local critical buckling stresses (R_{DL}), and (ii) yield and non-critical buckling stresses (R_y) – to avoid interaction with global buckling, all the columns have global critical buckling stresses much higher than their local, distortional and yield counterparts. The aim of the study is to identify combinations of these ratios for which L-D interaction is relevant, in the sense of affecting visibly the column elastic and elastic-plastic post-buckling behaviors, ultimate load and failure mode mechanisms – special attention is devoted to the ultimate strength erosion. The numerical ultimate strength data obtained above are then compared with the predictions of (i) the currently codified DSM (Direct Strength Method) strength curves for the design of columns failing in local and distortional modes, and (ii) available DSM-based design approaches specifically developed for local-distortional interactive failures – particular attention is devoted to those proposed by Silvestre *et al.* (2012). Then, experimental results available in the literature concerning failures in local-distortional interactive modes, namely those reported by Kwon & Hancock (1992), Kwon *et al.* (2009), Loughlan *et al.* (2012), Young *et al.* (2013) and Dinis *et al.* (2013a), dealing with lipped channel (mostly) and rack-section columns, are used to assess the quality of the estimates provided by the DSM-based design approaches. Finally, the paper closes with some considerations about the impact of the findings reported in this work on the design of cold-formed steel columns undergoing different levels of L-D interaction.

1. Introduction

Most cold-formed steel members exhibit slender thin-walled open cross-sections, a feature making them highly susceptible to several instability phenomena involving cross-section deformation, namely local and distortional buckling – Figs. 1(b)-(d) show buckled lipped channels cross-sections corresponding to column local, distortional and global (flexural-torsional and flexural) shapes. Moreover, since several commonly used cold-formed steel member geometries (cross-section shape/dimensions and unrestrained length) may exhibit fairly similar local (L) and distortional (D) critical buckling stresses, the corresponding post-buckling behavior (elastic or elastic-plastic), ultimate strength and failure mode

[1] Department of Civil Engineering Architecture and Georesources, ICIST, Instituto Superior Técnico, University of Lisbon, Portugal. <andrerdmartins@ist.utl.pt>, <dinis@civil.ist.utl.pt> and < dcamotim@civil.ist.utl.pt >
[2] Department of Civil Engineering, INESC, University of Coimbra, Portugal. <provid@dec.uc.pt>

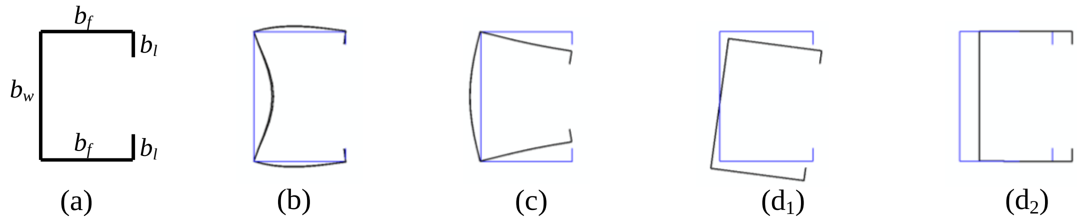

Figure 1: Lipped channel (a) geometry and buckled shapes associated with column (b) local (c) distortional and (d) global – (d_1) flexural-torsional (d_2) flexural – buckling

are likely to be affected, to a smaller or larger extent, by interaction effects involving these two instability phenomena – local-distortional (L-D) interaction.

A considerable amount of research activity has been recently devoted to local-distortional (L-D) interaction, involving mostly lipped channel columns and including experimental investigations, numerical simulations and design proposals – for instance, the works reported by Kwon & Hancock (1992), Yang & Hancock (2004), Dinis *et al*. (2007, 2009), Yap & Hancock (2009, 2011), Kwon *et al*. (2009), Silvestre *et al*. (2012), Young *et al*. (2013), Loughlan *et al.* (2012), Camotim *et al.* (2013) and Martins *et al.* (2013) . Although in a lesser amount, some research concerning columns with other cross-sections shapes is also available: (i) Dinis *et al*. (2011) (hat-sections), (ii) Silvestre *et al.* (2008) and Dinis *et al*. (2013a) (rack-sections), (iii) Dinis *et al*. (2012b) (zed, hat and rack-sections), and (iv) Dinis & Camotim (2012, 2013) (lipped channels and zed, hat and rack-sections). It was found that L-D interaction effects are relevant when the ratio between the critical local and distortional buckling stresses, denoted here $R_{DL}=f_{crd}/f_{crl}$, is either (i) in the close vicinity of 1.0 (comprised between 0.9 and 1.1) or (ii) significantly above 1.0, provided that the yield stress f_y is "high enough" to allow the development of L-D interaction prior to collapse – this means that the yield-to-critical stress ratio also plays a crucial role in assessing the relevance of L-D interaction effects. However, a systematic investigation aimed at identifying which combinations of the ratios involving the (i) local critical stress, (ii) distortional critical stress and (iii) yield stress leading to non-negligible L-D coupling effects is still lacking – the only available results addressing (partially) this issue have been reported by Dinis *et al*. (2009) and Martins *et al.* (2013), both exclusively for (plain) lipped channels columns.

Since the structural response and strength of cold-formed steel members is complex and not yet adequately reflected in several current design codes, a fair amount of research has been devoted to develop efficient (safe and economic) design rules for such members. The most relevant fruit of this research activity was the Direct Strength Method (DSM), which (i) has its roots in the work of Hancock *et al.* (1994), (ii) was originally proposed by Schafer & Peköz (1998), and (iii) has already been included in the latest versions of the Australian/New Zealand (AS/NZS 2005) and North American (AISI 2012) cold-formed steel specifications as an alternative to the traditional Effective Width Method (EWM) to estimate the load-carrying capacity of members subjected to uniform compression (columns) or bending (beams) – a detailed account of the most relevant DSM developments can be found in Schafer (2008). The DSM has been shown to provide an efficient and general approach to estimate the ultimate strength of cold-formed steel columns and beams failing in local (L), distortional (D), global (G) and local-global (L-G) interactive modes. Unfortunately, the consideration of these limit states is not sufficient for the design of such members, since interaction phenomena involving distortional buckling, namely, L-D, D-G and L-D-G may also erode significantly the member load-carrying capacity, thus leading to unacceptably low reliability indices, *i.e.*, to a high likelihood of reaching unsafe designs.

This paper deals solely with the design of columns against L-D interactive failures. Although several attempts have been made to extend the DSM approach, so that it covers also column L-D interactive failures, it is consensual that further research is still needed before the DSM can be successfully and generally applied to members affected by this type of mode interaction. Therefore, one of the main purposes of this work is also to contribute towards achieving this goal, by investigating the relevance of the L-D interaction effects, thus paving the way for the codification of a DSM-based design approach for columns affected by web-triggered L-D interaction. In the particular case of lipped channels columns (either pin-ended or fixed-ended) experiencing L-D interaction, the second and third authors performed extensive numerical simulations that (i) made it possible to obtain clear evidence that the current DSM local and distortional design curves cannot capture the ultimate strength erosion due to this coupling behavior and (ii) unveiled features that must appear in a DSM design approach intended for such members. These findings were incorporated into DSM-based design approaches recently proposed by Silvestre *et al*. (2012), for lipped channel channels only, later extended to zed, hat and rack-section columns by Dinis & Camotim (2012, 2013) – it is worth noting that these proposals concern exclusively columns affected by strong interaction stemming from the closeness between the local and distortional critical buckling stresses. Moreover, experimental results also confirmed the occurrence of considerable ultimate strength erosion due to L-D interaction in (i) fixed-ended lipped channel columns (plain or with intermediate stiffeners, *i.e.*, flange-triggered or web-triggered L-D interaction), as reported by various authors (Kwon & Hancock 1992, Yang & Hancock 2004, Yap 2008, Kwon *et al*. 2009, Yap & Hancock 2009, 2011, Loughlan *et al.* 2012, Young *et al*. 2013 and Dinis *et al.* 2013b) or (ii) fixed-ended rack-section columns, as reported by Dinis *et al.* (2013a).

This paper presents and discusses the results of a extensive numerical (ABAQUS shell finite element) investigation involving the determination the ultimate strength of (i) 484 lipped channel (C) (ii) 440 hat-section (H) (iii) 440 zed-section (Z) and (iv) 440 rack-section (R) fixed-ended columns exhibiting different cross-section dimensions and yield stresses, thus ensuring a wide variety of combinations of the stress ratios (i) $R_{DL}=f_{crd}/f_{crl}$, relating the distortional and local critical buckling stresses, and (ii) $R_y=f_y/f_{cr.max}$, quantifying the difference between the yield stress and the higher (non-critical) of the above two buckling stresses, *i.e.*, $f_{cr.max}=max(f_{crl}; f_{crd})$ – this is because, when f_{crd} and f_{crl} are not very close, the development of L-D interaction effects is also influenced by the closeness between f_y and $f_{cr.max}$. All the selected columns have cross-section dimensions that ensured that local buckling is triggered by the web, since (i) the mechanics of web-triggered and flange-triggered L-D interaction are quite different and (ii) the latter may cause an additional ultimate strength erosion that was clearly observed in the experimental tests reported by Dinis *et al.* (2013b)[3] – moreover, all the tests results considered in this work concern columns failing in web-triggered L-D interactive modes. The aim of this investigation is to extend a very recent study by the authors (Martins *et al.* 2013), carried out in the context of fixed-ended cold-formed plain lipped channel columns, to other plain (no wall intermediate stiffeners) cross-section shapes, namely hat, zed and rack-sections. In particular, it is sought to identify the R_{DL}-R_y range combinations for which the L-D interaction effects are relevant, in the sense of eroding visibly the column ultimate load and/or altering its failure mechanism nature. The numerical ultimate strength data obtained are also compared with their predictions provided by the available DSM strength curves/expressions developed for the design of columns failing in local, distortional and L-D interactive modes – special attention is devoted to the DSM approaches recently proposed by Silvestre *et al*. (2012) and Dinis & Camotim (2013), which account explicitly for L-D interaction. The ultimate strength erosion due to L-D interaction is also assessed by comparing the numerical failure loads with their estimates provided by the codified DSM local and distortional strength/design curves – generally speaking, both curves

[3] This type of L-D interaction is currently being studied by the authors – the results obtained will be reported in the near future.

overestimate the numerical and experimental ultimate loads, thus providing additional clear evidence of the occurrence of ultimate strength erosion due to L-D interaction.

Finally, the paper closes with some considerations concerning the impact of the findings reported in this work on the DSM design (ultimate strength prediction) of the cold-formed steel columns exhibiting different (i) (plain) cross-section shapes and (ii) levels of L-D interaction. In particular, the possibility of developing a general DSM-based approach capable of efficiently (safely and accurately) predicting the load-carrying capacity of all these different columns is addressed.

2. Buckling Analysis – Columns Geometry Selection

In order to perform an investigation involving the evaluation of the numerical ultimate strength of fixed-ended columns affected by various levels of L-D interaction, it is indispensable to begin by selecting columns with different "levels of closeness" between their local and distortional critical buckling stresses (R_{DL} values). These critical stresses can be obtained by means of various methods, such as shell finite element analyses (SFEA), finite strip analyses (FSA) or analyses based on Generalized Beam Theory (GBT). Since the column selection was made by a "trial-and-error" approach, it was decided to perform the buckling analysis using the GBT-based code GBTUL (Bebiano *et al*. 2008), mainly due to its computational efficiency and the structural clarity of the results obtained. Since the C, H and Z columns share the same local and distortional buckling behaviors (for identical cross-section dimensions, of course – note that local and distortional buckling are essentially governed by the web width and flange-lip assembly dimensions, respectively), the selection procedure adopted earlier (Martins *et al*. 2013) for the C columns was readily extended to their H and Z counterparts[4]. However, it should be noted that (i) the first 6 columns were modified, in order to have local buckling always triggered by the web, and (ii) 3 column geometries were added, in order to increase the number of columns with R_{DL} values (L-D interaction levels) comprised between 1.0 and 1.5. The end product of the columns geometry selection are the 27 distinct combinations of cross-section dimensions b_w, b_f, b_l, t (web/flange/lip widths and wall thickness – see Fig. 1(a) for the C columns) and lengths (L), which are provided in Table 1. The half-wave numbers exhibited by the critical local (n_l) and distortional (n_d) buckling modes are also given (the former only if $f_{crl}<f_{crd}$). These fixed-ended cold-formed steel (E=210GPa, v=0.3) columns (i) exhibit R_{DL} values in the range $0.42<R_{DL}<2.39$ and (ii) have global critical buckling stresses (ii$_1$) much higher than their local and distortional counterparts ($f_{crg}/f_{cr.max}>7.5$) and (ii$_2$) higher than all the column yield stresses considered (discussed later) ($f_{crg}/f_{y.max}>1.0$)[5], thus ensuring that interaction with flexural-torsional (C and H columns) or minor-axis flexural (Z columns) buckling does not occur. The values of the two stress ratios are also given in Table 1, but only for the H columns – f_{crg} value always lower than those of the corresponding C and Z columns, as is clearly shown in Fig. 2(a), which concerns column C11.

Fig. 2(b) shows illustrative mixed buckling modes, combining 2 D half-wave and 8 L half-waves, of columns whose post-buckling behavior and ultimate strength are strongly affected by L-D interaction.

[4] These C columns buckling results were already reported in Martins *et al*. (2013).

[5] In Table 1, two values concerning columns C11 e C12 are below 1.0. This is due to the fact that these column geometries were adopted in the C column investigation carried out by Martins *et al*. (2013) and C columns exhibit higher critical global buckling stress than their H counterparts (see Fig.2 (a)). Note also that the above two values are associated with maximum (critical) slenderness values equal to 3.50 in a region affected by "true" L-D interaction (close f_{crl} and f_{crd}). Since the high slenderness range is relevant only for the columns experiencing "secondary bifurcations", for which L-D interaction can develop even if f_{crl} and f_{crd} are not so close (provided that the yield stress is "sufficiently higher" – high slenderness), these two values of $f_{crg}/f_{y.max}$ below 1.0 have very little relevance. Indeed, a close inspection of the deformed configurations of these two columns showed no trace of L-D-G interaction.

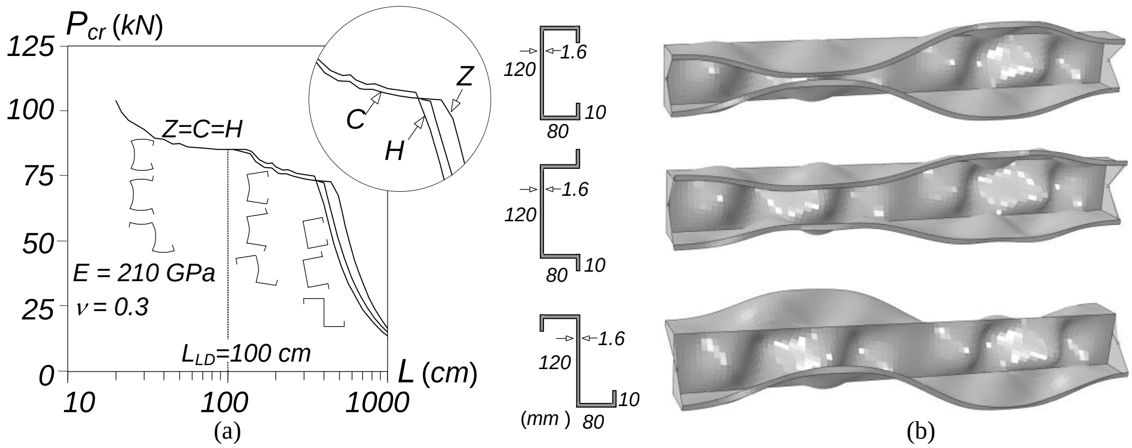

(a) (b)

Figure 2: (a) Critical buckling curves and (b) L_{LD} column mixed buckling modes concerning the C, H and Z

Table 1: Selected column geometries, critical local/distortional/global buckling stresses, buckling mode half-wave numbers and relevant stress ratios for the C, H and Z columns

	b_w (mm)	b_f (mm)	b_l (mm)	t (mm)	L (m)	f_{crd} (MPa)	n_d	f_{crl} (MPa)	n_l	R_{DL}	f_{crg} (MPa)	$\frac{f_{crg}}{f_{cr.\max}}$	$\frac{f_{crg}}{f_{y.\max}}$
C1	170	170	10	2.50	1.90	74	2	178	-	0.42	1343	7.5	1.49
C2	155	135	10	2.50	1.43	116	2	245	-	0.48	1911	7.8	1.34
C3	150	135	10	2.50	1.43	118	2	227	-	0.52	1799	9.6	1.25
C4	155	140	11	2.50	1.50	119	2	208	-	0.57	1738	8.3	1.19
C5	145	120	10	2.10	1.40	118	2	189	-	0.62	1714	9.0	1.19
C6	120	95	8	1.60	1.20	110	2	166	-	0.67	1583	9.5	1.16
C7	120	110	10	2.15	0.90	184	2	263	-	0.70	2856	10.9	1.27
C8	120	110	10	1.80	0.90	149	1	192	-	0.78	2852	14.8	1.55
C9	120	110	10	1.60	0.90	131	1	153	-	0.86	2850	18.6	1.77
C10	120	110	10	1.40	0.90	113	1	118	-	0.96	2849	24.1	2.04
C11	120	80	10	1.65	1.00	194	2	189	9	1.02	2093	10.5	0.90
C12	120	80	10	1.60	1.00	189	2	178	9	1.07	2092	10.8	0.96
C13	120	110	10	1.15	0.90	91	1	80	7	1.13	2307	25.4	2.36
C14	120	80	10	1.40	1.00	166	2	136	9	1.22	2090	12.4	1.25
C15	120	80	10	1.35	1.00	165	2	127	10	1.29	2090	12.4	1.34
C16	120	80	10	1.30	1.00	159	2	118	9	1.35	2089	12.8	1.44
C17	120	80	10	1.25	1.00	153	2	119	9	1.41	2089	13.3	1.56
C18	120	80	10	1.20	1.00	145	2	100	9	1.45	2088	13.8	1.69
C19	120	80	10	1.15	1.00	141	2	92	10	1.52	2088	14.3	1.84
C20	120	80	10	1.10	1.00	135	2	84	10	1.60	2087	15.0	2.01
C21	120	100	10	0.85	1.00	77	1	47	9	1.66	2255	28.7	3.92
C22	120	100	10	0.80	1.00	73	1	41	9	1.76	2254	31.0	4.42
C23	120	100	10	0.75	1.00	68	1	36	9	1.86	2254	32.5	5.03
C24	120	100	10	0.70	1.00	63	1	32	9	2.00	2254	35.1	5.77
C25	120	100	10	0.65	1.00	59	1	27	9	2.15	2254	38.0	6.69
C26	120	100	10	0.62	1.00	55	1	25	9	2.22	2254	40.4	7.35
C27	120	100	10	0.55	1.00	47	1	20	9	2.39	2254	47.7	9.33

The C, H and Z column P_{cr} vs. L behaviors only differ in the length associated with the transition between D to G critical buckling (intermediate-to-long columns). As reported by Dinis & Camotim (2013) and taking the C columns as reference, the G buckling loads (i_1) considerably increase for the Z columns, due to change from flexural-torsional to flexural buckling, and (i_2) slightly decrease for the H columns, due to the lower (about *10%*) warping constant, which outweighs the marginally higher major-axis inertia.

An objective of this paper is also to extend the findings obtained by Martins *et al.* (2013) to rack-section (R) columns, thus enabling the consideration of the four more commonly used plain cold-formed steel profiles (also those for which the column design can be carried out by means of the DSM – see, for instance, AISI 2012). It is necessary again to select columns with different levels of L-D interaction and, for comparison purposes, with R_{DL} values as close to those given in Table 1, for the C, H and Z columns, as possible. The selection procedure, which was performed once more with the code GBTUL, led to 27 distinct combinations of column (i) cross-section dimensions b_w, b_f, b_l, b_s, t (web/flange/lip/stiffener widths and wall thickness) and (ii) lengths (L), which are provided in Table 2 – they exhibit R_{DL} values in the range $0.42<R_{DL}<2.38$, virtually the same as for the C, H and Z columns. The half-wave numbers of the local and distortional critical buckling modes are also given, as well as the ratios between the global critical buckling stresses (flexural-torsional) and the (i) higher (non-critical) of the local and distortional buckling stresses ($f_{crg}/f_{cr.max}>5.24$), and (ii) maximum yield stress value ($f_{crg}/f_{y.max}>1.04$).

Table 2: Selected column geometries, critical local/distortional/global buckling stresses, buckling mode half-wave numbers and relevant stress ratios for the R columns

	b_w (mm)	b_f (mm)	b_s (mm)	b_l (mm)	t (mm)	L (m)	f_{crd} (MPa)	n_d	f_{crl} (MPa)	n_l	R_{DL}	f_{crg} (MPa)	$\frac{f_{crg}}{f_{cr.\max}}$	$\frac{f_{crg}}{f_{y.\max}}$
C1	140	135	6,5	10.0	2,45	1.60	113	2	272	-	0.42	1425	5.24	1.04
C2	140	130	7.5	10.0	2.50	1.40	141	2	291	-	0.49	1879	6.46	1.10
C3	140	130	7.5	10.0	2.33	1.40	131	2	252	-	0.52	1877	7.44	1.19
C4	220	210	10.0	10.0	2.50	3.30	62	3	108	-	0.57	811	7.54	1.08
C5	200	180	10.0	10.0	2.50	2.50	86	2	139	-	0.62	1172	8.46	1.12
C6	190	160	10.0	10.0	2.54	2.00	112	2	166	-	0.67	1650	9.94	1.22
C7	190	160	10.0	10.0	2.42	2.00	106	2	151	-	0.70	1649	10.93	1.28
C8	190	160	10.0	10.0	2.20	2.00	97	2	125	-	0.77	1648	13.15	1.40
C9	190	160	10.0	10.0	2.00	2.00	89	2	104	-	0.86	1648	15.88	1.53
C10	190	160	12.5	12.5	2.43	1.85	149	2	155	-	0.96	1995	12.91	1.12
C11	190	160	12.5	12.5	2.30	1.85	143	2	139	11	1.03	1995	13.93	1.18
C12	190	160	12.5	12.5	2.23	1.85	138	2	129	11	1.07	1995	14.46	1.25
C13	190	175	15.0	15.0	2.50	1.50	177	1	158	8	1.12	3173	17.91	1.65
C14	190	175	15.0	15.0	2.30	1.50	160	1	134	8	1.20	3172	19.83	1.94
C15	190	175	15.0	15.0	2.20	1.50	157	1	123	8	1.28	3171	20.17	2.12
C16	130	100	15.0	15.0	2.20	1.00	386	1	285	9	1.35	3693	9.56	1.06
C17	130	100	15.0	15.0	2.14	1.00	381	1	269	9	1.41	3693	9.70	1.12
C18	130	100	15.0	15.0	2.00	1.10	341	1	235	10	1.45	3052	8.96	1.06
C19	130	100	15.0	15.0	2.04	1.00	373	1	245	9	1.52	3692	9.91	1.23
C20	130	100	15.0	15.0	1.95	1.00	360	1	224	9	1.61	3691	10.25	1.35
C21	130	100	15.0	15.0	1.90	1.00	354	1	213	9	1.66	3691	10.42	1.42
C22	130	100	15.0	15.0	1.82	1.00	344	1	195	9	1.76	3690	10.73	1.54
C23	130	100	15.0	15.0	1.75	1.00	335	1	180	9	1.86	3689	11.02	1.67
C24	130	100	15.0	15.0	1.65	1.00	321	1	161	9	2.00	3689	11.49	1.87
C25	130	100	15.0	15.0	1.56	1.00	308	1	143	9	2.15	3688	11.99	2.10
C26	130	100	15.0	15.0	1.51	1.00	299	1	134	9	2.22	3688	12.35	2.23
C27	130	100	15.0	15.0	1.43	1.00	286	1	120	9	2.38	3687	12.87	2.49

3. Parametric Study: Scope and Numerical Results

This section presents the column ultimate load data concerning the four sets (C, H, Z, R) of 27 fixed-ended cold-formed steel columns characterized in the last section. As will be seen further ahead in the paper, L-D interaction may be relevant even when R_{DL} differs significantly from 1.0, provided that the yield stress is "sufficiently high". In order to confirm this assertion, yield stress values leading to a wide critical (local or distortional) slenderness [$\lambda_{cr}=(f_y/f_{cr})^{0.5}$] range are considered in this study – more specifically, ten λ_{cr} values, varying from 1.00 to 3.50 in approximately 0.25 intervals, correspond to yield stresses ranging roughly from (i) 240MPa to 2300MPa (C, H, Z columns) or (ii) 750 MPa to 3500MPa (R columns). Note that columns with f_y/f_{cr}<1.0 are not considered in this work, since their collapse is mainly governed by plasticity effects (only when R_{DL} is close to 1.0 does L-D interaction play a minor role). Moreover, the columns under investigation in this work are also highly sensitive to the shape of the initial geometrical imperfections, which has a strong influence on the normal stress pattern.

In the remainder of this section, (i) several relevant issues concerning the finite element modeling of the geometrically and materially non-linear behavior of thin-walled steel members are briefly described, (ii) the influence of the initial geometrical imperfection shape on the column ultimate strength is addressed – this shape is known to play a crucial role in mode interaction investigations (*e.g.*, Dinis *et al.* 2007), and (iii) the obtained failure load data is presented – these values will be subsequently used to assess the relevance of the L-D interaction effects in C, H, Z, R columns.

3.1 Finite Element Modeling

The column (i) elastic buckling and (ii) elastic-plastic post-buckling behaviors were determined by means of shell finite element analyses (SFEA), carried out in the code ABAQUS (Simulia Inc 2008), employing models already adopted in previous studies by Dinis *et al.* (2006, 2007, 2009) – a detailed account of the modeling issues can be found in these references. The main characteristics of these models are as follows:

(I) *Discretisation*. The column mid-surface was discretized into fine meshes of S4 elements (ABAQUS nomenclature – 4-node isoparametric shell elements with the shear stiffness obtained by a full integration rule). Since previous studies showed that using of elements with length-to-width ratios roughly equal to 1.0 provides accurate results, such elements were also adopted in this work. The rounded corners were neglected, since previous studies have shown that they have little impact on the column behavior (however, this assertion may not be true for other phenomena, like web crippling).

(II) *Support Conditions*. All the columns analyzed in this work have fixed end sections with warping and torsional rotations prevented. In order to avoid numerical difficulties related to the load application, both end sections are free to move axially (the rigid-body longitudinal translation is precluded by preventing one mid-span cross-section axial displacement). These fixed-ended support conditions were modeled by means of rigid end-plates attached to the end cross-section centroids.

(III) *Loading*. Compressive axial forces were applied at the column rigid end-plate points corresponding to the end cross-section centroids.

(IV) *Material Modelling*. The carbon steel material behavior, deemed isotropic and homogeneous, was modelled as (i) linear elastic (buckling analysis) or (ii) elastic perfectly-plastic (post-buckling analysis). In the latter case, the well-known Prandtl-Reuss model was adopted – it is based on J_2-flow plasticity theory and combines von Mises's yield criterion with its associated flow rule.

3.2 Initial Geometrical Imperfections

It is well known that the initial geometrical imperfection shape plays a key role in the non-linear analysis of thin-walled cold-formed steel columns (or any other structural system, for that matter), as its choice may alter considerably the corresponding post-buckling behavior and ultimate strength (*e.g.*, Dinis *et al.* 2007). Although various approaches can be adopted to characterize/define the initial geometrical imperfections in cold-formed steel members (*e.g.*, Schafer & Peköz 1998a or Zeinoddini & Schafer 2012), this work considers only "pure" distortional or local buckling mode shapes, which may be critical (in most cases) or non-critical, and small amplitudes (10% of the column wall thickness). This means that it was necessary to perform preliminary ABAQUS SFE buckling analyses to obtain the column initial geometrical imperfection shape to be incorporated in the ABAQUS SFE post-buckling analyses – obviously, the same SFE meshes were adopted in both analyses.

Previous studies showed that "pure" distortional initial imperfections are always the most detrimental when compared with "pure" local ones sharing the same overall amplitude – this can be easily explained by the lower D post-critical stiffness and strength, when compared with their L counterparts (*e.g.*, Camotim *et al*. 2005). However, this conclusion was based in the analysis of columns with R_{DL} values close to 1.0 (*i.e.*, $0.90<R_{DL}<1.10$) and may not remain true for columns with higher R_{DL} values, *i.e.*, $R_{DL}>1.10$. Therefore, it was decided to analyze all the columns with "pure" distortional initial geometrical imperfections, regardless of their R_{DL} values (*i.e.*, whether the column critical buckling mode is local or distortional). In addition, when $R_{DL}>1.0$, the columns were also analyzed with "pure" local initial geometrical imperfections. Unlike its local counterpart, the column distortional post-buckling behavior is asymmetric with respect to the imperfection "sign", which implies that it is necessary to identify the most detrimental "sign", *i.e.*, that leading to the lowest ultimate strengths. This identification has already been conducted by (i) Dinis *et al*. 2007, for C columns, and by (ii) Dinis & Camotim (2013), for H, Z, R fixed-ended columns, leading to the initial geometrical imperfection shapes depicted in Figs. 3(a)-(c) – since the same conclusions were drawn for the H and R columns, only the latter is presented. It is clearly demonstrated that, when there is only one distortional half-wave, (i) the most detrimental imperfection shape involves outward (C columns – Fig. 3(a_1)) or inward (H, R columns – Fig. 3(a_2)) mid-span flange-lip motions – in Z columns, the initial geometrical imperfection "sign" is obviously irrelevant due to the cross-section point-symmetry (see Fig. 3(a_3)). This is also when the columns exhibit an even distortional half-wave number, as there exist the same number of outward and inward half-waves – Figs. 3 (b_1)-(b_3) show C, R, Z columns with two half-waves. Concerning the local initial geometrical imperfection, their "sign" is again irrelevant, due to the local post-buckling symmetry – Figs. 3(c_1)-(c_3) show C, R, Z columns with multiple half-waves numbers. The distortional and local initial geometrical imperfections shared the same overall amplitude and were characterized by (i) maximum lip free edge vertical displacements v (also in the R columns, even if it is not the maximum displacement) equal to 10% of the wall thickness t at the cross-section with the highest outward or inward flange-lip motion, and (ii) maximum mid-web flexural displacement w, also equal to 10% of wall thickness t, respectively.

The inclusion of distortional (non-critical) initial imperfections in columns with R_{DL} values significantly higher than 1.0 is done through an auxiliary buckling analysis of an otherwise identical column with a

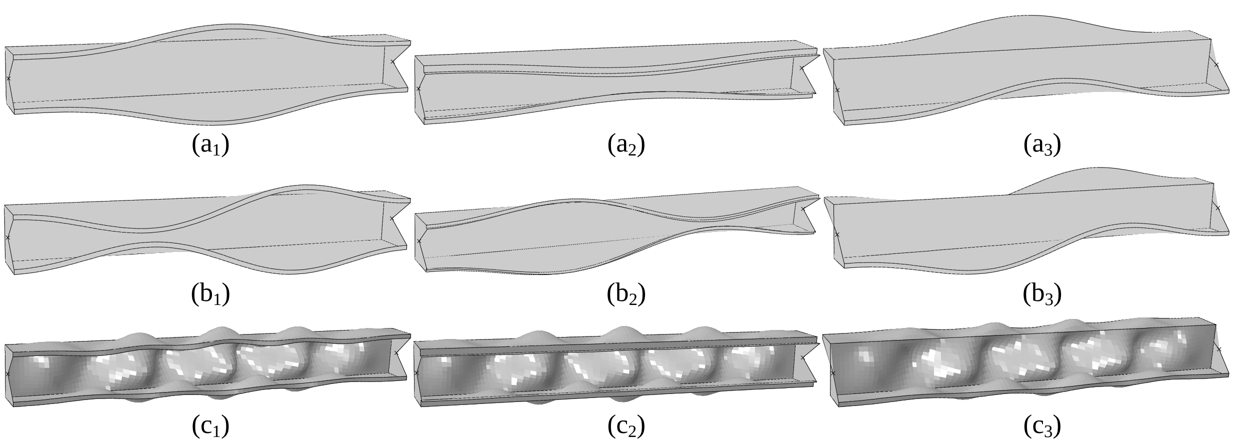

Figure 3: Initial geometrical imperfection shapes of C, Z and R columns exhibiting (a) one distortional half-wave (b) two distortional half-waves (c) multiple local half-waves

higher thickness value, selected to have a distortional critical buckling mode. The ensuing mid-surface deformed shape is then normalized and included in the column elastic-plastic second-order SFEA. Finally, it is still worth noting that, in this work, both the residual stress and corner strength effects (due to the cold-working of the brake-pressed corners) are neglected, since they have been shown to have little impact on the ultimate strength of cold-formed steel columns (Ellobody & Young 2005).

3.3 Column Ultimate Strength

The results concerning the ultimate strengths (f_u) obtained in this work, through ABAQUS second-order elastic-plastic SFEA, are given in the tables included in Annexes A (C columns), B (H and Z columns) and C (R columns). In Annex A, only the modifications mentioned in section 2 for the C columns are presented – the remaining results can be found in Martins *et al.* (2013). The above tables include ultimate strengths ($f_{u.D}$ and $f_{u.L}$, for columns with distortional or local critical initial geometrical imperfections – the latter only if R_{DL}>1.0), and their estimates provided by (i) the codified DSM design curves (f_{nl} or f_{nd}) and (ii) the two DSM-based approaches developed to account for the L-D interaction (f_{ndl} and f_{mndl}) – a few other relevant quantities are also given.

4. Relevance of Local-Distortional Interaction

The main results of the numerical investigation aimed at identifying the relevance of L-D interaction effects are presented and discussed next, thus extending the findings of Martins *et al*. (2013), obtained for C columns, to columns with other cross-section shapes, namely H, Z, R columns (and also the C columns not analyzed previously). The numerical ultimate strength data determined earlier are now used to identify R_{DL} and R_y ranges associated with the occurrence of relevant L-D interaction effects. Initially, the identification of the R_{DL} range associated with "true L-D interaction" is addressed – within this range, which corresponds to fairly close distortional and local critical buckling loads, the coupling effects may be said to be "intrinsic of the column" and, therefore, (i) gradually evolve as loading progresses and (ii) take place regardless of the yield stress value (provided, of course, that f_y/f_{cr} is not significantly below 1.0, in which case collapse is basically governed by plasticity). Then, attention is turned to the identification of the minimum R_y values allowing for the development of L-D interaction effects due to a "secondary (local or distortional) bifurcation", for all cross-sections shapes – these effects only emerge and grow as the applied stress nears the $f_{cr.max}$ level, provided that it falls considerably below the yield stress, particularly when the critical buckling stress is local, thus ensuring a high post-critical strength reserve.

4.1 True Local-Distortional Interaction – R_{DL} and R_y Upper and Lower Limits

Fig. 4(a) shows the upper portions (P/P_{cr} >0.5) of the P/P_{cr} vs v/t equilibrium paths (v is the mid-span flange-lip corner vertical displacement) of C13 (R_{DL}=1.13 – local critical buckling) lipped channel columns (i) containing D or L initial geometrical imperfections and (ii) exhibiting six R_y values (1.4, 2.0, 3.5, 5.5, 8.0 and ∞ – the latter corresponds to elastic behavior). Figs. 4(b$_1$)-(b$_4$) display the deformed configurations and plastic strain distributions near collapse of the columns with R_y=2.0 or R_y=5.5 and L or D initial imperfections – these deformed configurations are amplified either 2.5 (Fig. 4(b$_3$)) or 10 (remaining figures) times. The observation of these post-buckling results prompts the following remarks:

(i) Unlike the columns with D initial imperfections, which always exhibit outward mid-span flange-lip motions (akin to the initial imperfection shape), all the columns with L initial imperfections display inward mid-span flange-lip motions. This surprising feature is due to the presence of minor-axis bending, caused by effective centroid shifts towards the web stemming from stress redistribution (Young & Rasmussen 1999, despite the fixed ends). The associated outward web curvature "attracts" mid-span inward distortional deformations, which explains the failure modes in Figs. 4 (b$_1$) and (b$_3$).

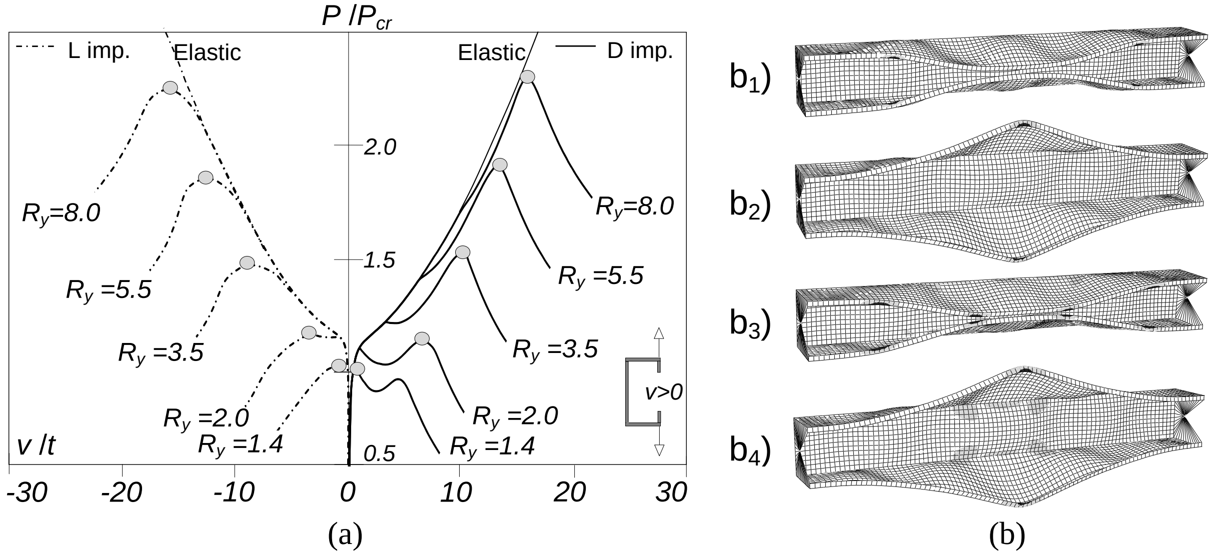

Figure 4: C13 lipped channel columns (a) P/P_{cr} vs v/t paths for D and L initial geometrical imperfections, and (b) failure modes and plastic strains for (b_1)-(b_4) R_y=2.0+L, R_y=2.0+D, R_y=5.5+L and R_y=5.5+D

(ii) In the columns with R_y closest to 1.0 (R_y=1.4), yielding starts when the normal stress distribution is still "not too far from uniform" and, therefore, precipitates a rather abrupt collapse, which occurs for a load that is practically imperfection-dependent.

(iii) In the columns with R_y>1.4, on the other hand, first yielding takes place when the normal stress distribution is already "highly non-uniform" and, therefore, does not lead to an immediate failure – collapse occurs either (iii_1) after a snap-through phenomenon and subsequent strength increase up to a limit point (columns with D imperfections) or (iii_2) following a fairly smooth stiffness decrease (columns with L imperfections). As R_y increases, the snap-through becomes less pronounced (it eventually disappears) and the elastic-plastic strength reserve grows considerably, because first yielding occurs at gradually more localized regions, thus impacting less the column stiffness – this can be confirmed by comparing the various R_y=*.*+D equilibrium paths.

(iv) In the columns with D imperfections and R_y<3.5 collapse occurs very soon after the yielding of the cross-section lips near the maximum outward distortional crest (*e.g.*, R_y=2.0+D – see Fig. 4(b_2)). As R_y grows, collapse occurs at a later stage, after the web-flange corner regions of the central L/3 segment have already yielded – see Fig. 4(b_4).

(v) On the other hand, the columns with L imperfections and R_y≤2.0 reach the ultimate strength when the lip free end regions of the outer half-wave most deformed cross-sections have yielded – *e.g.*, see Fig. 4(b_1), concerning R_y=2.0+L. For higher R_y values, collapse occurs once more at a later stage, when the lip free end and web-flange corner regions of the central L/3 segment have also yielded – see, for instance, Fig. 4(b_3), concerns R_y=5.5+L.

(vi) Regardless of the initial imperfections shape and R_y value, all columns with R_y≥2.0 exhibit visible L-D interaction. Moreover, note that the failure mode does not depend on R_y – *e.g.*, compare Figs. 4(b_2) and (b_4), which show the collapse mechanisms of the R_y=2.0+D and R_y=5.5+D columns.

Since L-D interaction occurs in all columns with R_{DL} close to 1.0 (even if it only causes significant ultimate strength erosion for R_y≥2.0, as shown later), it is important to identify when does "true L-D interaction" cease to occur, *i.e.*, the associated R_{DL} upper and lower limits. Such limits are obtained by means of a procedure involving the following steps:

(i) Select column sets with sequences of increasing and decreasing R_{DL} values, starting as close to 1.0 as possible, and exhibiting similar R_y values not too far from 1.0 (to avoid the yield stress influence).
(ii) Analyze all the columns within a set and, for each of them, observe and record the failure mode characteristics and location of the plastic strains at collapse. Only D initial imperfections are taken into consideration (they were shown by Dinis *et al*. 2007 to be the most detrimental).
(iii) Compare the failure mode characteristics and/or collapse plastic strain patterns of the columns with similar R_y values and identify the pairs of successive R_{DL} values associated with a change in them.

The above procedure was first adopted to identify R_{DL} upper and lower limits for C columns, starting with the identification of the lower limit, associated with the presence of L-D interaction when the column critical buckling is distortional (R_{DL}<1.0). Figs. 5(a)-(b) show the collapse modes and plastic strains of the R_{DL}=0.78+R_y=1.2 and R_{DL}=0.86+R_y=1.3 columns – note that the two column deformed shapes are amplified 3 times and the latter has its web magnified 150 times – since distortional buckling clearly precedes local buckling, the distortional deformations prevail at the column collapse and, thus, the huge magnification of the web deformed shape becomes necessary. The following conclusions can be drawn from the observation of these figures:
(i) The R_{DL}=0.78+R_y=1.2 column failure mode exhibits a perfect single-wave sinusoidal D shape – there is no trace of local deformations as illustrated in Fig. 5(a) (*i.e.*, no L-D interaction occurs).
(ii) Although barely perceptible, L-D interaction occurs close to collapse of the R_{DL} =0.86+R_y=1.3 columns – although the web deformed configuration appears to be a single-wave sinusoid, a minute local component can be detected by inspecting the magnified deformed web in Fig. 5(b), which provides evidence of an incipient local component (particularly near the fixed-ends).
(iii) Therefore, it seems fair to argue that the emergence of L-D interaction effects takes place somewhere in between the R_{DL}=0.78 and R_{DL}=0.86 values.

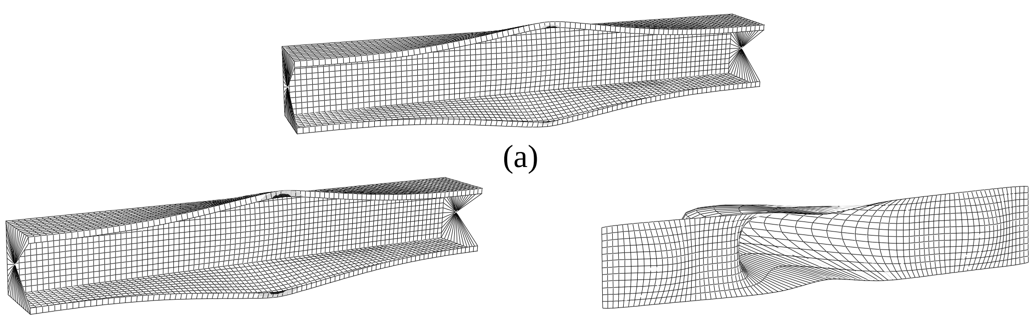
(a)
(b)

Figure 5: (a) R_{DL}=0.78+R_y=1.2 and (b) R_{DL}=0.86+R_y=1.3 C column and web deformed shapes and plastic strains at collapse

The same methodology was adopted to identify R_{DL} lower limits for the H, Z, R columns. Due to space limitations, no numerical results and figures are presented here. However, it was found that, also for the columns with these three cross-sections, the emergence of L-D interaction effects takes place somewhere in between the R_{DL}=0.78 and R_{DL}=0.86 values.

A similar procedure was adopted to identify the R_{DL} upper limit, which concerns columns with critical local buckling stresses (R_{DL}>1.0). Figs. 6(a)-(b) display the deformed shapes (amplified 20 times) and plastic strains of the R_{DL}=1.41+R_y=1.1 and R_{DL}=1.35+R_y=1.2 columns at the onset of collapse – detailed views of the column region with larger outward distortional deformations are also shown. These results prompt the following remarks:

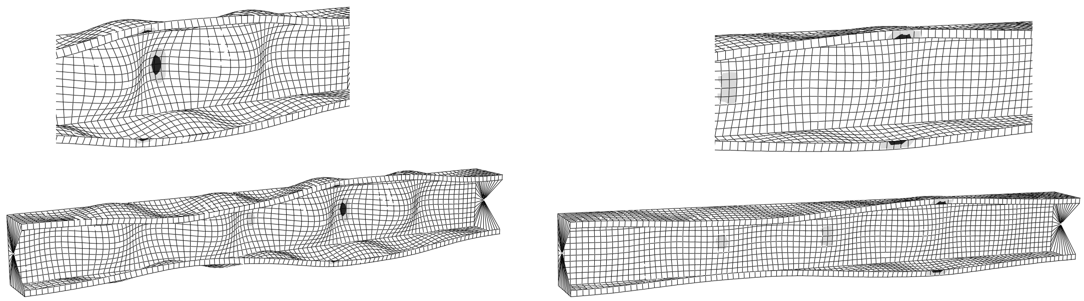

(a) (b)

Figure 6: (a) R_{DL}=1.41+R_y=1.1 and (b) R_{DL} =1.35+R_y=1.2 C column deformed shapes (with details) and plastic strain diagrams at collapse

(i) Although the two failure mode shapes share the same qualitative features, namely the combination of two D and several L half-waves, they are quantitatively quite different. Indeed, it is very clear that the L half-waves prevail in the R_{DL}=1.41+R_y=1.1 column failure mode, while the D ones are dominant in the R_{DL}=1.35+R_y=1.2 column collapse. Since both columns have L critical buckling modes and D initial imperfections, the dominance of the L (D) deformations in the failure mode may then be attributed to the absence (presence) of L-D interaction.

(ii) The above assertion is confirmed by the plastic strain diagrams of the two columns at the onset of collapse. In the R_{DL}=1.41+R_y=1.1 column, yielding starts at the web and flange crests (*i.e.*, central areas) of the most deformed L half-wave (see detail in Fig. 6(a)), which is a clear indication of a local failure (no visible L-D interaction occurs) – as will be seen later, the DSM prediction for the local failure of this column almost matches the numerical value ($f_{nl}/f_{u.D}$=1.01), thus confirming what had been anticipated. The presence of D deformations at collapse stems exclusively from the two half-wave D initial imperfection. In the R_{DL}=1.35+R_y=1.2 column, on the other hand, yielding starts at the lip free edge regions of the mid-span cross-section (see detail in Fig. 6 (b)), the trademark of distortional failure – thus, L-D interaction takes place, even if the ultimate strength erosion is small. The DSM prediction for a local failure slightly overestimates the numerical ultimate strength provided by the SFEA ($f_{nl}/f_{u.D}$=1.03) – minute ultimate strength erosion due to L-D interaction.

(iii) Thus, it may be argued that L-D interaction vanishes somewhere in between R_{DL}=1.35 and R_{DL}=1.41.

As before, for the upper limits, the same approach was adopted to identify R_{DL} lower limits for the H, Z, R columns and, due to space limitations, no numerical results and figures are presented. It was found that the transition between L failures and L-D collapses fits somewhere between (i) R_{DL}=1.13 and R_{DL}=1.22 (H columns), (ii) R_{DL}=1.22 and R_{DL}=1.29 (Z columns), and (iii) R_{DL}=1.28 and R_{DL}=1.35 (R columns).

Finally, it should be noted that (i) the above R_{DL} limits are in agreement with the findings of Dinis *et al.* (2009), Silvestre *et al.* (2012) and Dinis & Camotim (2013), who investigated the detrimental L-D interaction effects in columns with nearly coincident L and D critical buckling stresses ($0.9<R_{DL}<1.1$).

4.2 Secondary Bifurcation – R_y lower Limits

As mentioned earlier, L-D interaction may occur even when the L and D critical buckling stresses are far apart (*i.e.*, when R_{DL} is not close to 1.0). This interaction, due to a secondary (local or distortional) bifurcation, takes place if R_y (*i.e.*, the yield stress) is "large enough" to allow for the emergence and development of coupling effects before plasticity precipitates failure – indeed, all the selected columns may experience L-D interaction if the yield stress is "sufficiently high", since it is well known (*e.g.*, Camotim *et al.* 2005) that the column D and L post-critical strengths are fairly high (specially the latter).

Although the interaction may occur when R_{DL}>1.0 (critical L buckling) or R_{DL}<1.0 (critical D buckling), the former case is clearly more relevant, due to the considerably higher L post-critical strength (a more severe strength erosion is also expected for these columns).

After briefly presenting two illustrative examples of L-D interaction due to a "secondary" bifurcation (for columns with all cross-sections), namely concerning the (i) C1 (R_{DL}=0.42<1.0) and (ii) C27 (R_{DL}=2.39>1.0) columns, R_y lower limits (*i.e.*, yield stresses above which "secondary" bifurcation effects can emerge and develop) are obtained for all columns not experiencing "true" L-D interaction.

To illustrate the L-D interaction R_y-dependence of a column exhibiting L critical buckling, Figs. 7(a_1)-(a_2) depicts the upper portions (P/P_{cr}>0.50) of the C27 column elastic-plastic equilibrium paths P/P_{cr} vs v/t (v is again the mid-span top flange-lip corner vertical displacement) with C, H, Z (Fig. 7(a_1)) and R (Fig. 7(a_2)) cross-sections, and concerning (i) L initial imperfections, and (ii) R_y=0.9, 1.7, 2.6, 3.8. On the other hand, (i) Figs. 7(b_1)-(b_4) show the plastic strains at the onset of collapse of C, H, Z, R columns with R_y=0.9 (deformed shapes amplified 3, 4, 5 times in the C, H, Z columns, respectively) and (ii) Figs. 7(b_5)-(b_8) show similar results for R_y=3.8 (deformed shapes amplified 10 times in the H, R columns and 20 times in the C, Z columns). Due to space limitations, these two R_y values, which correspond to clearly distinct behaviors, are the only ones analyzed in detail in this work – however, a more detailed analysis can be found in Martins *et al*. (2013), for the lipped channel columns. The observation of the results presented in all the above figures leads to the following comments:

(i) All R_y=0.9 columns collapse abruptly with no trace of L-D interaction (see Figs. 7(b_1)-(b_4)) – only L deformations occur. In fact, the well-known "effective width" concept, originally proposed by von Karman, is clearly "illustrated" in these pictures, where the inability of the plate central regions to carry the compressive load forces the normal stresses to "migrate" towards the edges (when the load reaches its peak value), particularly towards the web-flange corners (the flanges are much more restrained by the web than by the lips – Silvestre & Camotim 2006), which is a trademark of local failure – note that, in these columns, the yield stress is such that f_y/f_{crl}=2.15 and f_y/f_{crd}=R_y=0.9.

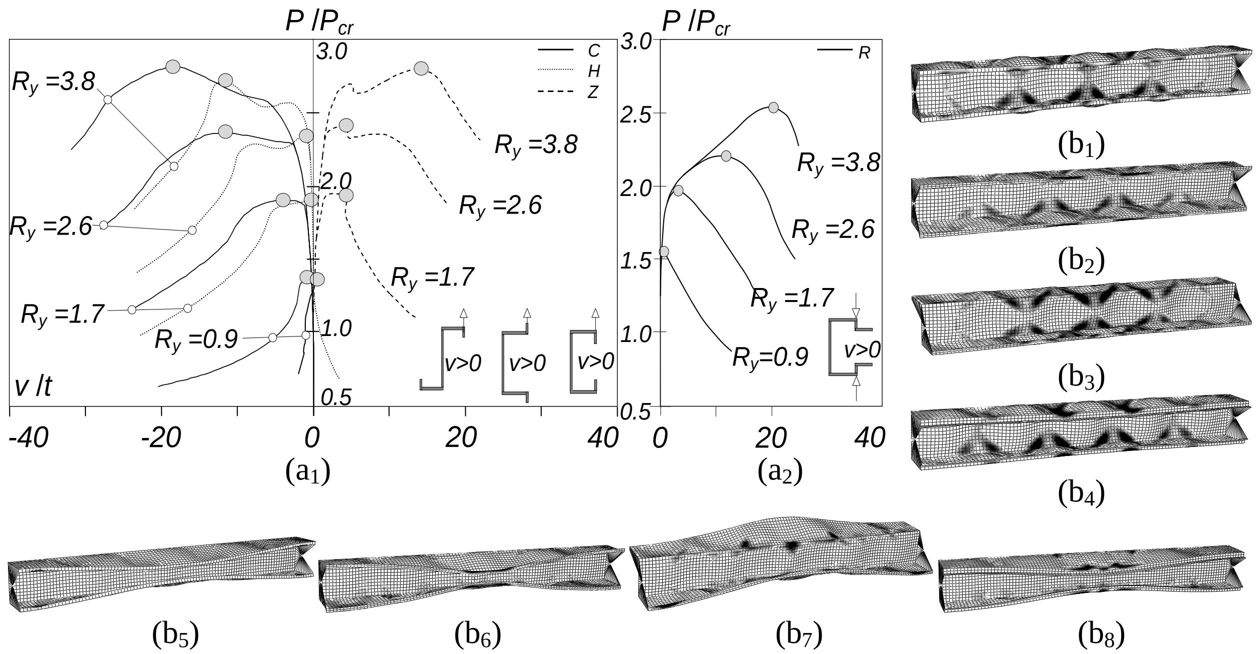

Figure 7: C27 column (a) P/P_{cr} vs v/t equilibrium paths with L imperfections for (a_1) C, H, Z and (a_2) R cross-sections, and (b) failure modes and plastic strains for (b_1)-(b_4) R_y=0.9+L and (b_5)-(b_8) R_y=3.8+L C, H, Z, R columns

(ii) The equilibrium paths associated with R_y=0.9 are distinct for the C, H, Z, R columns. Indeed, since none of the columns is affected by L-D interaction (they exhibit local failures) the most appropriated displacement to plot is the mid-span mid-web flexure (w), which explains the irregular behavior of the Z and H column equilibrium paths. However, a small mid-span inward flange-lip motions occurs in the C and R columns, due to global bending caused by the effective centroid shift effects – the same occurs in the H columns, but only for a bit higher R_y values (obviously this cannot take place in Z columns, due to the cross section point-symmetry).

(iii) The R_y=1.7 and R_y=2.6 columns exhibit local failures – no L-D interaction occurs, even in the presence of D initial imperfections.

(iv) All the R_y=3.8 C, H, Z, R columns exhibits L-D interaction (see Figs. 7(b_5)-(b_8)) and either (iv_1) fail after the occurrence of a snap-through phenomenon, followed by a subsequent applied load increase (C, H, Z columns – see Fig. 7(a_1)) or (iv_2) collapse occurs after a fairly smooth stiffness decrease (R column – see Fig. 7(a_2)). Note also that, as was observed in Figs. 4(b_1) and 4(b_3) for C columns, the C, H, R column with L initial imperfections exhibit mid-span inward flange-lip motions due to global bending stemming from effective centroid shift effects – as mentioned earlier, this does not apply to the Z column. These columns exhibit all local buckling and have a substantial post-critical strength reserve, which is responsible for a secondary (D) bifurcation that attracts distortional deformations and entails L-D interaction in the an elastic-plastic range, prior to collapse.

(v) For this particular column (R_{DL} value), it can be said that L-D interaction only develops if R_y is larger than a value comprised between 0.9 and 3.8. A more refined search narrowed the previous R_y interval down to between (i) 1.4 and 1.5 (C columns), (ii) 1.7 and 1.9 (H columns), (iii) 2.1 and 2.4 (Z columns) (iv) 1.6 and 1.7 (R columns) – see Fig. 9.

Next, a similar investigation is presented and discussed for the C1 column (R=0.42 – critical distortional buckling). Figs. 8(a_1)-(a_4) show four sets of five elastic-plastic equilibrium paths P/P_{cr} vs v/t concerning C, H, Z, R columns (v is the top flange-lip corner vertical displacement at the crest of the most deformed cross-section) associated with (i) R_y=0.4, 0.9, 1.7, 2.6, 5.1 and (ii) D initial geometrical imperfections. However, since the D post-buckling equilibrium paths concerning the Z columns are different for the top and bottom flange-lip assembly vertical displacements (Silvestre & Camotim 2003), all equilibrium paths shown in Fig. 8(a_3) correspond to the less stiff behavior (with outward motions). Figs. 8(b_1)-(d_4) depict the deformed configurations and plastic strain diagrams at the onset of collapse of the C, H, Z, R columns with (i) R_y=0.9 (Figs. 8(b_1)-(b_4)), and (ii) R_y=5.1 (Figs. 8(c_1)-(c_4)), while in Figs. 8(d_1)-(d_4) only the R_y=5.1 column web deformed configurations are depicted. The R_y=0.9 column deformed configurations are amplified either 5 times (C, H, R columns) or 10 times (Z column). As for the R_y=5.1 columns, the Z one is magnified 3 times and the C, H, R ones are not amplified – note also that the corresponding web deformed configurations are amplified either 20 times (C, H, Z columns) or only 15 times (R column). The observation of these post-buckling results prompts the following remarks:

(i) The R_y=0.9 columns fail without any trace of L-D interaction, since the deformed configuration at the onset of collapse is a perfect distortional two half-wave – see Figs. 8(b_1)-(b_4).

(ii) The R_y=5.1 columns exhibit L-D interaction, since local deformations were detected, even if they are not visible in Figs. 8(c_1)-(c_4). Indeed, a closer view of the web deformed configuration in Figs. 8(d_1)-(d_4) reveals very small amounts of local deformations in these columns – note that the web deformed configuration is depicted because the column L-D interaction is web-triggered.

(iii) For this R_{DL} value, L-D interaction only develops if R_y is larger than a value comprised between 0.9 and 5.1. A subsequent search narrowed the above R_y range to the interval comprised between

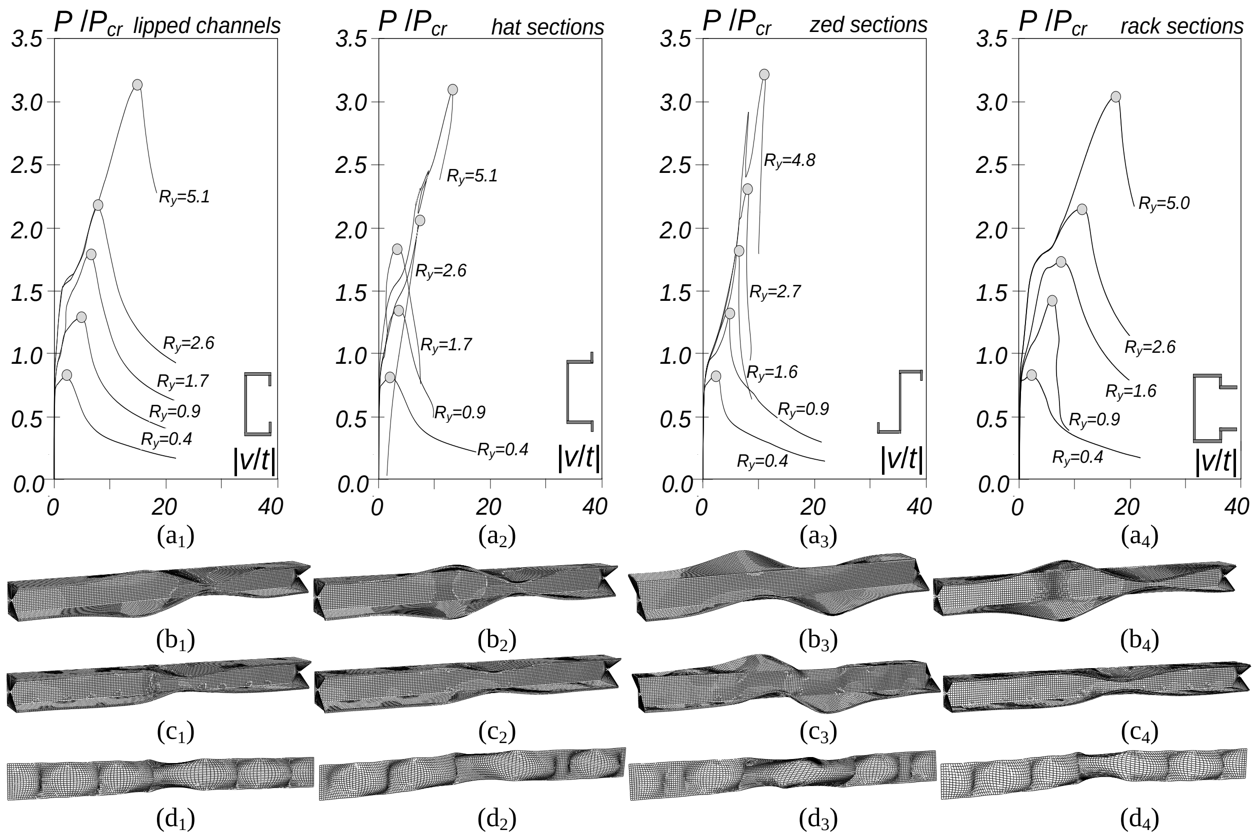

Figure 8: C1 column (a) P/P_{cr} vs v/t equilibrium paths with D imperfections for (a_1)-(a_4) C, H, Z, R cross-sections, (b)-(c) failure modes and plastic strains for (b_1)-(b_4) R_y=0.9+D and (c_1)-(c_4) R_y=5.1+D C, H, Z, R columns, and (d) web deformed configurations and plastic strains at collapse for Ry=5.0+D (d_1)-(d_4) C, H, Z, R columns

1.6 and 1.7 (C columns), (ii) 1.5 and 1.6 (H columns), (iii) 1.6 and 1.7 (Z columns) and (iv) 1.4 and 1.5 (R columns) – see Fig. 9.

(iv) The fact that the deformed configuration local component is small even for high yield stresses (*e.g.*, R_y=5.1) may explain the quite low ultimate strength erosion due to L-D interaction, particularly when compared to that exhibited by the columns buckling in critical local modes (this issue will be addressed in section 5). In fact, the failure modes of columns with high R_y values are characterized by the yielding of the mid-span lip free end regions, a trademark of distortional collapses – this is why the DSM D strength curve always predicts their failure loads quite accurately (see section 5).

In order to attempt to identify the R_{DL}-R_y range combinations leading to the occurrence of visible L-D interaction effects, all columns not exhibiting "true" L-D interaction (*i.e.*, those with R_{DL} values not close to 1.0) were analyzed with various yield stresses (R_y or λ_{cr} values). The results obtained are given in Fig. 9, for both R_{DL}<1.0 (D critical buckling) and R_{DL}>1.0 (L critical buckling) – in the latter case only L imperfections were considered. Since the correlation between the "R_y lower limits" and R_{DL} was far from illuminating, it is preferable to focus on plots involving "λ_{cr} lower limits". Initially they consisted of relatively small intervals containing the "λ_{cr} lower limits", in the sense that they separate columns undergoing or not L-D interaction. However, in order to address all the columns studied (C, H, Z, R) and taking into account that the λ_{cr} bounded intervals were found to be rather short, it was decided, for the sake of clarity, to plot only the average of the upper and lower bounds of those intervals. The observation of this figure leads to the followings comments:

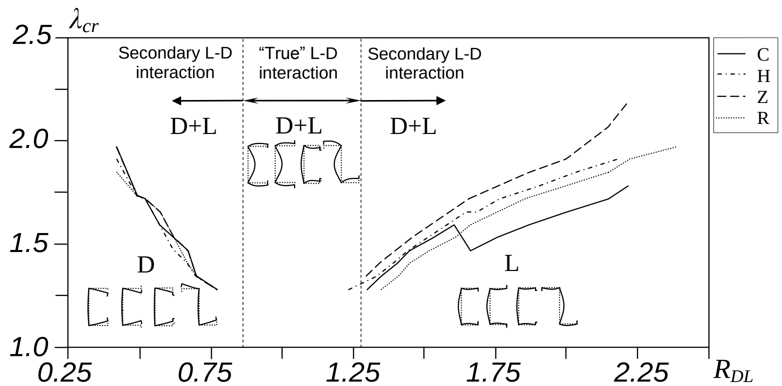

Figure 9: R-λ_{cr} combinations associated with the transition between pure individuals (L or D) and L-D interactive behaviors for C, H, Z and R cross-sections

(i) First of all, and generally speaking, the transition between "pure" distortional ("pure" local) and L-D interactive behaviors occurs for growing λ_{cr} values as R_{DL} decreases (increases) – the only exception concerns the transition between the R_{DL}=1.60 and R_{DL}=1.66 in C columns (discussed below).

(ii) Since it was found that the collapse mechanisms of columns with R_{DL}<1.0 exhibit predominantly distortional deformations, the occurrence of L-D interaction (if the yield stress is "high enough", *i.e.*, for yield stresses above the curve depicted in Fig. 9) always involves quite small L deformations. It was also observed that the transitions between "pure" distortional and L-D collapses are very similar for the four columns considered.

(iii) Conversely, the transitions between "pure" local and L-D collapses may be quite distinct, particularly if the comparison is made between the C and Z columns – the Z columns curve is always above the remaining ones. Moreover, the curves concerning the H and R columns are quite close.

(iv) In the C columns, the transition curve exhibits a singularity between R_{DL}=1.60 and R_{DL}=1.66. In between these two values, the half-wave number exhibited by the column critical distortional buckling mode (n_d) changes from two to one (see Table 1). It was observed that (iv$_1$) the failure modes of columns C15 to C20 (both with n_d=2) exhibited mid-span outward flange-lip motions and, conversely, (iv$_2$) those of columns C21 to C27 (all with n_d=1) exhibits mid-span inward flange-lip motions, regardless of the initial imperfection shape (L+, L–, D+ or D–). This stems from the presence of minor-axis bending caused by the effective centroid shifts towards the web, caused by the "highly non-uniform" stress redistribution (see section 4.1).

It is still worth mentioning that the above results concerning the columns with R_{DL}>1.0 provide numerical confirmation for the experimental evidence of the occurrence of L-D interaction when the R_{DL} values significantly exceed 1.0, namely those reported by (i) Young *et al.* (2013), for fixed-ended C columns with R_{DL} values comprised between 1.73 and 2.71, and (ii) Dinis *et al.* (2013a), for fixed-ended R columns with R_{DL} values varying between 1.31 and 1.46.

5. Direct Strength Method (DSM) Design – Assessment of the Ultimate Strength Estimates

The motivation for developing the Direct Strength Method (DSM) was overcoming the difficulties associated with the application of the classical Effective Width Method (EWM) to more complex cold-formed steel cross-sections (those exhibiting large wall numbers, including more or less involved lips and/or intermediate stiffeners). The DSM was originally proposed by Schafer and Peköz (1998b) about fifteen years ago, following a seminal idea of Hancock (Hancock *et al.* 1994), and has been continuously improved since then, mostly due to the research activity carried out by Schafer and his collaborators. The method has been shown to provide an efficient and general approach to obtain efficient (safe and accurate) estimates of the ultimate strength of cold-formed steel columns and beams on the sole basis of the steel yield stress and elastic critical buckling stresses (for the whole cross-section, rather than for individual walls/plates, like in the traditional EWM) associated with local, distortional and global modes. For columns, the DSM nominal strengths against local (f_{nl}) and distortional (f_{nd}) failures are provided by "Winter-type" expressions (calibrated against a fairly large numbers of experimental and numerical failure loads, mostly involving fixed-ended columns) that can be found in Schafer's state-of-the-art report (Schafer 2008). Regarding the columns experiencing L-D interaction, there are also specific DSM approaches to predict their load-carrying capacity. The first two of them, proposed by Schafer (2002), consist of replacing f_y by either (i) f_{nd} in the f_{nl} equations (NLD approach – f_{nld}) or (ii) f_{nl} in the f_{nd} equations (NDL approach – f_{ndl}) – the former was later employed by Yang and Hancock (2004) and Kwon *et al.* (2009). Silvestre *et al.* (2012) assessed the performance of these two approaches, for fixed-ended lipped channel columns[6], and concluded that they provide similar results, even if the quality of the f_{ndl} estimates was found to be marginally higher – this is why this work adopts the NDL approach, defined as

$$f_{ndl}=\begin{cases} f_{nl} & , \quad \lambda_d \le 0.561 \\ f_{nl}\ \left(\lambda_{dl}\right)^{-1.2}\ \left[1-0.25\left(\lambda_{dl}\right)^{-1.2}\right], & \lambda_d > 0.561 \end{cases} \tag{1}$$

where $\lambda_{dl}=(f_{nl}/f_{crd})^{0.5}$ is a distortional slenderness based on the local strength, and $\lambda_d=(f_y/f_{crd})^{0.5}$ is the distortional slenderness. Moreover, these authors also showed that the f_{nd} values (i) provide accurate column ultimate strength estimates in the low-to-moderate distortional slenderness range (λ_d<1.5), but (ii) lead to excessively conservative predictions for more slender columns (λ_d≥1.5). For the latter, Silvestre *et al.* (2012) showed that the ultimate strength is best estimated by adopting (i) the current DSM distortional strength expression (f_{nd}), for λ_d<1.5, and (ii) a modified local strength f_{nl}^* (instead of the usual f_{nl}), for λ_d≥1.5 – the corresponding DSM approach is termed here "modified NDL approach – MNDL". The modified local strength (i) depends on the critical half-wave length ratio L_{crd}/L_{crl} (obtained from simply supported column signature curves and given in the tables included in Annexes A to C for C, H, Z and R columns), and (ii) leads to f_{nd} and f_{ndl} values for $L_{crd}/L_{crl} \le 4$ and $L_{crd}/L_{crl} \ge 8$, respectively – it is given by

$$f_{nl}^*=\begin{cases} f_y & , \quad \dfrac{L_{crd}}{L_{crl}} \le 4 \\ f_y+\left(1-0.25\,\dfrac{L_{crd}}{L_{crl}}\right)\times\left(f_y-f_{nl}\right), & 4<\dfrac{L_{crd}}{L_{crl}}<8 \\ f_{nl} & , \quad \dfrac{L_{crd}}{L_{crl}} \ge 8 \end{cases} \tag{2}$$

It is worth noting that the DSM MNDL approach just presented was developed, calibrated and validated on the basis of numerical (SFEA) ultimate strengths concerning fixed-ended lipped channel columns exhibiting R_{DL} values comprised between 0.90 and 1.10 – this means that those numerical results were restricted to columns strongly affected by L-D interaction, for which the ultimate strength erosion is most severe (they are all included in the "true L-D interaction" region determined in section 4.1).

[6] These findings were subsequently extended to H, Z, R columns by Dinis & Camotim (2013).

The numerical ultimate strengths (f_u) obtained previously are compared next with their estimates provided (i) by the current DSM local and distortional strength curves (f_{nl} and f_{nd}) and also (ii) by the DSM approaches specifically developed to deal with L-D interactive failures (NDL and MNDL – f_{ndl} and f_{mndl}) – these four ultimate strength estimates are also given in the tables included in Annexes A to C. The aim of this study is to assess (i) how the combined R_{DL} and R_y values affect the ultimate strength erosion due to L-D interaction (and, if possible, provide preliminary guidelines about its relevance) and (ii) how the available DSM-based approaches predict the C, H, Z, R columns L-D interactive failure loads. The results presented concern only a representative fraction of the analyzed columns, covering the whole R_{DL} range considered: columns C1-5-9-12-16-21-24-27 (R_{DL}=0.42-0.62-0.86-1.07-1.35-1.66-2.00-2.39) – this set of columns provides sufficient information to quantify the influence of R_{DL} on the quality of the DSM ultimate strength predictions. For the sake of clarity, it was decided to present and discuss separately two sets of results: (i) those concerning the ultimate strength of C, H, Z columns (section 5.1), whose values are very similar (as explained in section 2), and (ii) a comparison between the C column results (which are also representative of the H, Z columns) with their R column counterparts (section 5.2). Each of the above 8 columns was analyzed with 11 distinct yield stresses, thus making it possible to cover a quite wide critical (distortional or local) slenderness range, which is essential to identify the columns affected by L-D interaction caused by a "secondary (L or D) bifurcation".

5.1 Lipped channel, hat-section and zed-section columns

Figs. 10(a$_1$)-(b$_4$) and 11(a$_1$)-(b$_4$) provide the variations of f_u/f_y with λ_l or λ_d for the 8 sets of C, H, Z columns listed above. While only D initial imperfections were considered for the columns with R_{DL}<1.0 (distortional critical buckling), all columns with R_{DL}>1.0 (local critical buckling) were analyzed with L (white circles, squares, triangles and rhombuses) and D (grey circles, squares, triangles and rhombuses) initial imperfections. The numerical f_u/f_y values are compared, separately for each R_{DL} value, with their (i) f_{nl} or f_{nd} and (ii) f_{ndl} and f_{mndl} estimates – note that f_{mndl} values were also determined outside the R_{DL} domain prescribed for the application of the MNDL approach. The comparative analysis of all these numerical ultimate strengths and associated DSM estimates prompts the following remarks:

(i) First of all, all the numerical f_u/f_y values are well aligned along "Winter-type" curves.

(ii) The observation of Figs. 10 and 11 shows that the C, H, Z column ultimate strength stresses concerning the same R_{DL} values are nearly coincident, even if (i) the collapse mechanism (and yielding pattern) are clearly distinct, as reported in section 4, and (ii) the configurations of the most detrimental D imperfections are different (*e.g.*, the 1 D half-wave shapes for the C and H columns).

(iii) For R_{DL}=0.42 and R_{DL}=0.62, the f_{nd} values provide safe and fairly accurate ultimate strength estimates for the C, H, Z columns considered, which means that there is no perceptible erosion due to L-D interaction (note that, for these columns, $f_{nd} \equiv f_{mndl}$). Indeed, these columns exhibit failure modes characterized by the yielding of the lip free end regions (their locations depend on the number of distortional half-waves) – this explains why the current DSM distortional strength curve predicts adequately the ultimate strength of these columns and no relevant strength erosion stemming from a secondary L bifurcation is detected.

(iv) The ultimate strengths of the R_{DL}=0.86 columns, which already exhibit "true" L-D interaction, are no longer appropriately predicted by the current DSM distortional strength curve (see Fig. 10(b$_3$)) – instead, it is necessary to resort to the f_{mndl} estimates.

(v) Concerning the R_{DL}>1.0 columns, the first remark concerns the fact that the vast majority of f_u values associated with L and D initial imperfections are very similar. The few exceptions are stocky columns whose ultimate strengths are generally very well predicted by the DSM local strength curve, which means that they are not affected by L-D interaction (low R_y values).

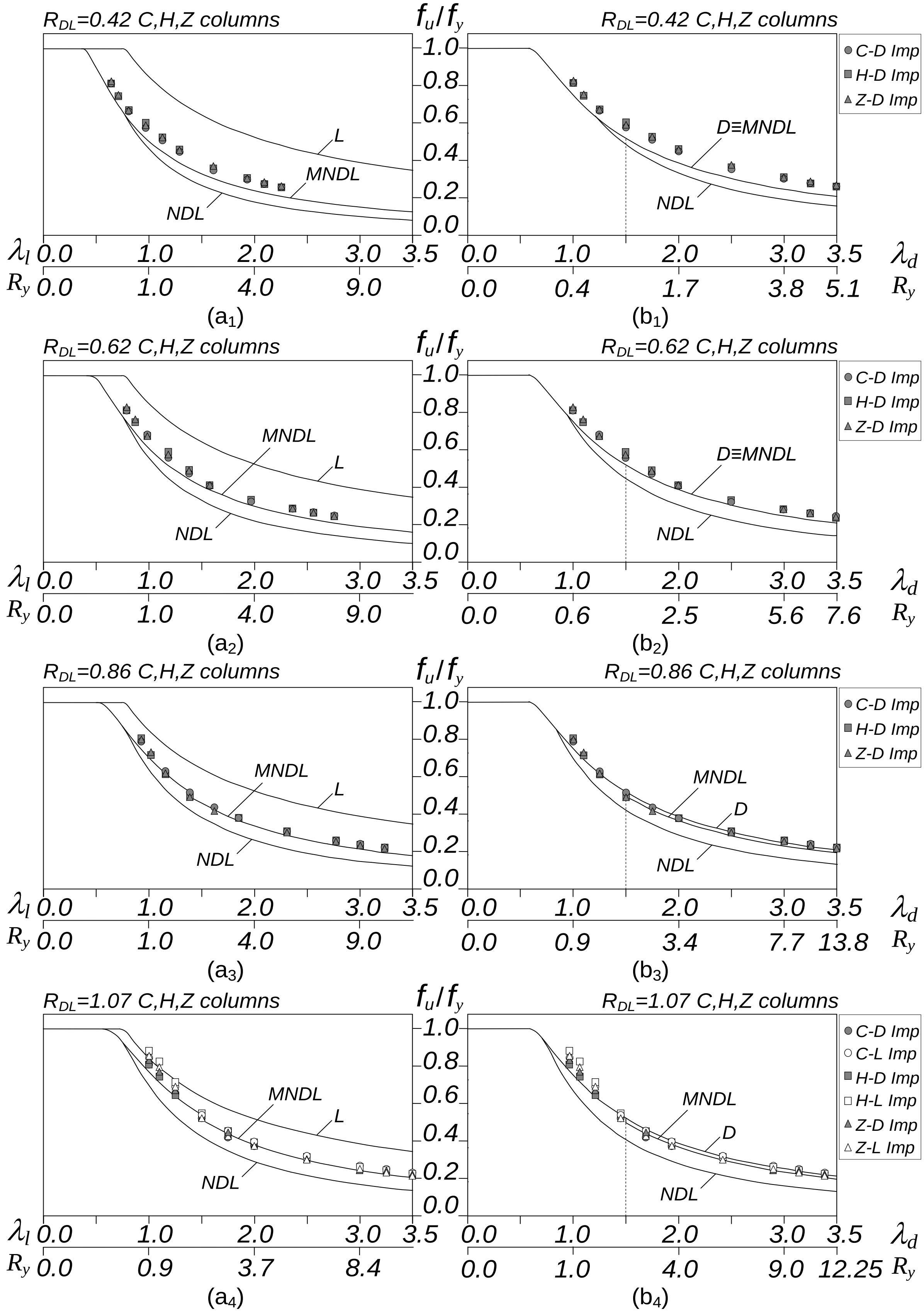

Figure 10: Variation of f_u/f_y and corresponding DSM predictions with (a) λ_l or (b) λ_d for ($_1$)-($_4$) R_{DL}=0.42-0.62-0.86-1.07 columns

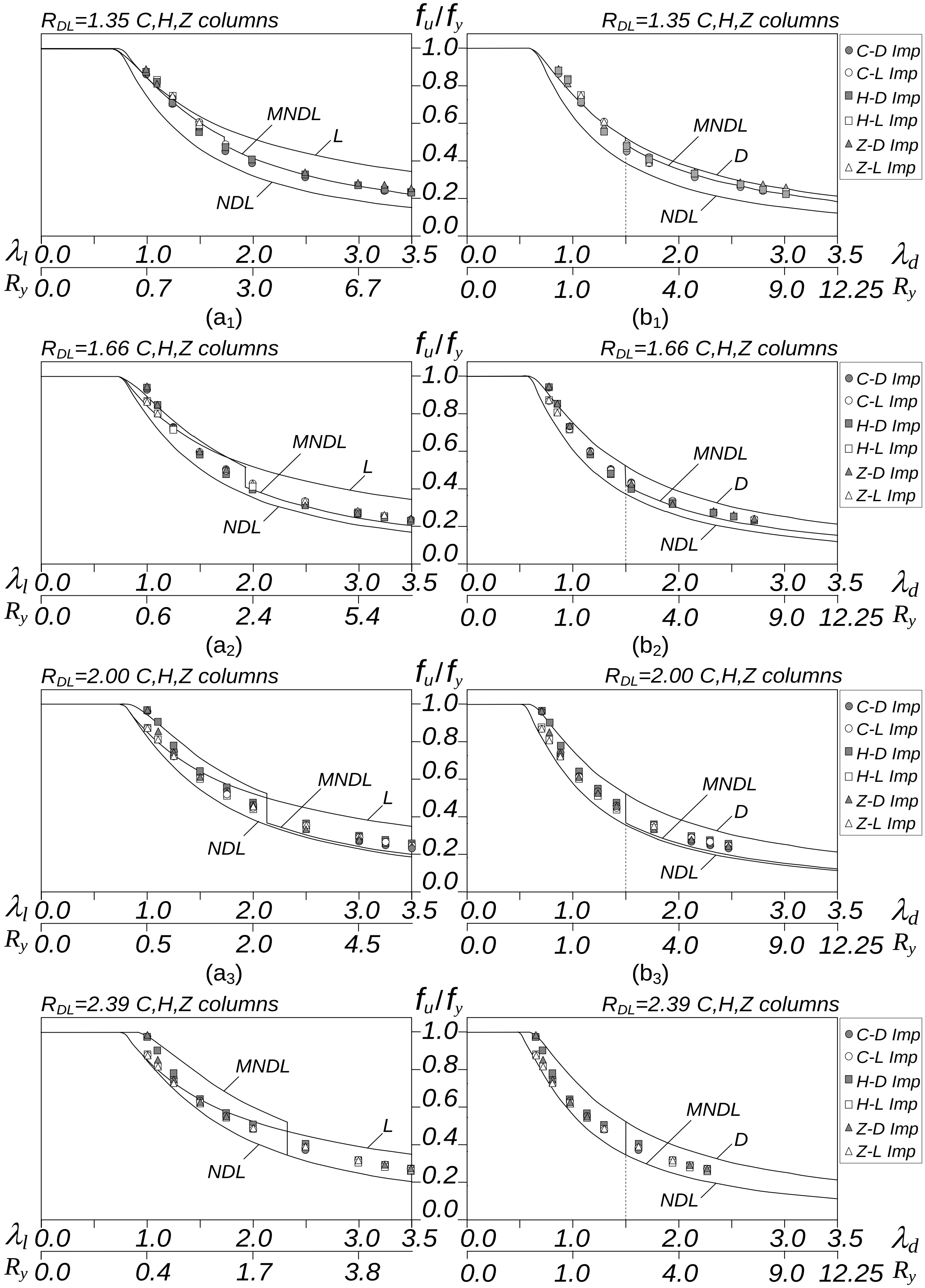

Figure 11: Variation of f_u/f_y and corresponding DSM predictions with (a) λ_l or (b) λ_d for ($_1$)-($_4$) R_{DL}=1.35-1.66-2.00-2.39 columns

(vi) For the particular case of the R_{DL}=1.07 columns, Figs. 10(a_4)-(b_4) clearly show that L-D interaction occurs in the whole slenderness range, as had already been concluded in section 4.1 (this column exhibits "true" L-D interaction) – note the difference (erosion) between the numerical ultimate loads and their f_{nl} prediction. Moreover, these figures also evidence the merits of the MNDL approach, as the f_{mndl} values provide quite good estimates for the whole slenderness range.

(vii) Practically all failure loads concerning the most slender R_{DL}>1.0 columns are clearly overestimated by the current DSM local and distortional strength curves – undeniable evidence of the occurrence of significant L-D interaction (the R_y values are "high enough").

(viii) For R_{DL}=1.35, R_{DL}=1.66, R_{DL}=2.00 and R_{DL}=2.39, the occurrence of a secondary D bifurcation is noticeable in Figs. 11(a_1)-(a_4). The R_y and λ_{cr} values for which L-D interaction becomes less relevant (lower limits, in the sense of ceasing to cause ultimate strength erosion) clearly increase with R_{DL}.

(ix) Finally, it may be concluded that, generally speaking, the R_{DL}>1.0 column ultimate strength tends to be less overestimated by the f_{nl} values as R_{DL} increases (switch from "true" L-D interaction to "secondary D bifurcation") and λ_l decreases (lower R_y values), which corresponds to less relevant L-D interaction effects (as concluded earlier). The number of fairly accurate estimates, indicating local failures, grows with R_{DL}. Conversely, the f_{nd} values provide overestimations that increase as R_{DL} increases and λ_l decreases – for $R_{DL}\leq$1.35, such overestimations are invariably quite small and only become "visible" for columns with intermediate slenderness values.

5.2 Lipped channel and rack-section columns

Figs. 12(a_1)-(b_4) and 13(a_1)-(b_4) provide the variations of f_u/f_y with λ_l or λ_d for the 8 sets of C, R columns considered (they are similar to Figs. 10(a_1)-(b_4) and 11(a_1)-(b_4)), in order to compare the C column earlier findings (also valid for the H, Z columns) with the R column results. Like in section 5.1, (i) only D initial imperfections were considered for the R_{DL}<1.0 columns, (ii) all R_{DL}>1.0 columns were analyzed with L (white circles, squares, triangles and rhombus) and D (grey circles, squares, triangles and rhombus) initial imperfections. Again, the numerical f_u/f_y values are compared, separately for each R_{DL} value, with their (i) f_{nl} or f_{nd} and (ii) f_{ndl} and f_{mndl} estimates. The comparison leads to the following comments:

(i) First of all, the comments (i) and (iii) to (ix) of the previous section remain perfectly valid for the results presented in Figs. 12(a_1)-(b_4) and 13(a_1)-(b_4).

(ii) Generally speaking, on the basis of the observation of Figs. 10-11 and Figs. 12-13, can be stated that, for similar R_{DL} values, the R columns ultimate loads are lower than their C column counterparts, which implies that the former columns are more affected by L-D interaction than the latter (and also the H, Z columns).

5.3 Assessment of the numerical ultimate strength estimates

On the basis of the significant amount of numerical ultimate strengths obtained in this work, concerning C, H, Z, R columns affected by L-D interaction, it is possible to draw some preliminary conclusions concerning the quality of their DSM-based predictions. Figs. 14(a)-(c) show, respectively, the variations of (i) f_u/f_{nd} with the local slenderness λ_l, (ii) f_u/f_{nl} with the distortional slenderness λ_d, and (iii) f_u/f_{ndl} with the distortional slenderness λ_d, for the C, H, Z, R columns analyzed[7]. However, note that Figs. 14(a)-(b) include only results of columns with R_{DL}<1.0 and R_{DL}>1.0, respectively, while all column results are displayed in Fig. 14(c). Moreover, the grey circles in these three figures correspond to the R column ultimate strengths. The observation of these figures prompts the following comments:

[7] The inclusion of the apparently "illogical" f_u/f_{nd} vs. λ_l and f_u/f_{nl} vs. λ_d plots (instead of the more "logical" f_u/f_{nd} vs. λ_d and f_u/f_{nl} vs. λ_l ones) is done to improve the "readability" – the values are much less "on top of each other".

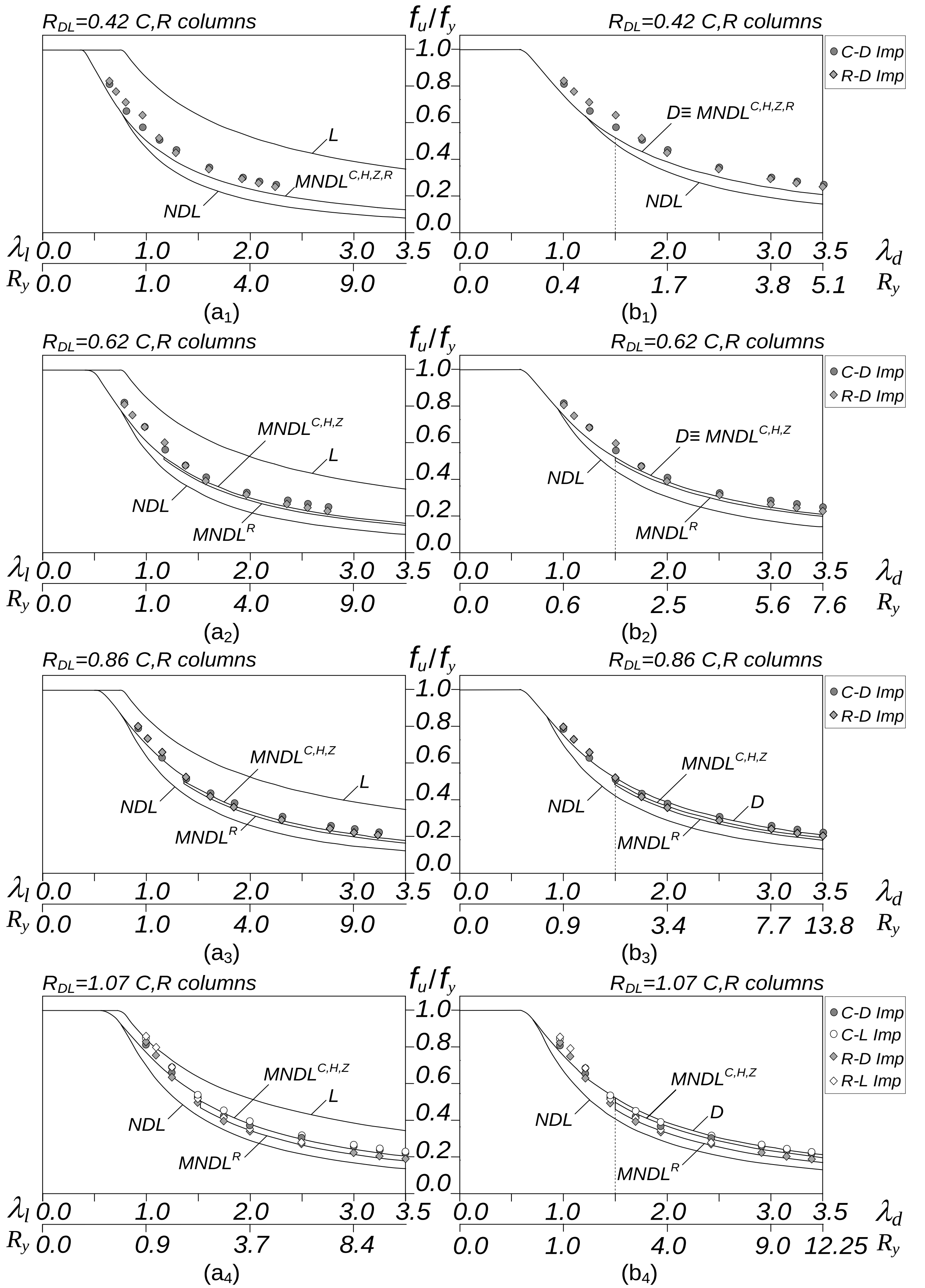

Figure 12: Variation of f_u/f_y and corresponding DSM predictions with (a) λ_l or (b) λ_d for $(_1)$-$(_4)$ R_{DL}=0.42-0.62-0.86-1.07 columns

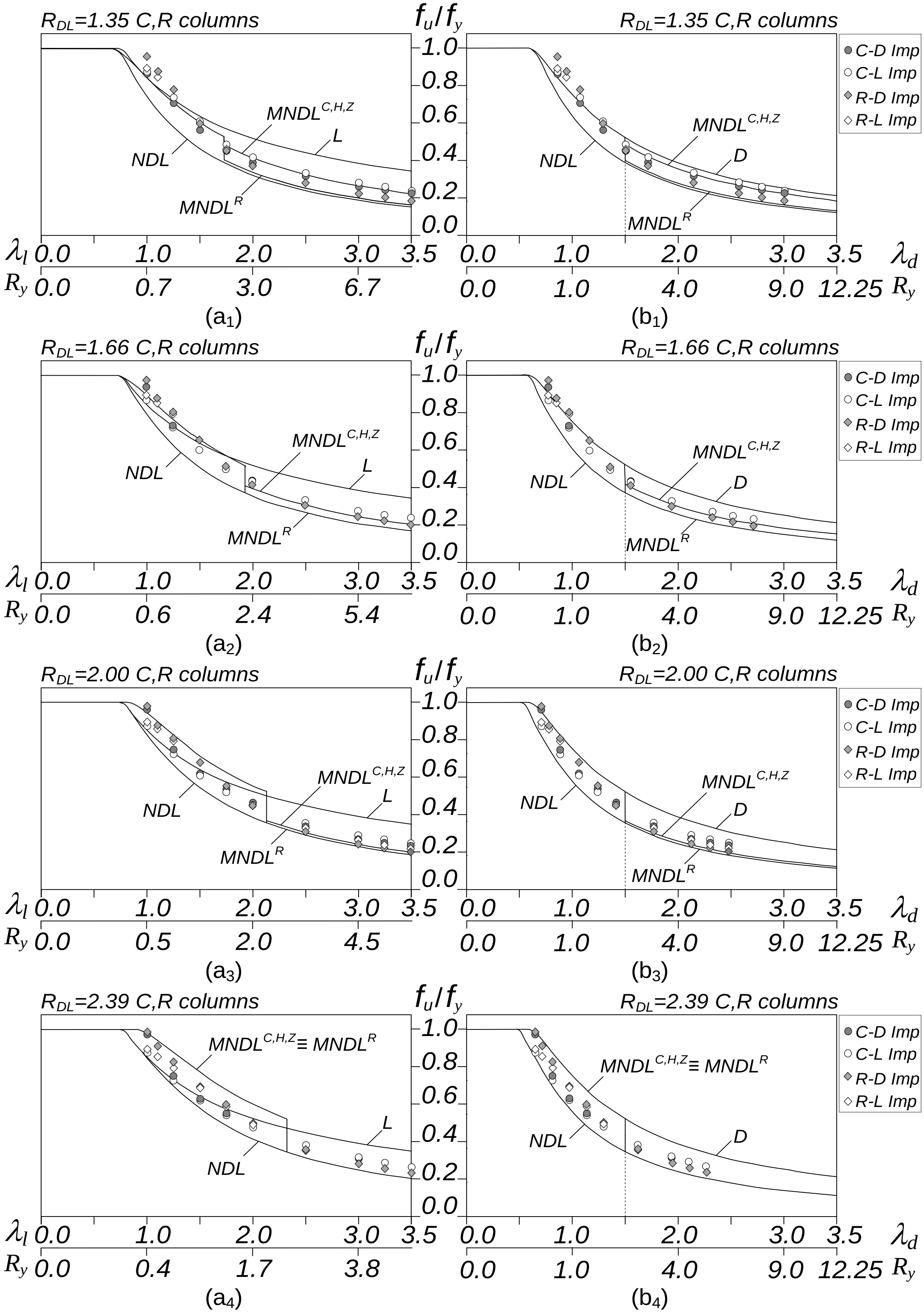

Figure 13: Variation of f_u/f_y and corresponding DSM predictions with (a) λ_l or (b) λ_d for $(_1)$-$(_4)$ R_{DL}=1.35-1.66-2.00-2.39 columns

(i) First of all, as mentioned already by several authors, the current DSM expressions (NL and ND) are not able to predict adequately the ultimate strength erosion caused by the L-D interaction, particularly the NL approach, whose estimates have mean and standard deviation values equal to 0.82 and 0.15 (minimum value of 0.52!). The ND predictions exhibit much higher quality: they are clearly more accurate and mostly safe, as reflected in the mean and standard deviation values of 1.08 and 0.08 – note that all unsafe estimates in Fig. 14(a) concern columns affected by "true" L-D interaction.

(ii) The NDL approach always provides safe ultimate strength estimates (the minimum value of 1.02) – see Fig. 14(c) (and also Figs. 10-13(a_1)-(b_4)). However, as already observed by Silvestre *et al*. (2012) and Dinis & Camotim (2013), a considerable fraction of the estimates concerning columns with R_{DL} values close to 1.0 (strong "true" L-D interaction), are overly conservative – nevertheless, this approach can be quite useful for designers, particularly in the preliminary column design stages.

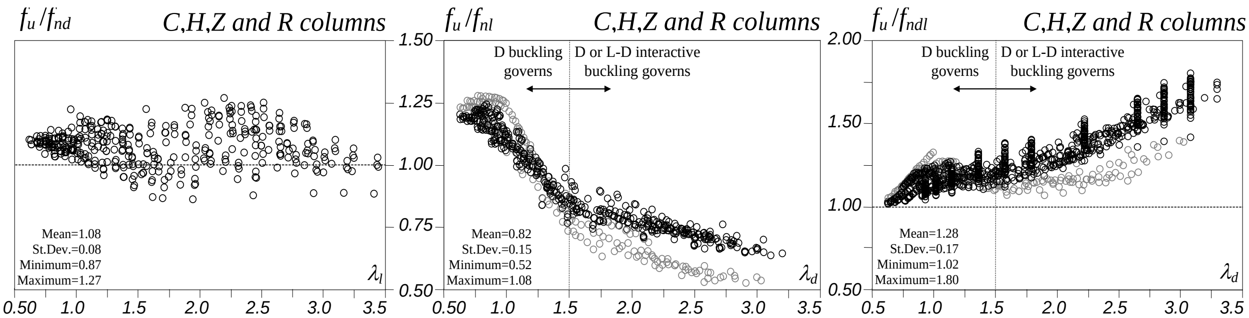

(a) (b) (c)

Figure 14: Variation of (a) f_u/f_{nd} with λ_l, (b) f_u/f_{nl} with λ_d and (c) f_u/f_{ndl} with λ_d (C, H, Z, R columns)

Figs. 15($a_{1\text{-}3}$)-($b_{1\text{-}3}$) show the variation of f_u/f_{mndl} with the distortional slenderness λ_d for the ($_1$-C, $_2$-H, $_3$-Z) columns (i) C10-C13 (R_{DL} between 0.96 and 1.13 – Fig. 15(a)), and (ii) C7-C20 (R_{DL} between 0.70 and 1.60 – Fig. 15(b)) – only the former fall inside the R_{DL} range considered by Silvestre *et al*. (2012) and Dinis & Camotim (2013), to assess the quality of the DSM MNDL ultimate strength estimates. It is worth noting that f_u is taken as (i) $f_{u,D}$, for $R_{DL}\leq 1.0$, and (ii) the lowest of $f_{u,D}$ and $f_{u,L}$, for $R_{DL}>1.0$. As for Figs. 16(a)-(b), they provide similar results for the R columns. Finally, Fig. 16(c) shows the variation of f_u/f_{mndl} with the distortional slenderness for all C, H, Z, R columns with $0.70<R_{DL}<1.60$. The observation of the results shown in the above figures makes it possible to conclude that (on the basis of the limited number of numerical results obtained in this work, of course):

(i) The MNDL approach, which was developed specifically for columns with R_{DL} values comprised between 0.90 and 1.10, provides quite good predictions for the R_{DL}=0.96, R_{DL}=1.07 and R_{DL}=1.13 C, H, Z, R columns in the whole slenderness range – note that only the R_{DL}=1.07 column results were displayed in Figs. 10(a_4)-(b_4) (C, H, Z columns) and Figs. 12(a_4)-(b_4) (R columns).

(ii) The MNDL was found to provide also quite good estimates for C, H, Z columns with R_{DL} values falling outside its intended domain of application, namely values comprised between (ii_1) 0.70 and 0.90 (Figs. 15(a_1)-(a_3)), and (ii_2) 1.10 and 1.60 (Figs. 15(b_1)-(b_3)) – indeed, the ultimate strengths of columns C7, C8, C9, C13, C14, C15, C16, C17 were efficiently predicted. Figs. 16(a)-(b) show that this assertion (efficient MNDL estimates) can also be extended to R columns in the same R_{DL} range.

(iii) The quality of the f_{mndl} estimates is very similar for the C10-C12 and C7-C17 C, H, Z columns (Fig. 15), as attested by (iii_1) the closeness of the corresponding averages and standard deviations (iii_2) the strong resemblance between the f_{mndl}/f_u vs λ_d "clouds" and (iii_3) the fact that the minimum and maximum values are very similar. Moreover, the overwhelming majority of column ultimate strength predictions are safe ($f_u/f_{mndl}>1$) – the "level of safety" increases with the slenderness λ_d.

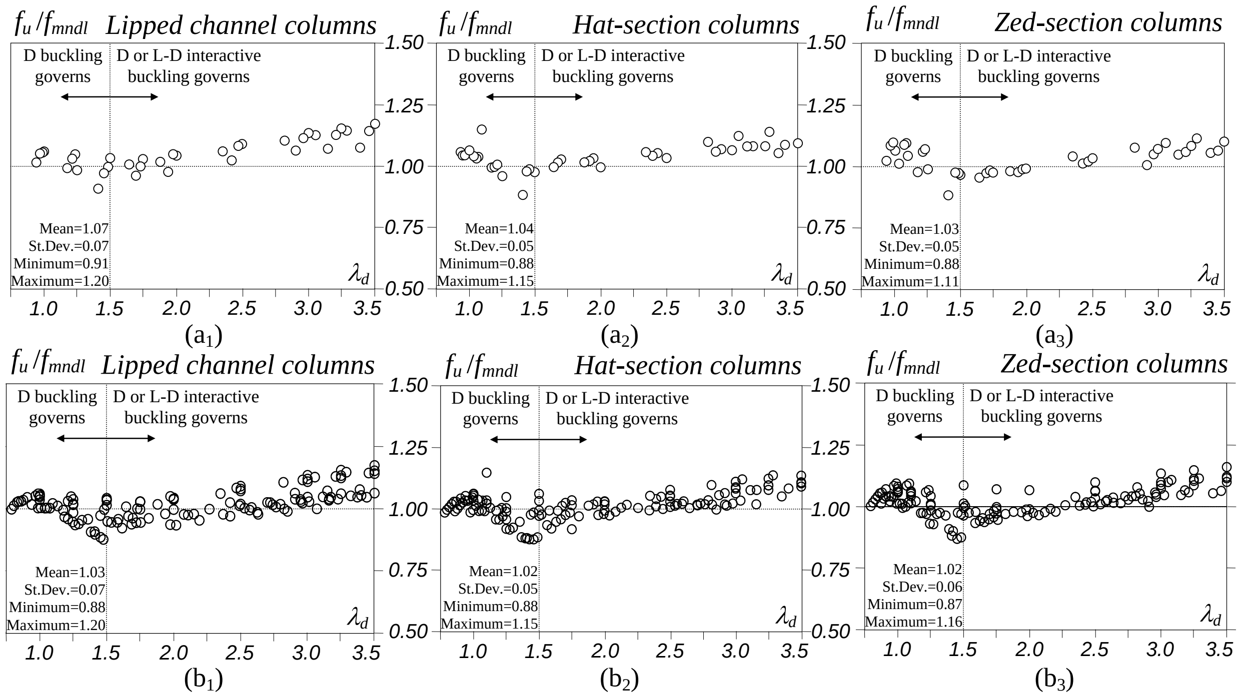

Figure 15: Variation of f_u/f_{mndl} with λ_d for columns (a) C10-C13 (0.96<R_{DL}<1.13) and (b) C7-C20 (0.70<R_{DL}<1.60)

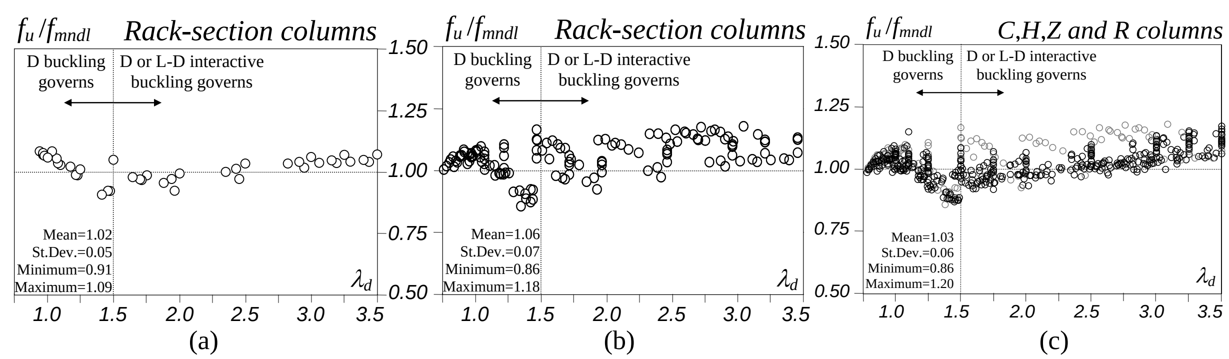

Figure 16: Variation of f_u/f_{mndl} with λ_d for columns (a) C10-C13 (0.96<R_{DL}<1.13) and (b) C7-C20 (0.70<R_{DL}<1.60)

(iv) Despite the reduced number of columns analyzed in the 0.90<R_{DL}<1.10 range, the average and standard deviation of their f_u/f_{mndl} values are very similar to those reported by Silvestre *et al.* (2012) and Dinis & Camotim (2013). However, the quality of the other values reported earlier by these same authors (Dinis *et al.* 2009) is considerably lower (average and standard derivation equal to 1.09 and 0.11, respectively) – most likely, this was due to a poor column geometry selection, in the sense that the global (flexural-torsional) critical buckling loads are not "above enough" their local and distortional counterparts, which led to some amount of mode interaction involving global buckling modes, thus causing additional ultimate strength erosion.

(v) It seems fair to expect that it will be possible to extend the domain of application of the DSM MNDL design approach, developed and validated for fixed-ended columns with 0.90<R_{DL}<1.10, to C, H, Z, R columns in the range 0.70<R_{DL}<1.60, as clearly shown in Fig. 16(c) (mean and standard deviation values equal to 1.03 and 0.06).

5.4 Assessment of the experimental ultimate strengths reported in the literature

It is well known that the development of the column DSM design/strength curves/expressions was validated against fairly large numbers of experimental and numerical failure loads, mostly concerning fixed-ended columns. Following the assessment of the numerical ultimate strength data estimation, presented in the previous section, attention is now turned to the prediction of the experimental failure loads, in order to assess the generality of the available DSM-based design approaches developed to handle L-D interaction, thus paving the way for their codification.

The experimental results available in the literature and considered in this work are those reported by Kwon & Hancock (1992), Kwon *et al.* (2009), Loughlan *et al.* (2012), Young *et al.* (2013) and Dinis *et al.* (2013a), all concerning column specimens compressed between fixed-ended cross-sections, which fully prevent local/global rotations and warping – with the exception of the tests reported by Dinis *et al.* (2013a), which concern R columns, all the above results deal with C columns. A total of 54 test results were gathered and it is worth noting that those selected concern exclusively column specimens for which (i) local buckling is triggered by the web (plain cross-section columns with flanges wider than the web were excluded – a different kind of L-D interaction phenomenon that is currently under investigation by the authors), and (ii) L-D interactive failures were experimentally observed[8]. Since the overwhelming majority of the experimental data concerns columns with critical local buckling stresses (*i.e.*, R_{DL}>1.0) (only very few tests on columns with critical distortional buckling stresses were found), an experimental program covering the R_{DL}<1.0 range is planned for the near future.

5.4.1 Kwon & Hancock (1992)

Table 3 concerns the tests carried out by Kwon & Hancock (1992) and provides the corresponding (i) critical buckling stresses (f_{crl}, f_{crd}, f_{crg}), (ii) R_{DL} values, (iii) experimental ultimate stresses (f_{Exp}), (iv) their estimates yielded by the ND, NDL and MNDL DSM approaches and (v) the corresponding experimental-to-predicted ultimate stress ratios – the measured (mean) steel properties were E=210GPa and f_y=590MPa. The observation of this table shows that, with a single exception (specimen CH1-5-800), all columns have almost coincident f_{crl} and f_{crd} values, *i.e.*, experience "true" L-D interaction for all slenderness values. Figs. 17(a)-(b) plot f_{Exp}/f_{MNDL} and f_{Exp}/f_{NDL} against the distortional slenderness (almost coincident with the local one, since R_{DL}≈1.0). It is clear that the f_{MNDL} values predict very accurately the four experimental failure loads (mean and standard deviation equal to 1.00 and 0.04), which provides experimental confirmation for the fact that, as mentioned in sections 5.1 and 5.2, the predictions of the MNDL approach (developed specifically for columns exhibiting strong "true" L-D interaction) correlate very well with the numerical failure loads. On the other hand, the f_{NDL} values heavily underestimate the above four experimental failure loads (mean and standard deviation equal to 1.46 and 0.15).

Finally, the "single" CH1-5-800 specimen is affected by L-D interaction caused by a "secondary local bifurcation", since R_{DL} is much lower than 1.0 (0.61) and R_y is very high (7.13). For this column all the conclusions drawn in section 5.1 and illustrated in Fig. 12(b_2) apply: (i) the NDL estimate is very conservative (f_{Exp}/f_{ndl}=1.70) and the most accurate prediction is provided by the distortional strength curve (f_{Exp}/f_{nd}=1.13), which is not surprising because D deformations govern the column collapse.

---

[8] In a few cases, the authors of the experimental investigations reported (i) distortional failures (tests T1.9-MS-4, T2.4-HSS-(1 to 6) of Young *et al.* 2013), (ii) flexural-torsional failures (tests T1.9-MS-8, T2.4-MS-1 of Young *et al.* 2013, and test A-8-2-800 of Kwon *et al.* 2009), (ii_3) local-flexural-torsional interactive failures (tests A-6-1-800, A-6-1-1000, A-6-1-1200, A-8-1-800, A-8-1-1000, A-8-1-1200, A-8-2-1000, A-8-2-1200 of Kwon *et al.* 2009), and (ii_4) one local-distortional-global (flexural-torsional) interactive failure (test T1.0-HSS-3 of Young *et al.* 2013) – note that the original specimen labels are kept in this paper.

Table 3: Results concerning the tests carried out by Kwon & Hancock (1992): critical buckling stresses, experimental ultimate stresses and observed failure modes, and DSM ultimate strength predictions (stresses in MPa)

Specimen	f_y	f_{crl}	f_{crd}	f_{crg}	R_{DL}	Experimental		ND		NDL		MNDL			
						f_{Exp}	Failure	f_{nd}	f_{Exp}/f_{nd}	f_{ndl}	f_{Exp}/f_{ndl}	L_{crd}	L_{crl}	L_{crd}/L_{crl}	f_{exp}/f_{mndl}
CH1-5-800	590	82.8	50.6	3709	0.61	148	L+D	130.4	1.13	86.7	1.70	460	110	4.2	1.17
CH1-6-800	590	78.8	67.6	3769	0.86	147	L+D	154.2	0.96	100.3	1.47	520	110	4.7	1.03
CH1-7-400	590	83.1	83.1	15438	1.00	160	L+D	173.6	0.92	112.7	1.42	570	110	5.2	1.04
CH1-7-600	590	81.7	86.7	6824	1.06	156	L+D	177.9	0.88	114.8	1.36	560	110	5.1	0.98
CH1-7-800	590	81.0	82.5	3844	1.02	150	L+D	172.9	0.86	111.7	1.34	560	110	5.1	0.97

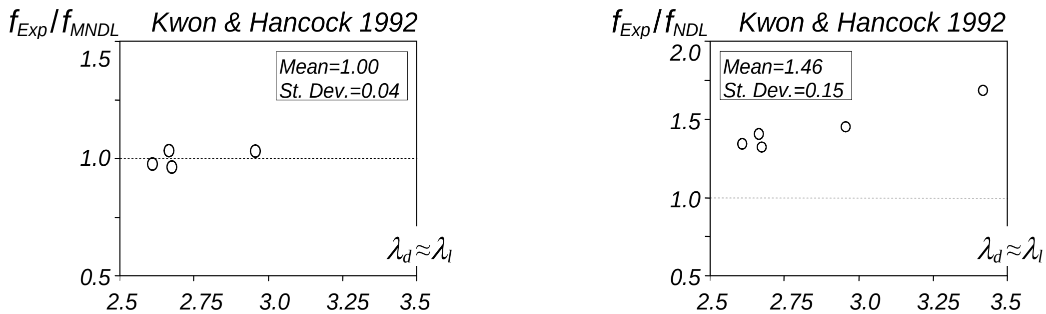

(a) (b)

Figure 17: Tests of Kwon & Hancock (1992): plots of the ratios (a) f_{Exp}/f_{mndl} and (b) f_{Exp}/f_{ndl} against λ_d

5.4.2 Loughlan et al. (2012)

Table 4 concerns the tests reported by Loughlan *et al.* (2012) and gives the specimen (i) critical buckling stresses (f_{crl}, f_{crd}, f_{crg}), (ii) R_{DL} and R_y values, (iii) experimental ultimate stresses (f_{Exp}), (iv) their estimates yielded by the NL and NDL approaches and (v) the corresponding experimental-to-predicted ultimate

Table 4: Results concerning the tests carried out by Loughlan *et al.* (2012): critical buckling stresses, experimental ultimate stresses and observed failure modes, and DSM ultimate strength predictions (stresses in MPa)

Specimen	f_y	f_{crl}	f_{crd}	f_{crg}	R_{DL}	R_y	Experimental		λ_l	NL		NDL	
							f_{Exp}	Failure		f_{nl}	f_{Exp}/f_{nl}	f_{ndl}	f_{Exp}/f_{ndl}
1-1000	209	28.9	127.8	3177	4.42	1.64	101.0	L+D	2.69	88.3	1.14	75.8	1.33
1-1200	209	28.5	122.5	2207	4.30	1.71	100.5	L+D	2.71	87.8	1.14	74.5	1.35
1-1400	209	28.8	106.5	1622	3.70	1.96	99.4	L+D	2.69	88.2	1.13	71.1	1.40
1-1600	209	28.8	99.5	1243	3.45	2.10	99.9	L+D	2.69	88.2	1.13	69.3	1.44
1-1800	209	28.8	97.6	983	3.39	2.14	91.5	L+D	2.69	88.2	1.04	68.8	1.33
2-1000	209	39.8	150.1	2461	3.77	1.39	107.3	L+D	2.29	99.3	1.08	86.5	1.24
2-1200	209	39.8	127.7	1710	3.21	1.64	102.1	L+D	2.29	99.3	1.03	81.9	1.25
2-1400	209	39.8	119.6	1257	3.01	1.75	108.8	L+D	2.29	99.3	1.10	80.0	1.36
2-1600	209	39.6	118.4	964	2.99	1.77	106.6	L+D	2.30	99.2	1.08	79.6	1.34
2-1800	209	39.4	111.9	762	2.84	1.87	108.8	L+D	2.30	99.0	1.10	77.9	1.40
3-1000	209	56.2	150.5	1803	2.68	1.39	127.1	L+D	1.93	112.6	1.13	94.2	1.35
3-1200	209	56.3	143.5	1254	2.55	1.46	128.9	L+D	1.93	112.7	1.14	92.6	1.39
3-1400	209	55.8	136.9	923	2.45	1.53	126.4	L+D	1.94	112.3	1.13	90.9	1.39
3-1600	209	55.2	132.4	708	2.40	1.58	114.3	L+D	1.95	111.9	1.02	89.6	1.28
3-1800	209	55.2	130.8	560	2.37	1.60	124.1	L+D	1.95	111.9	1.11	89.1	1.39
4-1000	209	85.1	222.8	1681	2.62	0.94	123.8	L+D	1.57	130.6	0.95	118.0	1.05
4-1200	209	84.4	194.3	1168	2.30	1.08	135.9	L+D	1.57	130.2	1.04	113.0	1.20
4-1400	209	84.2	176.2	859	2.09	1.19	123.8	L+D	1.58	130.1	0.95	109.3	1.13
4-1600	209	83.8	171.0	659	2.04	1.22	134.4	L+D	1.58	129.9	1.03	108.0	1.24
4-1800	209	83.7	166.0	521	1.98	1.26	120.7	L+D	1.58	129.9	0.93	106.9	1.13

stress ratios – the measured (mean) steel properties were $E=193GPa$ and $f_y=209MPa$. The observation of this table shows that these experimental are clearly different from those reported by Kwon & Hancock (1992), since the local buckling stresses are now always critical and significantly below their distortional counterparts ($1.98<R_{DL}<4.42$). This is not surprising since the authors mention that the purpose of this experimental investigation, conducted about 25 years ago, was to assess the influence of local buckling on the compressive strength of fixed-ended C columns. In the light of the numerical findings of sections 4.2 and 5.1, it can be concluded that the tested specimens either fail in local modes or experience L-D interaction due to a "secondary D bifurcation" [9]. It is worth noting that only the last four specimens (4-1200, 4-1400, 4-1600 and 4-1800) exhibit combinations of R_{DL} and λ_l values matching those dealt with in the numerical investigation presented in section 5.1 (see Figs. 11(a_3)-(a_4)) – all the remaining specimens have significantly higher R_{DL} and/or λ_l values.

With one exception, all column critical distortional buckling stresses are below the yield stress – R_y varies between 1.08 and 2.14 (R_y=0.94 for the exception – specimen 4-1000). In view of the high R_{DL} values ($R_{DL}\geq1.98$, *i.e.*, outside the range covered by the DSM-based MNDL design approach), the columns tested would be expected to fail either in local modes (lower R_y values) or in L-D interactive modes stemming from a "secondary D bifurcation" (higher R_y values). This assertion is confirmed by looking at Figs. 18(a)-(b), where the f_{Exp}/f_{NL} and f_{Exp}/f_{NDL} ultimate stress ratios are plotted against the column local slenderness. It is observed that (i) the f_{NL} values provide fairly good ultimate strength estimates (f_{Exp}/f_{NL} mean value and standard deviation equal to 1.07 and 0.07, and only three overestimations) and (ii) the f_{NDL} values considerably underestimate the experimental failure loads (f_{Exp}/f_{NL} mean value and standard deviation equal to 1.30 and 0.11, and no overestimation).

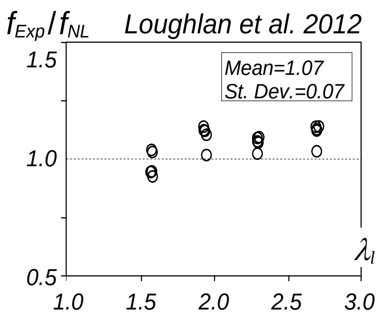

(a)

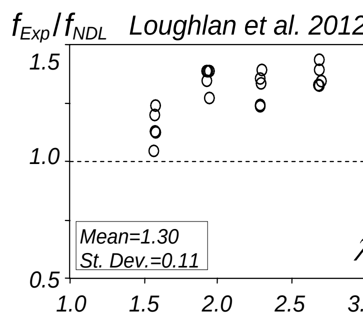

(b)

Figure 18: Tests of Loughlan *et al*. (2012): plots of the ratios (a) f_{Exp}/f_{nl} and (b) f_{Exp}/f_{ndl} against λ_l

5.4.3 Kwon et al (2009), Young et al. (2013) and Dinis et al. (2013a)

Table 5 concerns the last set of experimental data, namely the tests carried out by Kwon *et al.* (2009)[10], (specimens A), Young *et al.* (2013) (specimens T) and Dinis *et al.* (2013a) (specimens RS). It gives the (i) critical buckling stresses (f_{crl}, f_{crd}, f_{crg}), (ii) R_{DL} and R_y values, (iii) experimental ultimate stresses (f_{Exp}), (iv) their estimates yielded by the NDL and MNDL DSM approaches, and (v) the corresponding experimental-to-predicted ultimate stress ratios.

[9] In the opinion of Young *et al*. (2013), which is shared by the authors, local failures were wrongly interpreted as L-D interactive failures, due to the fact that "distortional deformations" suddenly appear at collapse. They are triggered by severe yielding at the web-flange junctions, caused by the normal stress redistribution stemming from the heavy local deformations, and do not originate on the emergence of distortional buckling effects.

[10] Note that the specimens A-6-1-400, A-6-2-1000, A-8-2-400 were excluded from these data because they have webs and flanges with the same width, *i.e.*, exhibit flange-triggered L-D interaction (situation not covered in this work).

Table 5: Results concerning the tests of Kwon *et al* (2009), Young *et al* (2013), Dinis *et al.* (2013a): critical buckling stresses, experimental ultimate stresses and observed failure modes, and DSM ultimate strength predictions (stresses in MPa)

Specimen	f_y	f_{crl}	f_{crd}	f_{crg}	R_{DL}	R_y	Experimental		NDL		MNDL			
							f_{Exp}	Failure	f_{ndl}	f_{Exp}/f_{ndl}	L_{crd}	L_{crl}	L_{crd}/L_{crl}	f_{Exp}/f_{mndl}
T1.0-HSS-1	536	82.5	148.8	348	1.80	3.6	140.8	L+D	144.9	0.97	980	100	9.8	-
T1.0-HSS-2	536	90.4	156.1	335	1.73	3.4	146.0	L+D	150.9	0.97	980	90	10.9	-
T1.2-HSS-1	588	60.7	105.2	2104	1.73	5.6	126.3	L+D	119.3	1.06	1200	140	8.6	-
T1.2-HSS-2	588	60.9	116.7	2122	1.92	5.0	131.2	L+D	125.6	1.04	1250	140	8.9	-
T1.2-HSS-3	588	54.7	96.3	2173	1.76	6.1	121.6	L+D	112.0	1.09	1300	150	8.7	-
T1.5-HSS-1	494	175.1	321.9	1789	1.84	1.5	248.0	L+D	228.4	1.09	850	100	8.5	-
T1.5-HSS-2	494	153.6	303.1	1973	1.97	1.6	229.6	L+D	216.8	1.06	860	110	7.8	-
T1.5-HSS-2R	494	156.9	310.6	1984	1.98	1.6	228.7	L+D	219.9	1.04	860	110	7.8	-
T1.5-HSS-3	494	45.1	82.4	2220	1.83	6.0	101.2	L+D	94.7	1.07	1750	200	8.8	-
T1.5-HSS-4	494	44.1	94.5	2272	2.14	5.2	104.0	L+D	100.7	1.03	1850	200	9.3	-
T1.9-MS-1	336	114.3	280.7	5112	2.46	1.2	171.0	L+D	168.2	1.02	1200	160	7.5	-
T1.9-MS-2	336	113.4	307.4	5162	2.71	1.1	173.9	L+D	172.8	1.01	1200	160	7.5	-
T1.9-MS-3	336	117.0	273.3	5302	2.34	1.2	157.5	L+D	167.7	0.94	1250	160	7.8	-
T1.9-MS-5	336	255.1	470.7	1004	1.85	0.7	237.4	L+D	238.9	0.99	1300	120	10.8	-
T1.9-MS-6	336	66.4	132.6	2475	2.00	2.5	110.2	L+D	111.7	0.99	1600	210	7.6	-
T1.9-MS-7	336	65.5	147.0	2500	2.24	2.3	112.4	L+D	116.3	0.97	1650	210	7.9	-
RS-1	500	233.0	318.9	493	1.37	1.6	259	L+D	262	0.99	590	60	9.8	0.99
RS-2	500	196.3	265.4	394	1.35	1.9	218	L+D	234	0.93	700	60	11.7	0.93
RS-3	500	166.8	244.1	357	1.46	2.0	210	L+D	218	0.96	760	70	10.9	0.96
RS-4-1	464	153.0	214.9	311	1.40	2.2	184	L+D	202	0.91	820	70	11.7	0.91
RS-4-2	500	147.8	213.8	305	1.45	2.3	185	L+D	201	0.92	830	70	11.9	0.92
RS-5	550	244.3	320.1	490	1.31	1.7	257	L+D	260	0.99	700	70	10.0	0.99
RS-6	550	214.0	296.0	454	1.38	1.9	239	L+D	245	0.98	770	70	11.0	0.98
RS-7	550	200.1	262.4	391	1.31	2.1	213	L+D	229	0.93	850	80	10.6	0.93
RS-8-1	550	172.7	227.3	315	1.32	2.4	197	L+D	209	0.94	900	80	11.3	0.94
RS-8-2	550	165.6	225.3	314	1.36	2.4	198	L+D	206	0.96	920	80	11.5	0.96
A-8-1-400	671	232.5	585.1	3378	2.52	1.2	334	L+D	334	1.00	380	45	8.4	0.65
A-8-3-1000	671	99.6	256.1	1021	2.57	2.6	209	L+D	203	1.03	410	65	6.3	0.81
A-8-4-1000	671	99.0	132.8	878	1.34	5.1	166	L+D	150	1.11	250	60	4.2	0.75

First of all, note that all column specimens tested buckle in critical L modes (R_{DL}>1.0). Then, it is also observed that (i) all C column specimens tested by Young *et al.* (2013) and (ii) two of the three C column specimens tested by Kwon *et al.* (2009) exhibit R_{DL} values falling outside the domain of application of the MNDL approach (0.70<R_{DL}<1.60), defined in sections 5-1 and 5.2 – indeed, they are in the range 1.73≤R_{DL}≤2.71. Conversely, (i) the remaining C column specimen tested by Kwon *et al.* (2009) and (ii) all R column specimens tested by Dinis *et al*. (2013a) fall inside the above domain of application (1.31≤R_{DL}≤1.46). Concerning the R_y values, decisive for the possible occurrence of L-D interaction caused by a "secondary D bifurcation", they are in the intervals 1.2<R_y<5.1 (Kwon *et al.* 2009), 0.7<R_y<6.1 (Young *et al.* 2013) and 1.6<R_y<2.4 (Dinis *et al.* 2013a). Only one specimen tested by Young *et al.* (2013) (T1.9-MS-6) has R_y below 1.1 – probably, its observed L-D interactive failure mode is a "disguised local failure mode" (like in most of the specimens tested by Loughlan *et al.* 2012).

Figs. 19(a)-(c) plot the f_{Exp}/f_{NDL} values against the local slenderness from the three sets of tests. Note that all the columns eligible for the application of the MNDL design approach[11] have L_{crd}/L_{crl} values higher than 8.0, which means that the f_{MNDL} and f_{NDL} estimates coincide. It is observed that the f_{NDL} values predict

[11] Recall that it was shown, in sections 5.1 and 5.2, that the MNDL approach is only valid within the 0.70<R_{DL}<1.60 range.

quite satisfactorily the three sets of test results considered: the mean and standard deviations of the f_{Exp}/f_{NDL} ratios are equal to (i) 1.02 and 0.05 (Young *et al.* 2013a), (ii) 1.05 and 0.05 (Kwon *et al.* 2009) and (iii) 0.95 and 0.03 (Dinis *et al.* 2013a). The slight overestimations of the R column predictions are most certainly due to the fact that most of these columns exhibit critical global buckling stresses visibly below the yield stress ($0.57<f_{crg}/f_y<0.99$), which implies the occurrence of non-negligible interaction with global buckling – naturally, the added ultimate strength erosion is not captured by the NDL approach.

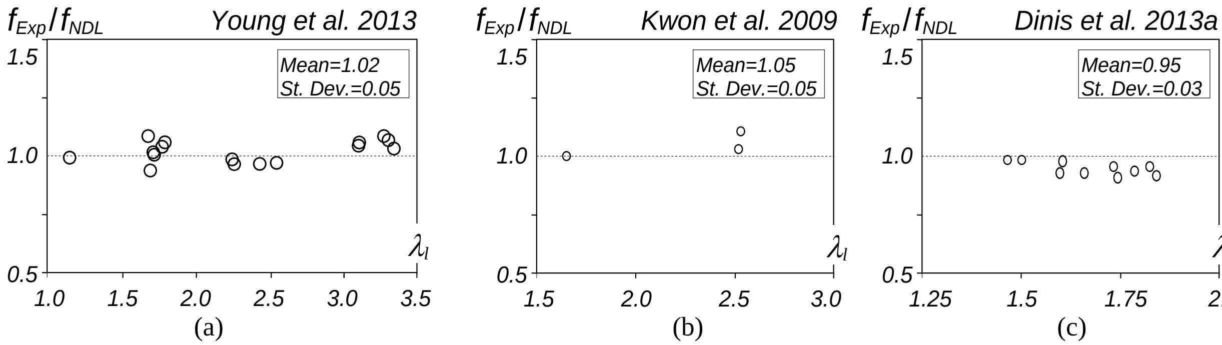

Figure 19: Tests of Kwon *et al.* (2009), Young *et al.* (2013) and Dinis *et al.* (2013a): plots of the ratios f_{Exp}/f_{ndl} against λ_l

5.4.4 Summary

Finally, this section summarizes the findings of the previous ones and makes it possible to compare the full set of experimental column ultimate strengths available in the literature with their estimates provided by the NDL and MNDL DSM design approaches, *i.e.*, those that were specifically developed to capture the ultimate strength erosion due to L-D interaction. Figs. 20(a)-(b) plot the appropriate sets of f_{Exp}/f_{NDL} and f_{Exp}/f_{MNDL} ratios against the local slenderness – the use of the word "appropriate" means that (i) Fig. 20(a) includes all experimental results and (ii) Fig. 20(b) includes only the results concerning specimens with $0.70<R_{DL}<1.60$, *i.e.*, all tests of Kwon & Hancock (1992) and Dinis *et al.* (2013a), and specimen A-8-4-1000 from Kwon *et al.* (2009). The first plot clearly shows that the NDL approach provides generally safe predictions of the experimental failure loads (all the unsafe ones correspond to f_{Exp}/f_{NDL} values above 0.91), but a fair number of them are overly conservative – the overall f_{Exp}/f_{NDL} mean and standard deviation are equal to 1.15 and 0.19. As for the second plot, it evidences the quality of the f_{MNDL} estimates, reflected in the overall f_{Exp}/f_{MNDL} mean and standard deviation of 0.97 and 0.09 – note that the "negatively isolated" value concerns the single specimen tested by Kwon *et al.* (2009), whose removal would improve the above indicators to 0.98 and 0.07. It should still be recalled that a large fraction of the f_{MNDL} overestimations correspond to the R column tests reported by Dinis *et al.* (2013a), for which the closeness of the global buckling stress is certainly responsible for an added failure load erosion.

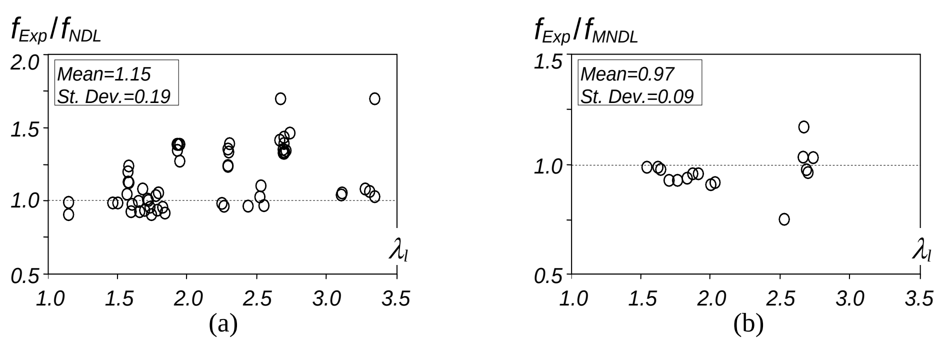

Figure 20: Experimental tests reported in the literature: plots of the ratios (a) f_{Exp}/f_{ndl} and (b) f_{Exp}/f_{mndl} against λ_l

6. Concluding Remarks

An extensive numerical investigation about the relevance of web-triggered L-D interaction effects on the post-buckling behavior, ultimate strength and DSM design of fixed-ended cold-formed steel plain lipped channel, hat-section, zed-section and rack-section columns was reported. All the columns analyzed had cross-section dimensions, lengths and yield stresses selected to ensure a wide variety of ratios between the (i) distortional and local critical buckling stresses (R_{DL}), and (ii) yield and non-critical buckling stresses (R_y). In order to prevent the occurrence of interaction phenomena involving global buckling, the column selection ensured that the global critical buckling stresses were (i) much larger than their distortional and local counterparts, and also (ii) higher than the maximum yield stress considered. ABAQUS geometrically and materially non-linear SFEA were employed to assess the structural response of columns (i) containing critical-mode initial imperfections with small amplitudes (10% of the wall thickness) and (ii) exhibiting a linear-elastic-perfectly-plastic constitutive law (typical of carbon steels) – residual stresses and corner strength effects were neglected, since they have been shown to have little impact on the ultimate strength of cold-formed steel columns.

The results obtained made it possible to reach preliminary conclusions concerning the identification of the combinations of the above stress ratios for which of web-triggered L-D interaction is relevant, in the sense that it erodes visibly the ultimate strength of C, H, Z and R columns and/or alters their failure mode characteristics. After providing numerical evidence about the presence or absence of L-D interaction, its influence on the ultimate strength erosion was assessed by comparing the numerical column failure loads with their estimates supplied by (i) the current DSM local (NL) and distortional (ND) strength curves, and (ii) two DSM-based design approaches specifically developed to estimate failure loads of columns affected by L-D interaction (NDL and MNDL – Schafer 2002 and Silvestre *et al.* 2012) – besides assessing the quality of the predictions, it was also possible to establish their domains of application. Next, the experimental results available in the literature on columns collapsing in web-triggered L-D modes, namely those reported by Kwon & Hancock (1992), Kwon *et al*. (2009), Loughlan *et al*. (2012), Young *et al*. (2013) and Dinis *et al.* (2013a), which consist of lipped channel (mostly) and rack-section columns, were used to assess the quality of the various DSM-based design approaches.

The numerical results presented and discussed in this work provided clear evidence that web-triggered cold-formed steel columns may be affected by two types of L-D interaction: (i) one due to the closeness between the local and distortional critical buckling stresses (R_{DL} in the vicinity of 1.0), characterized by the simultaneous presence of L and D deformations since the early loading stages and denoted as "true" L-D interaction, and (ii) the other caused by a "secondary (L or D) bifurcation", which occurs when the L and D critical buckling stresses are not so close and stems from the high (moderate) L (D) post-critical strength reserve strength – collapses must take place visibly below the yield stress, whose value plays a key role in this type of L-D interaction coupling (*e.g.*, it explains why L-D interaction was observed in the tests carried out by Young *et al.* 2013 and Dinis *et al.* 2013a, involving columns with R_{DL} values ranging from 1.73 to 2.71 and from 1.31 to 1.46, respectively). This investigation addressed also the determination of the minimum yield stresses required to enable the development of this second type of L-D interaction in C, H, Z and R columns exhibiting different R_{DL} values – enough "room" must be provided for L-D interaction to emerge and develop before yielding precipitates the column failure.

The DSM-based ultimate strength estimation confirmed what had already been concluded by other researchers, namely that the current DSM NL and ND strength curves cannot capture the ultimate strength erosion stemming from L-D interaction. However, the NDL and MNDL approaches were found to predict satisfactorily both the numerical and experimental ultimate strengths of columns experiencing web-triggered L-D interaction. While the former underestimates the vast majority of numerical and experimental ultimate strengths (often by a quite large amount), the latter yields quite accurate and mostly safe predictions for the numerical and experimental failure loads of C, H, Z, R columns with R_{DL} values comprised between 0.70 and 1.60. The ultimate strength erosion due to web-triggered L-D interaction was found to be more relevant in columns exhibiting "true" L-D interaction than in those undergoing "secondary (L or D) bifurcation" L-D effects (even when if local buckling precedes distortional buckling – the worst case). Although the available experimental failure loads were reasonably well estimated by the NDL and MNDL design, they do not cover all the important parameter ranges – therefore, additional carefully planned test programs need to be conducted, in order to completely clear the path leading to the codification of a DSM design approach for columns affected by L-D interaction. In particular, because the overwhelming majority of available test results concern columns with R_{DL} well above 1.0, the future tests must involve specimens with different cross-sections and R_{DL} values close to and/or quite below 1.0.

Since this paper dealt exclusively with columns exhibiting web-triggered local buckling, it must be complemented with similar work on columns undergoing flange-triggered local buckling, namely columns with "v-shaped" intermediate stiffeners and sigma-section columns – research on this subject is currently underway). Finally, taking advantages of the modal features of the Generalized Beam Theory (GBT) analyses, an in-depth investigation on the mechanics underlying the various local-distortional coupling phenomena is also planned for the near future.

Acknowledgements

The first and fourth authors gratefully acknowledge the financial support of FCT (*Fundacão para a Ciência e a Tecnologia* – Portugal), through the (i) doctoral scholarship SFRH/BD/87746/2012 and (ii) project grant Pest-C/EEI/UI0308/2011, respectively.

References

American Iron and Steel Institute (AISI) (2012), *North American Specification* (NAS) *for the Design of Cold-Formed Steel Structural Members* (AISI-S100-12), Washington DC.

Australian/New Zealand Standard (AS/NZS) (2005), *Cold-Formed Steel Structures* – AS/NZS 4600 (2nd edition), Sydney-Wellington.

Bebiano R, Pina P, Silvestre N, Camotim D (2008), *GBTUL 1.0β – Buckling and Vibration Analysis of Thin-Walled Members*, DECivil/IST, Technical University of Lisbon. (*http://www.civil.ist.utl.pt/gbt*)

Camotim D, Silvestre N, Dinis PB (2005) "Numerical analysis of cold-formed steel members", *International Journal of Steel Structures*, **5**(1), 63-78.

Camotim D, Dinis PB, Young B, Silvestre N (2013), "Local-distortional interaction in cold-formed steel columns: non-linear behaviour, ultimate strength and DSM design", *Proceedings of 5th International Conference of Structural Engineering, Mechanics and Computation* (SEMC 2013 – Cape Town, 2-4/9), A. Zingoni (ed.), Taylor & Francis (London), pp. 7-8. (full paper in CD-ROM Proceedings – 17-22)

Dinis PB, Camotim D (2006), "On the use of shell finite element analysis to assess the local buckling and post-buckling behaviour of cold-formed steel thin-walled members", *Book of Abstracts of III European Conference on Computational Mechanics: Solids, Structures and Coupled Problems in Engineering* (III ECCM – Lisboa, 5-9/6), C.A.M. Soares *et al.* (eds.) Springer, 689. (full paper in CD-ROM Proceedings).

Dinis PB, Camotim D (2010), "Local/distortional mode interaction in cold-formed steel lipped channel beams", *Thin-Walled Structures*, **48**(10-11), 771-785.

Dinis PB, Camotim D (2012), "Direct strength method to predict the resistance of cold-formed steel columns against local-distortional interactive failure", *Proceedings of 11th International Conference on Computational Structures Technology* (CST 2012 – Dubrovnik, 3-7/9), B. Topping (ed.), Civil-Comp Press (Stirling), Paper 30.

(full paper in USB Key Drive Proceedings)

Dinis PB, Camotim D (2013), "Cold-formed steel columns undergoing local-distortional coupling: behaviour and direct strength prediction against interactive failure", *submitted for publication*.

Dinis PB, Camotim D, Silvestre N (2007), "FEM-based analysis of the local-plate/distortional mode interaction in cold-formed steel lipped channel columns", *Computers & Structures,* **85**(19-20), 1461-1474.

Dinis PB, Silvestre N, Camotim D (2009), "On the relevance of local-distortional interaction in the post-buckling behaviour and strength of cold-formed steel lipped channel columns", *Proceedings of 12th International Conference on Civil, Structural and Environmental Engineering Computing* (CC 2009 – Funchal, 1-4/9) Civil-Comp Press (Stirling), Paper 12. (full paper in CD-ROM Proceedings)

Dinis PB, Camotim D, Fena R (2011), "Local/distortional mode interaction in hat-section columns: post-buckling behaviour, strength and DSM design", *Proceedings of 6th European Conference on Steel and Composite Structures*, (EUROSTEEL 2011 – Budapest, 31/8-2/9), 69-74.

Dinis PB, Camotim D, Fena R (2012b), "Post-buckling, strength and design of cold-formed steel lipped channel, zed-section and hat-section columns affected by local-distortional interaction", *USB Proceedings of SSRC Annual Stability Conference* (Grapevine – 18-21/4).

Dinis PB, Young B, Camotim D (2013a), "Local-distortional interaction in cold-formed steel rack-section columns", *Thin-Walled Structures,* in press.

Dinis PB, Young B, Camotim D (2013b) "Strength, interactive failure and design of web-stiffened lipped channel columns exhibiting distortional buckling", *Thin-Walled Structures,* in press.

Ellobody E, Young B (2005), "Behavior of cold-formed steel plain angle columns", *Journal of Structural Engineering* (ASCE), **131**(3), 457-466.

Hancock GJ, Kwon YB, Bernard ES (1994), "Strength design curves for thin-walled sections undergoing distortional buckling", *Journal of Constructional Steel Research,* **31**(2-3), 169-186.

Kwon YB, Hancock GJ (1992), "Tests of cold-formed channels with local and distortional buckling", *Journal of Structural Engineering* (ASCE), **118**(7), 1786-1803.

Kwon YB, Kim BS, Hancock GJ (2009), "Compression tests of high strength cold-formed steel channel with buckling interaction", *Journal of Constructional Steel Research,* **65**(2), 278-89.

Loughlan J, Yidris N, Jones K (2012), "The failure of thin-walled lipped channel compression members due to coupled local-distortional interactions and material yielding", *Thin-Walled Structures,* **61**(December), 14-21.

Martins AD, Dinis PB, Camotim D, Providência P (2013), "The relevance of local-distortional interaction effects in lipped channel columns", *Proceedings of 14th International Conference Civil, Structural and Environmental Engineering Computing* (CC 2013 – Cagliari, 3-6/9), B.H.V. Topping, P. Iványi (eds.), Civil-Comp Press (Stirling), Paper 8. (full paper in CD-ROM Proceedings)

Schafer BW (2002), "Local, distortional and Euler buckling in thin-walled columns", *Journal of Structural Engineering* (ASCE), **128**(3), 289-299.

Schafer BW (2008), "Review: the direct strength method of cold-formed steel member design" *Journal of Constructional Steel Research,* **64**(7-8), 766-778.

Schafer BW, Peköz T (1998a), "Computational modeling of cold-formed steel: characterizing geometric imperfections and residual stresses", *Journal of Constructional Steel Research,* **47**(3), 193-210.

Schafer BW, Peköz T (1998b), "Direct strength predition of cold-formed steel members using numerical elastic buckling solutions", *Thin-Walled Structures - Research and Development* (ICTWS'98 – Singapore, 2-4/12), N. Shanmugam, J.Y.R. Liew, V. Thevendran (eds.), Elsevier, 137-144.

Silvestre N, Camotim D (2003), "Non-linear generalized beam theory for cold-formed steel members", *International Journal of Structural Stability and Dynamics,* **3**(4), 461-490.

Silvestre N, Camotim D (2006), "Local-plate and distortional postbuckling behavior of cold-formed steel lipped channel columns with intermediate stiffeners", *Journal of Structural Engineering* (ASCE), **132**(4), 529-540.

Silvestre N, Dinis PB, Camotim D (2008), "DSM design of simply supported rack-section columns against local/distortional interactive buckling", *Proceedings of 5th International Conference on Coupled Instabilities in Metal Structures*, (CIMS 2008 – Sydney 23-25/6), K. Rasmussen, T. Wilkinson (eds.), 417-424.

Silvestre N, Camotim D, Dinis PB (2012), "Post-buckling behaviour and direct strength design of lipped channel columns experiencing local/distortional interaction", *Journal of Constructional Steel Research*, **73**(June), 12-30.

Simulia Inc. (2008), *ABAQUS Standard* (version 6.7-5).

Yang D, Hancock GJ (2004), "Compression tests of high strength steel channel columns with interaction between local and distortional buckling", *Journal of Structural Engineering* (ASCE), **130**(12), 1954-1963.

Yap DCY, Hancock GJ (2009), "Interaction of local and distortional modes in thin-walled sections", *Proceedings of 6th International Conference on Advances in Steel Structures* (ICASS'09 – Hong Kong, 16-18/12), S.L. Chan (ed.), 35-48.

Yap, D.C.Y., Hancock, G.J. (2011), "Experimental study of high strength cold-formed stiffened-web C-sections in compression", *Journal of Structural Engineering* (ASCE), vol. 137(2), pp. 162-72.

Yap DCY (2008), "Local and distortional buckling of high strength cold-formed steel section", Ph.D. Thesis, School of Civil Engineering, University of Sydney, Australia.

Young B, Rasmussen KJR (1999), "Shift of effective centroid in channel columns", *Journal of Structural Engineering* (ASCE), **125**(5), 524-531.

Young B, Silvestre N, Camotim D (2013), "Cold-formed steel lipped channel columns influenced by local-distortional interaction: strength and DSM design", *Journal of Structural Engineering* (ASCE), **139**(6), 1059-1074.

Zeinoddini VM, Schafer BW (2012), "Simulation of geometric imperfections in cold-formed steel members using spectral representation approach", *Thin-Walled Structures*, **60**(November), 14-21.

ANNEX A – LIPPED CHANNEL COLUMN RESULTS

Table A1: C columns: SFEA ultimate strengths and corresponding DSM estimates (dimensions in *mm*, stresses in *MPa*) – I

			SFEA	DSM			NDL			MNDL			
	λ_d	f_y	f_u	f_{nl}	f_{nd}	$\frac{f_{nd}}{f_u}$	λ_{dl}	f_{ndl}	$\frac{f_{ndl}}{f_u}$	f^*_{nl}	λ^*_{dl}	f_{mndl}	$\frac{f_{mndl}}{f_u}$
C1 (L_{crd}=675; L_{crl}=175)	1.00	74	60	74	55	0.92	1.00	55	0.92	74	1.00	55	0.92
	1.10	89	67	89	62	0.92	1.10	62	0.92	89	1.10	62	0.92
	1.25	115	77	113	71	0.93	1.24	70	0.92	115	1.25	71	0.93
	1.50	166	96	144	86	0.90	1.40	80	0.84	166	1.50	86	0.90
	1.75	226	115	177	101	0.88	1.55	89	0.78	226	1.75	101	0.88
	2.00	295	133	211	114	0.86	1.69	97	0.74	295	2.00	114	0.86
	2.50	461	163	283	141	0.86	1.96	112	0.69	461	2.50	141	0.86
	3.00	664	199	357	166	0.83	2.20	125	0.63	664	3.00	166	0.83
	3.25	779	217	395	178	0.82	2.32	131	0.60	779	3.25	178	0.82
	3.50	904	235	435	190	0.81	2.43	137	0.58	904	3.50	190	0.81
C2 (L_{crd}=575; L_{crl}=150)	1.00	116	96	116	87	0.91	1.00	87	0.91	116	1.00	87	0.91
	1.10	141	107	141	98	0.91	1.10	98	0.91	141	1.10	98	0.91
	1.25	182	125	170	112	0.90	1.21	108	0.87	182	1.25	112	0.90
	1.50	262	152	218	136	0.90	1.37	124	0.81	262	1.50	136	0.90
	1.75	356	179	267	159	0.89	1.51	138	0.77	356	1.75	159	0.89
	2.00	465	202	318	180	0.89	1.65	150	0.74	465	2.00	180	0.89
	2.50	727	251	425	222	0.88	1.91	173	0.69	727	2.50	222	0.88
	3.00	1047	302	536	261	0.87	2.15	193	0.64	1047	3.00	261	0.87
	3.25	1229	342	594	281	0.82	2.26	202	0.59	1229	3.25	281	0.82
	3.50	1425	369	652	299	0.81	2.37	211	0.57	1425	3.50	299	0.81
C3 (L_{crd}=575; L_{crl}=150)	1.00	118	97	118	88	0.91	1.00	88	0.91	118	1.00	88	0.91
	1.10	142	109	141	99	0.91	1.09	98	0.90	142	1.10	99	0.91
	1.25	184	127	167	114	0.90	1.19	108	0.85	184	1.25	114	0.90
	1.50	265	153	214	138	0.90	1.35	123	0.81	265	1.50	138	0.90
	1.75	360	182	262	161	0.88	1.49	137	0.76	360	1.75	161	0.88
	2.00	470	205	312	182	0.89	1.63	150	0.73	470	2.00	182	0.89
	2.50	735	253	417	224	0.89	1.88	172	0.68	735	2.50	224	0.89
	3.00	1058	308	526	264	0.86	2.11	192	0.63	1058	3.00	264	0.86
	3.25	1242	334	582	284	0.85	2.22	202	0.60	1242	3.25	284	0.85
	3.50	1441	361	639	303	0.84	2.33	211	0.58	1441	3.50	303	0.84
C4 (L_{crd}=625; L_{crl}=175)	1.00	119	97	119	89	0.92	1.00	89	0.92	119	1.00	89	0.92
	1.10	144	109	138	100	0.92	1.08	97	0.90	144	1.10	100	0.92
	1.25	186	128	164	115	0.90	1.17	107	0.84	186	1.25	115	0.90
	1.50	268	152	209	139	0.92	1.33	123	0.81	268	1.50	139	0.92
	1.75	365	179	257	162	0.91	1.47	136	0.76	365	1.75	162	0.91
	2.00	476	201	305	185	0.92	1.60	149	0.74	476	2.00	185	0.92
	2.50	744	249	407	227	0.91	1.85	171	0.69	744	2.50	227	0.91
	3.00	1072	302	513	268	0.89	2.08	191	0.63	1072	3.00	268	0.89
	3.25	1258	328	568	287	0.88	2.18	201	0.61	1258	3.25	287	0.88
	3.50	1458	354	624	306	0.87	2.29	210	0.59	1458	3.50	306	0.87
C5 (L_{crd}=575; L_{crl}=150)	1.00	118	96	116	88	0.92	1.00	88	0.92	118	1.00	88	0.92
	1.10	142	107	133	99	0.92	1.06	95	0.88	142	1.10	99	0.92
	1.25	184	126	158	114	0.91	1.16	104	0.83	184	1.25	114	0.91
	1.50	264	148	201	138	0.93	1.31	119	0.81	264	1.50	138	0.93
	1.75	360	171	246	160	0.94	1.45	133	0.78	360	1.75	160	0.94
	2.00	470	192	293	182	0.95	1.58	145	0.76	470	2.00	182	0.95
	2.50	735	238	390	224	0.94	1.82	167	0.70	735	2.50	224	0.94
	3.00	1058	300	491	264	0.88	2.04	186	0.62	1058	3.00	264	0.88
	3.25	1242	329	544	283	0.86	2.15	195	0.59	1242	3.25	283	0.86
	3.50	1440	357	597	302	0.85	2.25	204	0.57	1440	3.50	302	0.85
C6 (L_{crd}=475; L_{crl}=125)	1.00	110	90	106	82	0.92	0.98	81	0.90	110	1.00	82	0.92
	1.10	133	101	121	92	0.92	1.05	87	0.87	133	1.10	92	0.92
	1.25	172	117	144	106	0.91	1.14	96	0.82	172	1.25	106	0.91
	1.50	247	138	183	129	0.94	1.29	110	0.80	247	1.50	129	0.94
	1.75	337	151	224	150	1.00	1.43	122	0.81	337	1.75	150	1.00
	2.00	440	178	267	171	0.96	1.56	134	0.75	440	2.00	171	0.96
	2.50	687	223	355	210	0.94	1.80	154	0.69	687	2.50	210	0.94
	3.00	989	283	448	247	0.87	2.02	172	0.61	989	3.00	247	0.87
	3.25	1161	307	495	265	0.86	2.12	180	0.59	1161	3.25	265	0.86
	3.50	1347	330	544	283	0.86	2.22	188	0.57	1347	3.50	283	0.86

Table A2: C columns: SFEA ultimate strengths and corresponding DSM estimates (dimensions in *mm*, stresses in *MPa*) – II

			SFEA		DSM				NDL			MNDL		
	λ_l	f_y	$f_{u.D}$	$f_{u.L}$	f_{nl}	f_{nd}	$\frac{f_{nl}}{f_{u.D}}$	$\frac{f_{nl}}{f_{u.L}}$	f_{ndl}	$\frac{f_{ndl}}{f_{u.D}}$	$\frac{f_{ndl}}{f_{u.L}}$	f_{mndl}	$\frac{f_{mndl}}{f_{u.D}}$	$\frac{f_{mndl}}{f_{u.L}}$
C11 (L_{crd}=480; L_{crl}=100)	1.00	189	152	158	160	143	1.06	1.02	129	0.85	0.82	143	0.94	0.90
	1.10	228	170	177	182	160	1.08	1.03	140	0.83	0.79	160	0.94	0.90
	1.25	295	194	200	216	185	1.12	1.08	155	0.80	0.78	185	0.95	0.93
	1.50	425	223	227	274	224	1.23	1.21	177	0.79	0.78	224	1.00	0.99
	1.75	578	249	259	334	261	1.34	1.29	197	0.79	0.76	248	1.00	0.96
	2.00	755	*	295	396	297	*	1.34	216	*	0.73	281	*	0.95
	2.50	1180	*	372	526	365	*	1.41	249	*	0.67	343	*	0.92
	3.00	1699	*	449	661	430	*	1.47	279	*	0.62	403	*	0.90
	3.25	1994	*	487	731	462	*	1.50	292	*	0.60	431	*	0.89
	3.50	2312	*	525	802	493	*	1.53	305	*	0.58	459	*	0.88
C15 (L_{crd}=530; L_{crl}=100)	1.00	127	109	110	108	105	0.99	0.98	94	0.87	0.86	105	0.97	0.95
	1.10	153	122	125	122	118	1.00	0.98	103	0.84	0.82	118	0.97	0.95
	1.25	198	141	144	145	138	1.03	1.01	114	0.81	0.79	138	0.98	0.96
	1.50	285	161	170	184	168	1.14	1.08	132	0.82	0.78	168	1.05	0.99
	1.75	388	173	186	224	197	1.30	1.21	148	0.85	0.79	183	1.06	0.98
	2.00	507	196	208	266	225	1.36	1.28	162	0.83	0.78	207	1.06	1.00
	2.50	792	242	262	353	279	1.46	1.35	188	0.78	0.72	254	1.05	0.97
	3.00	1140	291	317	444	329	1.53	1.40	211	0.73	0.67	298	1.02	0.94
	3.25	1338	316	344	491	354	1.56	1.43	222	0.70	0.65	319	1.01	0.93
	3.50	1552	340	371	538	378	1.59	1.45	232	0.68	0.63	340	1.00	0.92
C19 (L_{crd}=570; L_{crl}=100)	1.00	92	83	82	78	81	0.94	0.96	72	0.86	0.88	81	0.97	0.99
	1.10	111	94	93	89	91	0.95	0.96	79	0.84	0.85	91	0.97	0.98
	1.25	144	108	109	105	107	0.98	0.97	88	0.82	0.81	107	1.00	0.99
	1.50	207	127	130	134	132	1.06	1.03	102	0.81	0.79	132	1.04	1.01
	1.75	282	140	141	163	155	1.17	1.16	115	0.83	0.82	155	1.11	1.11
	2.00	368	152	147	193	178	1.27	1.32	127	0.84	0.87	159	1.04	1.08
	2.50	575	188	182	257	221	1.37	1.41	148	0.79	0.82	194	1.04	1.07
	3.00	829	227	221	323	262	1.42	1.46	167	0.73	0.75	228	1.00	1.03
	3.25	972	247	241	357	282	1.45	1.48	175	0.71	0.73	244	0.99	1.01
	3.50	1128	266	260	391	301	1.47	1.51	183	0.69	0.71	260	0.98	1.00

* Due to numerical difficulties, no ultimate strength could be obtained for these columns.

ANNEX B – HAT-SECTION AND ZED-SECTION COLUMN RESULTS

Table B1: H and Z columns: SFEA ultimate strengths and corresponding DSM estimates (dimensions in *mm*, stresses in *MPa*) – I

			SFEA		DSM			NDL				MNDL				
	λ_d	f_y	f_u^H	f_u^Z	f_{nd}	$\frac{f_{nd}}{f_u^H}$	$\frac{f_{nd}}{f_u^Z}$	λ_{dl}	f_{ndl}	$\frac{f_{ndl}}{f_u^H}$	$\frac{f_{ndl}}{f_u^Z}$	f_{nl}^*	λ_{dl}^*	f_{mndl}	$\frac{f_{mndl}}{f_u^H}$	$\frac{f_{mndl}}{f_u^Z}$
C1 (L_{crd}=675; L_{crl}=175)	1.00	74	60	61	55	0.92	0.91	1.00	55	0.92	0.91	74	1.00	55	0.92	0.91
	1.10	89	67	68	62	0.93	0.92	1.10	62	0.93	0.92	89	1.10	62	0.93	0.92
	1.25	115	78	78	71	0.92	0.92	1.23	70	0.91	0.92	115	1.25	71	0.92	0.92
	1.50	166	100	98	86	0.87	0.88	1.40	80	0.81	0.83	166	1.50	86	0.87	0.88
	1.75	226	119	119	101	0.85	0.85	1.55	89	0.75	0.76	226	1.75	101	0.85	0.85
	2.00	295	135	136	115	0.85	0.84	1.69	97	0.72	0.73	295	2.00	115	0.85	0.84
	2.50	460	165	173	141	0.85	0.82	1.95	112	0.68	0.66	460	2.50	141	0.85	0.82
	3.00	663	204	204	166	0.82	0.81	2.20	125	0.62	0.62	663	2.99	166	0.82	0.81
	3.25	778	214	223	178	0.83	0.80	2.31	131	0.61	0.60	778	3.24	178	0.83	0.80
	3.50	902	231	241	190	0.82	0.79	2.42	137	0.59	0.57	902	3.49	190	0.82	0.79
C2 (L_{crd}=575; L_{crl}=150)	1.00	116	96	97	87	0.91	0.90	1.00	87	0.91	0.90	116	1.00	87	0.91	0.90
	1.10	141	107	109	98	0.91	0.89	1.10	98	0.91	0.89	141	1.10	98	0.91	0.89
	1.25	182	125	125	113	0.90	0.90	1.21	109	0.87	0.87	182	1.25	113	0.90	0.90
	1.50	262	160	156	137	0.85	0.87	1.36	124	0.78	0.79	262	1.50	137	0.85	0.87
	1.75	357	187	186	159	0.85	0.85	1.51	138	0.74	0.74	357	1.75	159	0.85	0.85
	2.00	466	204	207	181	0.89	0.87	1.65	151	0.74	0.73	466	2.00	181	0.89	0.87
	2.50	728	258	251	223	0.86	0.88	1.90	173	0.67	0.69	728	2.49	223	0.86	0.88
	3.00	1048	312	317	262	0.84	0.82	2.14	193	0.62	0.61	1048	2.99	262	0.84	0.82
	3.25	1230	340	345	281	0.83	0.81	2.25	203	0.60	0.59	1230	3.24	281	0.83	0.81
	3.50	1426	366	371	300	0.82	0.81	2.36	212	0.58	0.57	1426	3.49	300	0.82	0.81
C3 (L_{crd}=575; L_{crl}=150)	1.00	118	97	99	88	0.92	0.89	1.00	88	0.92	0.89	118	1.00	88	0.92	0.89
	1.10	142	108	110	99	0.92	0.90	1.09	98	0.91	0.89	142	1.10	99	0.92	0.90
	1.25	184	127	127	114	0.90	0.90	1.19	108	0.86	0.85	184	1.25	114	0.90	0.90
	1.50	265	162	158	138	0.85	0.87	1.35	124	0.76	0.78	265	1.50	138	0.85	0.87
	1.75	360	190	190	161	0.85	0.85	1.49	138	0.72	0.72	360	1.75	161	0.85	0.85
	2.00	471	210	210	183	0.87	0.87	1.63	150	0.72	0.71	471	2.00	183	0.87	0.87
	2.50	736	262	259	225	0.86	0.87	1.88	173	0.66	0.67	736	2.49	225	0.86	0.87
	3.00	1059	318	316	265	0.83	0.84	2.11	193	0.61	0.61	1059	2.99	265	0.83	0.84
	3.25	1243	346	351	285	0.82	0.81	2.22	202	0.59	0.57	1243	3.24	285	0.82	0.81
	3.50	1442	373	379	304	0.81	0.80	2.33	211	0.57	0.56	1442	3.49	304	0.81	0.80
C4 (L_{crd}=625; L_{crl}=175)	1.00	119	97	99	90	0.92	0.90	1.00	90	0.92	0.90	119	1.00	90	0.92	0.90
	1.10	144	109	111	100	0.92	0.90	1.07	98	0.90	0.88	144	1.10	100	0.92	0.90
	1.25	186	127	127	115	0.91	0.91	1.17	108	0.85	0.85	186	1.25	115	0.91	0.91
	1.50	268	162	157	140	0.86	0.89	1.32	123	0.76	0.78	268	1.50	140	0.86	0.89
	1.75	365	189	188	163	0.86	0.87	1.47	137	0.73	0.73	365	1.75	163	0.86	0.87
	2.00	477	206	206	185	0.90	0.90	1.60	150	0.73	0.72	477	1.99	185	0.90	0.90
	2.50	745	256	254	228	0.89	0.89	1.85	172	0.67	0.67	745	2.49	228	0.89	0.89
	3.00	1072	312	305	269	0.86	0.88	2.07	192	0.62	0.63	1072	2.99	269	0.86	0.88
	3.25	1258	339	344	288	0.85	0.83	2.18	202	0.60	0.58	1258	3.24	288	0.85	0.83
	3.50	1459	365	371	307	0.84	0.83	2.29	210	0.58	0.57	1459	3.49	307	0.84	0.83
C5 (L_{crd}=575; L_{crl}=150)	1.00	118	96	98	89	0.93	0.90	0.99	88	0.92	0.90	118	1.00	89	0.93	0.90
	1.10	143	107	109	99	0.93	0.90	1.06	95	0.89	0.87	143	1.10	99	0.93	0.90
	1.25	184	125	125	114	0.92	0.91	1.16	105	0.84	0.84	184	1.25	114	0.92	0.91
	1.50	266	156	153	138	0.89	0.90	1.31	120	0.77	0.78	266	1.50	138	0.89	0.90
	1.75	361	177	177	161	0.91	0.91	1.44	133	0.76	0.75	361	1.75	161	0.91	0.91
	2.00	472	193	195	184	0.95	0.93	1.57	146	0.76	0.74	472	2.00	184	0.95	0.93
	2.50	738	244	223	226	0.93	1.01	1.82	168	0.69	0.75	738	2.50	226	0.93	1.01
	3.00	1062	299	303	266	0.89	0.87	2.04	187	0.63	0.62	1062	2.99	266	0.89	0.87
	3.25	1247	325	329	285	0.88	0.86	2.15	197	0.60	0.59	1247	3.24	285	0.88	0.86
	3.50	1446	350	354	304	0.87	0.85	2.25	205	0.59	0.58	1446	3.49	304	0.87	0.85
C6 (L_{crd}=475; L_{crl}=125)	1.00	111	90	92	83	0.93	0.90	0.98	82	0.91	0.89	111	1.00	83	0.93	0.90
	1.10	134	100	103	93	0.93	0.90	1.05	88	0.88	0.86	134	1.10	93	0.93	0.90
	1.25	174	117	116	107	0.92	0.92	1.14	97	0.84	0.84	174	1.25	107	0.92	0.92
	1.50	250	143	142	130	0.91	0.91	1.29	111	0.78	0.78	250	1.50	130	0.91	0.91
	1.75	340	161	163	152	0.95	0.92	1.43	124	0.77	0.75	340	1.75	152	0.95	0.92
	2.00	444	178	181	173	0.97	0.95	1.56	135	0.76	0.74	444	2.00	173	0.97	0.95
	2.50	694	227	217	212	0.93	0.97	1.79	156	0.69	0.72	694	2.50	212	0.93	0.97
	3.00	999	277	284	250	0.90	0.87	2.01	174	0.63	0.61	999	3.00	250	0.90	0.87
	3.25	1173	305	303	268	0.88	0.88	2.12	182	0.60	0.60	1173	3.25	268	0.88	0.88
	3.50	1360	329	331	286	0.87	0.86	2.22	190	0.58	0.57	1360	3.50	286	0.87	0.86
C7 (L_{crd}=525; L_{crl}=110)	1.00	183	143	145	138	0.96	0.94	0.97	134	0.94	0.92	183	0.99	138	0.96	0.94
	1.10	221	160	161	154	0.96	0.95	1.04	145	0.91	0.89	221	1.09	154	0.96	0.95
	1.25	286	187	184	178	0.95	0.96	1.13	160	0.86	0.86	284	1.24	178	0.95	0.96
	1.50	412	228	226	216	0.95	0,95	1.28	183	0.80	0.80	407	1.48	214	0.94	0.92
	1.75	560	259	258	251	0.97	0.97	1.41	204	0.79	0.78	552	1.73	250	0.96	0.93
	2.00	732	293	291	286	0.98	0.97	1.54	223	0.76	0.76	720	1.97	284	0.97	0.94
	2.50	1144	368	366	352	0.96	0.95	1.77	256	0.70	0.69	1120	2.46	348	0.95	0.91
	3.00	1647	447	443	414	0.93	0.93	1.99	286	0.64	0.64	1609	2.95	410	0.92	0.88
	3.25	1933	483	480	444	0.92	0.92	2.10	300	0.62	0.62	1886	3.19	440	0.91	0.87
	3.50	2242	519	517	474	0.91	0.91	2.20	314	0.60	0.60	2185	3.43	469	0.90	0.86

Table B2: H and Z columns: SFEA ultimate strengths and corresponding DSM estimates (dimensions in *mm*, stresses in *MPa*) – II

			SFEA		DSM			NDL				MNDL				
	λ_d	f_y	f_u^H	f_u^Z	f_{nd}	$\frac{f_{nd}}{f_u^H}$	$\frac{f_{nd}}{f_u^Z}$	λ_{dl}	f_{ndl}	$\frac{f_{ndl}}{f_u^H}$	$\frac{f_{ndl}}{f_u^Z}$	f_{nl}^*	λ_{dl}^*	f_{mndl}	$\frac{f_{mndl}}{f_u^H}$	$\frac{f_{mndl}}{f_u^Z}$
C8 (L_{crd}=575; L_{crl}=125)	1.00	150	119	121	113	0.95	0.93	0.96	107	0.90	0.88	147	0.99	113	0.95	0.93
	1.10	181	129	133	126	0.98	0.94	1.02	116	0.90	0.87	175	1.08	126	0.98	0.94
	1.25	234	146	146	145	0.99	0.99	1.11	128	0.88	0.87	222	1.21	145	0.99	0.99
	1.50	337	175	173	176	1.01	1.01	1.25	146	0.84	0.84	312	1.44	169	0.97	0.99
	1.75	459	199	198	205	1.03	1.03	1.39	163	0.82	0.82	417	1.66	196	0.98	1.00
	2.00	599	228	*	233	1.02	*	1.51	178	0.78	*	536	1.89	221	0.97	*
	2.50	937	291	292	287	0.99	0.98	1.74	205	0.70	0.70	817	2.33	269	0.93	0.94
	3.00	1349	351	351	338	0.96	0.96	1.96	229	0.65	0.65	1156	2.77	315	0.90	0.92
	3.25	1583	380	382	362	0.95	0.94	2.06	240	0.63	0.62	1347	2.99	338	0.89	0.91
	3.50	1836	409	411	387	0.95	0.94	2.15	251	0.61	0.61	1552	3.21	359	0.88	0.90
C9 (L_{crd}=600; L_{crl}=120)	1.00	131	105	105	99	0.94	0.93	0.94	92	0.88	0.87	128	0.98	99	0.94	0.93
	1.10	159	113	116	110	0.98	0.94	1.01	100	0.88	0.85	152	1.08	110	0.98	0.94
	1.25	205	126	127	127	1.01	0.99	1.10	110	0.87	0.86	193	1.21	127	1.01	0.99
	1.50	295	147	146	154	1.05	1.05	1.23	126	0.86	0.86	272	1.44	148	1.00	1.00
	1.75	402	157	168	180	1.14	1.06	1.36	140	0.89	0.83	363	1.66	171	1.09	1.01
	2.00	525	197	*	204	1.04	*	1.49	153	0.78	*	467	1.88	193	0.98	*
	2.50	820	248	249	251	1.01	1.00	1.71	176	0.71	0.70	712	2.32	235	0.95	0.94
	3.00	1181	299	301	296	0.99	0.98	1.92	197	0.66	0.65	1008	2.76	276	0.92	0.91
	3.25	1387	324	326	317	0.98	0.97	2.02	207	0.64	0.63	1175	2.98	295	0.91	0.90
	3.50	1608	349	350	339	0.97	0.96	2.12	216	0.62	0.61	1354	3.20	314	0.90	0.89
C10 (L_{crd}=625; L_{crl}=120)	1.00	114	91	91	85	0.94	0.94	0.93	78	0.86	0.86	109	0.98	85	0.94	0.94
	1.10	138	99	99	96	0.97	0.96	0.99	84	0.86	0.84	130	1.07	96	0.97	0.96
	1.25	178	106	108	110	1.04	1.01	1.07	93	0.88	0.86	164	1.20	110	1.04	1.01
	1.50	256	123	121	133	1.09	1.09	1.21	107	0.87	0.88	229	1.42	126	1.02	1.03
	1.75	349	*	141	156	*	1.10	1.34	119	*	0.84	305	1.63	146	*	1.03
	2.00	455	164	162	177	1.08	1.08	1.46	130	0.79	0.80	390	1.85	164	1.00	1.01
	2.50	711	207	206	218	1.05	1.05	1.68	150	0.72	0.72	593	2.28	200	0.97	0.97
	3.00	1024	250	250	256	1.03	1.02	1.88	167	0.67	0.66	836	2.70	234	0.94	0.93
	3.25	1202	271	271	275	1.02	1.01	1.98	175	0.65	0.64	972	2.92	250	0.92	0.92
	3.50	1394	292	292	293	1.01	1.00	2.07	183	0.63	0.62	1119	3.13	267	0.91	0.91

Table B3: H and Z columns: SFEA ultimate strengths and corresponding DSM estimates (dimensions in *mm*, stresses in *MPa*) – III

			SFEA				DSM					NDL					MNDL				
	λ_l	f_y	$f_{u.D}^H$	$f_{u.L}^H$	$f_{u.D}^Z$	$f_{u.L}^Z$	f_{nl}	$\frac{f_{nl}}{f_{u.D}^H}$	$\frac{f_{nl}}{f_{u.L}^H}$	$\frac{f_{nl}}{f_{u.D}^Z}$	$\frac{f_{nl}}{f_{u.L}^Z}$	f_{ndl}	$\frac{f_{ndl}}{f_{u.D}^H}$	$\frac{f_{ndl}}{f_{u.L}^H}$	$\frac{f_{ndl}}{f_{u.D}^Z}$	$\frac{f_{ndl}}{f_{u.L}^Z}$	f_{mndl}	$\frac{f_{mndl}}{f_{u.D}^H}$	$\frac{f_{mndl}}{f_{u.L}^H}$	$\frac{f_{mndl}}{f_{u.D}^Z}$	$\frac{f_{mndl}}{f_{u.L}^Z}$
C11 (L_{crd}=475; L_{crl}=100)	1.00	189	152	166	157	161	161	1.06	0.97	1.03	1.00	131	0.87	0.79	0.83	0.81	145	0.96	0.87	0.91	0.89
	1.10	229	169	187	175	180	183	1.09	0.98	1.04	1.01	142	0.84	0.76	0.80	0.78	163	0.97	0.87	0.91	0.89
	1.25	296	189	208	197	201	216	1.15	1.04	1.10	1.07	157	0.83	0.76	0.79	0.77	188	0.99	0.91	0.94	0.92
	1.50	426	225	227	224	217	275	1.22	1.21	1.22	1.26	180	0.80	0.79	0.79	0.82	228	1.01	1.00	1.00	1.03
	1.75	580	261	259	256	246	335	1.28	1.30	1.31	1.36	201	0.77	0.78	0.77	0.80	252	0.96	0.97	0.98	1.02
	2.00	758	295	294	287	281	398	1.35	1.35	1.38	1.41	220	0.75	0.75	0.75	0.77	285	0.97	0.97	0.99	1.01
	2.50	1184	375	366	359	354	528	1.41	1.44	1.47	1.49	254	0.68	0.69	0.69	0.70	348	0.93	0.95	0.97	0.98
	3.00	1705	445	435	432	428	664	1.49	1.53	1.53	1.55	284	0.64	0.65	0.65	0.65	408	0.92	0.94	0.94	0.95
	3.25	2000	479	472	466	462	734	1.53	1.56	1.57	1.58	298	0.62	0.63	0.63	0.63	437	0.91	0.93	0.94	0.94
	3.50	2320	510	505	500	495	805	1.58	1.59	1.61	1.62	311	0.61	0.62	0.61	0.62	465	0.91	0.92	0.93	0.94
C12 (L_{crd}=475; L_{crl}=100)	1.00	178	144	156	148	152	151	1.05	0.97	1.02	0.99	125	0.87	0.80	0.83	0.81	138	0.96	0.89	0.92	0.90
	1.10	216	160	177	166	171	172	1.08	0.97	1.03	1.00	135	0.85	0.76	0.80	0.78	155	0.97	0.88	0.92	0.89
	1.25	278	179	198	187	192	204	1.14	1.03	1.09	1.06	150	0.84	0.76	0.79	0.77	179	1.00	0.91	0.94	0.92
	1.50	401	213	218	212	209	258	1.21	1.19	1.22	1.23	172	0.81	0.79	0.80	0.81	218	1.02	1.00	1.01	1.02
	1.75	546	247	244	243	233	315	1.28	1.29	1.29	1.35	192	0.78	0.79	0.78	0.81	241	0.97	0.99	0.99	1.03
	2.00	713	*	278	272	266	374	*	1.35	1.37	1.40	210	*	0.76	0.76	0.78	272	*	0.98	1.00	1.02
	2.50	1114	*	347	340	336	497	*	1.43	1.46	1.47	243	*	0.70	0.70	0.71	333	*	0.96	0.98	0.99
	3.00	1604	423	413	391	406	625	1.48	1.51	1.59	1.53	272	0.64	0.66	0.68	0.66	390	0.92	0.94	1.00	0.96
	3.25	1882	451	451	451	439	690	1.53	1.53	1.53	1.57	285	0.63	0.63	0.62	0.64	418	0.93	0.93	0.93	0.95
	3.50	2183	469	481	484	471	757	1.61	1.57	1.56	1.60	298	0.64	0.62	0.61	0.62	445	0.95	0.93	0.92	0.95
C13 (L_{crd}=700; L_{crl}=120)	1.00	80	69	66	68	64	68	0.99	1.02	1.00	1.05	57	0.83	0.85	0.83	0.88	63	0.92	0.95	0.92	0.98
	1.10	97	77	74	76	71	77	1.00	1.05	1.01	1.08	62	0.80	0.84	0.81	0.86	71	0.92	0.96	0.93	0.99
	1.25	125	81	83	81	80	91	1.12	1.10	1.12	1.15	68	0.84	0.82	0.84	0.86	82	1.01	0.99	1.01	1.03
	1.50	180	88	93	88	88	116	1.32	1.25	1.32	1.31	78	0.89	0.85	0.89	0.89	99	1.13	1.07	1.13	1.12
	1.75	245	102	102	101	99	141	1.39	1.39	1.40	1.42	88	0.86	0.86	0.87	0.88	103	1.01	1.01	1.03	1.05
	2.00	319	117	117	116	115	168	1.43	1.43	1.44	1.46	96	0.82	0.82	0.83	0.83	115	0.98	0.98	1.01	1.02
	2.50	499	147	150	148	148	222	1.51	1.48	1.50	1.50	111	0.75	0.74	0.75	0.75	139	0.95	0.93	0.96	0.96
	3.00	719	178	184	179	180	280	1.57	1.52	1.56	1.55	124	0.70	0.68	0.69	0.69	162	0.91	0.88	0.93	0.92
	3.25	843	194	200	195	195	309	1.59	1.55	1.58	1.58	130	0.67	0.65	0.67	0.67	173	0.89	0.86	0.91	0.91
	3.50	978	209	216	210	210	339	1.62	1.57	1.61	1.61	136	0.65	0.63	0.65	0.65	183	0.88	0.85	0.90	0.90

* Due to numerical difficulties, no ultimate strength could be obtained for these columns.

Table B4: H and Z columns: SFEA ultimate strengths and corresponding DSM estimates (dimensions in *mm*, stresses in *MPa*) – IV

			SFEA				DSM					NDL					MNDL				
	λ_l	f_y	$f^H_{u.D}$	$f^H_{u.L}$	$f^Z_{u.D}$	$f^Z_{u.L}$	f_{nl}	$\frac{f_{nl}}{f^H_{u.D}}$	$\frac{f_{nl}}{f^H_{u.L}}$	$\frac{f_{nl}}{f^Z_{u.D}}$	$\frac{f_{nl}}{f^Z_{u.L}}$	f_{ndl}	$\frac{f_{ndl}}{f^H_{u.D}}$	$\frac{f_{ndl}}{f^H_{u.L}}$	$\frac{f_{ndl}}{f^Z_{u.D}}$	$\frac{f_{ndl}}{f^Z_{u.L}}$	f_{mndl}	$\frac{f_{mndl}}{f^H_{u.D}}$	$\frac{f_{mndl}}{f^H_{u.L}}$	$\frac{f_{mndl}}{f^Z_{u.D}}$	$\frac{f_{mndl}}{f^Z_{u.L}}$
C14 (L_{crd}=525; L_{crl}=100)	1.00	137	116	121	118	119	116	1.00	0.96	0.98	0.98	100	0.86	0.82	0.84	0.83	111	0.96	0.92	0.93	0.93
	1.10	166	131	137	131	135	132	1.01	0.96	1.01	0.98	109	0.83	0.79	0.82	0.80	125	0.95	0.91	0.95	0.92
	1.25	214	146	160	147	156	156	1.07	0.98	1.06	1.00	121	0.83	0.75	0.81	0.77	145	0.99	0.91	0.98	0.92
	1.50	308	168	187	169	178	198	1.18	1.06	1.17	1.11	139	0.83	0.74	0.82	0.77	177	1.05	0.95	1.04	0.98
	1.75	419	195	196	196	187	242	1.24	1.24	1.23	1.29	155	0.80	0.79	0.79	0.82	196	1.00	1.00	0.97	1.02
	2.00	547	221	216	224	210	287	1.30	1.33	1.28	1.37	171	0.77	0.79	0.75	0.80	222	1.01	1.03	0.97	1.03
	2.50	855	276	274	286	266	381	1.38	1.39	1.33	1.43	198	0.72	0.72	0.68	0.74	272	0.99	0.99	0.92	0.99
	3.00	1231	326	328	345	323	479	1.47	1.46	1.39	1.48	222	0.68	0.68	0.64	0.68	320	0.98	0.97	0.90	0.96
	3.25	1445	348	355	374	351	530	1.52	1.49	1.41	1.51	233	0.67	0.66	0.62	0.66	343	0.98	0.97	0.89	0.95
	3.50	1676	373	381	404	377	581	1.56	1.53	1.44	1.54	243	0.65	0.64	0.60	0.64	365	0.98	0.96	0.87	0.94
C15 (L_{crd}=525; L_{crl}=100)	1.00	127	110	111	111	112	108	0.99	0.97	0.97	0.97	95	0.87	0.86	0.85	0.84	106	0.97	0.96	0.95	0.94
	1.10	154	124	126	123	127	123	0.99	0.98	1.00	0.97	104	0.84	0.82	0.83	0.81	120	0.97	0.95	0.96	0.94
	1.25	199	139	146	140	146	145	1.05	1.00	1.04	0.99	116	0.83	0.79	0.82	0.78	139	1.01	0.96	0.99	0.94
	1.50	286	158	165	164	169	185	1.17	1.12	1.12	1.09	134	0.85	0.81	0.80	0.78	171	1.08	1.03	1.03	1.00
	1.75	390	183	180	183	179	225	1.23	1.25	1.23	1.26	150	0.82	0.83	0.81	0.82	183	1.00	1.02	1.00	1.03
	2.00	509	208	205	210	197	267	1.29	1.30	1.27	1.35	164	0.79	0.80	0.77	0.82	208	1.00	1.01	0.99	1.06
	2.50	795	259	259	268	250	355	1.37	1.37	1.32	1.42	191	0.74	0.74	0.70	0.75	254	0.98	0.98	0.95	1.02
	3.00	1145	307	308	323	304	446	1.45	1.45	1.38	1.47	214	0.70	0.70	0.65	0.70	297	0.97	0.96	0.92	0.98
	3.25	1344	329	325	351	330	493	1.50	1.52	1.40	1.49	225	0.69	0.69	0.63	0.67	318	0.97	0.98	0.91	0.97
	3.50	1559	351	354	378	*	541	1.54	1.53	1.43	*	236	0.67	0.67	0.61	*	339	0.96	0.96	0.90	*
C16 (L_{crd}=550; L_{crl}=100)	1.00	118	103	103	104	104	100	0.97	0.97	0.96	0.96	89	0.87	0.87	0.85	0.85	100	0.97	0.97	0.95	0.95
	1.10	143	117	118	116	118	114	0.97	0.97	0.98	0.96	98	0.83	0.83	0.83	0.82	113	0.96	0.96	0.96	0.94
	1.25	185	131	137	132	137	135	1.03	0.99	1.02	0.98	109	0.83	0.79	0.81	0.78	132	1.00	0.96	0.98	0.95
	1.50	266	148	157	154	160	171	1.16	1.09	1.11	1.07	126	0.85	0.80	0.81	0.78	161	1.09	1.03	1.03	0.99
	1.75	362	171	168	172	171	209	1.22	1.24	1.21	1.22	141	0.83	0.84	0.81	0.81	190	1.11	1.13	0.99	1.00
	2.00	472	194	192	194	185	248	1.28	1.29	1.28	1.34	155	0.80	0.81	0.79	0.83	196	1.01	1.02	1.00	1.04
	2.50	738	242	242	246	234	329	1.36	1.36	1.34	1.40	181	0.75	0.75	0.72	0.76	240	0.99	0.99	0.96	1.01
	3.00	1063	288	289	298	284	414	1.44	1.43	1.39	1.45	203	0.70	0.70	0.67	0.70	282	0.98	0.97	0.93	0.97
	3.25	1247	310	308	337	309	457	1.48	1.49	1.36	1.48	213	0.69	0.69	0.62	0.68	302	0.97	0.98	0.88	0.96
	3.50	1446	329	339	365	330	502	1.52	1.48	1.37	1.52	223	0.68	0.66	0.60	0.66	321	0.98	0.95	0.86	0.96
C17 (L_{crd}=550; L_{crl}=100)	1.00	109	96	96	97	96	93	0.97	0.97	0.95	0.96	84	0.87	0.87	0.85	0.86	94	0.98	0.98	0.95	0.96
	1.10	132	110	109	109	110	105	0.96	0.97	0.97	0.96	91	0.83	0.84	0.83	0.82	106	0.96	0.97	0.96	0.95
	1.25	171	123	127	122	128	125	1.01	0.98	1.02	0.97	102	0.83	0.80	0.83	0.79	124	1.01	0.97	1.00	0.95
	1.50	246	140	148	139	150	158	1.13	1.07	1.14	1.05	118	0.85	0.80	0.84	0.78	152	1.09	1.03	1.08	1.00
	1.75	334	160	157	154	163	193	1.21	1.23	1.25	1.18	133	0.83	0.85	0.85	0.80	179	1.12	1.14	1.14	1.08
	2.00	437	181	178	174	173	229	1.27	1.29	1.32	1.32	146	0.81	0.82	0.83	0.83	185	1.02	1.04	1.05	1.05
	2.50	683	225	225	220	218	304	1.35	1.35	1.38	1.39	170	0.76	0.76	0.76	0.77	227	1.01	1.01	1.01	1.02
	3.00	983	269	270	268	264	383	1.42	1.42	1.43	1.45	192	0.71	0.71	0.70	0.71	266	0.99	0.99	0.98	0.99
	3.25	1154	290	291	292	288	423	1.46	1.45	1.45	1.47	201	0.69	0.69	0.68	0.69	285	0.98	0.98	0.96	0.97
	3.50	1338	310	*	316	310	464	1.50	*	1.47	1.49	211	0.68	*	0.66	0.67	304	0.98	*	0.94	0.96
C18 (L_{crd}=550; L_{crl}=100)	1.00	101	89	88	91	89	86	0.96	0.97	0.94	0.96	78	0.87	0.88	0.85	0.87	88	0.98	0.99	0.95	0.97
	1.10	122	104	101	103	102	97	0.93	0.96	0.94	0.95	86	0.82	0.85	0.82	0.83	99	0.96	0.98	0.95	0.96
	1.25	157	120	118	114	119	115	0.96	0.98	1.01	0.97	96	0.80	0.81	0.83	0.79	116	0.97	0.99	1.00	0.96
	1.50	227	140	139	131	141	146	1.04	1.05	1.11	1.03	111	0.79	0.80	0.84	0.78	143	1.02	1.03	1.07	1.00
	1.75	308	151	148	144	155	178	1.18	1.20	1.24	1.15	125	0.83	0.84	0.85	0.79	169	1.12	1.14	1.15	1.07
	2.00	403	174	166	162	161	211	1.22	1.27	1.30	1.31	138	0.79	0.83	0.84	0.84	175	1.00	1.05	1.06	1.07
	2.50	629	216	209	205	203	281	1.30	1.34	1.37	1.38	160	0.74	0.77	0.77	0.78	214	0.99	1.03	1.03	1.04
	3.00	906	256	252	249	247	353	1.38	1.40	1.42	1.43	181	0.71	0.72	0.71	0.72	251	0.98	1.00	0.99	1.00
	3.25	1064	281	271	272	268	390	1.39	1.44	1.43	1.45	190	0.68	0.70	0.69	0.70	269	0.96	0.99	0.97	0.99
	3.50	1234	306	287	294	288	428	1.40	1.49	1.45	1.48	199	0.65	0.69	0.66	0.68	287	0.94	1.00	0.96	0.98
C19 (L_{crd}=575; L_{crl}=100)	1.00	93	83	82	83	82	79	0.95	0.97	0.95	0.96	73	0.88	0.89	0.87	0.88	82	0.98	1.00	0.98	0.98
	1.10	112	95	93	95	95	89	0.95	0.96	0.94	0.94	80	0.84	0.86	0.83	0.83	93	0.98	1.00	0.96	0.97
	1.25	145	109	111	109	110	106	0.97	0.96	0.97	0.96	89	0.82	0.81	0.81	0.81	109	1.00	0.98	0.99	0.98
	1.50	208	129	130	128	131	134	1.04	1.04	1.05	1.03	104	0.81	0.80	0.80	0.78	134	1.04	1.04	1.03	1.01
	1.75	283	140	141	142	140	164	1.17	1.17	1.15	1.17	117	0.84	0.83	0.81	0.82	158	1.13	1.13	1.09	1.11
	2.00	370	146	155	157	149	194	1.34	1.26	1.24	1.30	129	0.89	0.84	0.81	0.85	158	1.08	1.02	1.01	1.06
	2.50	578	189	194	197	189	258	1.36	1.33	1.31	1.37	151	0.80	0.78	0.75	0.78	193	1.02	0.99	0.98	1.03
	3.00	833	228	233	239	231	324	1.42	1.39	1.36	1.41	170	0.74	0.73	0.70	0.72	225	0.99	0.97	0.95	0.98
	3.25	977	247	252	261	252	358	1.45	1.42	1.37	1.42	178	0.72	0.71	0.67	0.70	241	0.98	0.96	0.93	0.96
	3.50	1133	267	266	281	272	393	1.48	1.48	1.40	1.44	187	0.70	0.70	0.65	0.67	256	0.96	0.96	0.92	0.95
C20 (L_{crd}=575; L_{crl}=100)	1.00	85	77	75	78	75	72	0.93	0.96	0.92	0.96	67	0.87	0.90	0.85	0.89	76	0.98	1.01	0.96	1.00
	1.10	102	87	86	87	86	82	0.94	0.96	0.94	0.95	74	0.85	0.86	0.84	0.85	86	0.99	1.01	0.97	0.99
	1.25	132	100	101	101	101	97	0.97	0.96	0.96	0.96	83	0.83	0.82	0.81	0.81	101	1.01	1.00	0.99	0.99
	1.50	191	120	120	120	121	123	1.02	1.02	1.02	1.01	97	0.81	0.81	0.79	0.79	125	1.04	1.04	1.03	1.02
	1.75	259	131	132	132	132	150	1.14	1.14	1.13	1.13	109	0.83	0.83	0.81	0.81	148	1.13	1.12	1.10	1.10
	2.00	339	138	143	145	138	178	1.29	1.24	1.23	1.29	120	0.87	0.84	0.82	0.86	147	1.07	1.03	1.02	1.07
	2.50	529	176	179	182	174	236	1.34	1.32	1.30	1.35	141	0.80	0.79	0.76	0.79	180	1.02	1.01	0.99	1.04
	3.00	762	210	215	221	213	297	1.41	1.38	1.34	1.39	158	0.75	0.74	0.70	0.73	211	1.00	0.98	0.96	1.00
	3.25	895	229	233	240	232	328	1.43	1.41	1.37	1.41	167	0.73	0.72	0.68	0.71	226	0.98	0.97	0.95	0.98
	3.50	1038	247	246	255	252	360	1.46	1.46	1.41	1.43	175	0.71	0.71	0.67	0.68	240	0.97	0.98	0.95	0.96

* Due to numerical difficulties, no ultimate strength could be obtained for these columns.

Table B5: H and Z columns: SFEA ultimate strengths and corresponding DSM estimates (dimensions in *mm*, stresses in *MPa*) – V

			SFEA				DSM					NDL					MNDL				
	λ_l	f_y	$f^H_{u.D}$	$f^H_{u.L}$	$f^Z_{u.D}$	$f^Z_{u.L}$	f_{nl}	$\frac{f_{nl}}{f^H_{u.D}}$	$\frac{f_{nl}}{f^H_{u.L}}$	$\frac{f_{nl}}{f^Z_{u.D}}$	$\frac{f_{nl}}{f^Z_{u.L}}$	f_{ndl}	$\frac{f_{ndl}}{f^H_{u.D}}$	$\frac{f_{ndl}}{f^H_{u.L}}$	$\frac{f_{ndl}}{f^Z_{u.D}}$	$\frac{f_{ndl}}{f^Z_{u.L}}$	f_{mndl}	$\frac{f_{mndl}}{f^H_{u.D}}$	$\frac{f_{mndl}}{f^H_{u.L}}$	$\frac{f_{mndl}}{f^Z_{u.D}}$	$\frac{f_{mndl}}{f^Z_{u.L}}$
C21 (L_{crd}=775; L_{crl}=110)	1.00	47	44	41	44	41	40	0.91	0.98	0.91	0.98	37	0.85	0.92	0.85	0.92	47	1.07	1.16	0.96	1.04
	1.10	57	48	46	48	46	45	0.95	1.00	0.95	1.00	41	0.86	0.90	0.85	0.90	48	1.00	1.06	1.00	1.05
	1.25	73	53	52	53	52	54	1.01	1.03	1.01	1.03	46	0.87	0.89	0.86	0.88	57	1.07	1.09	1.06	1.07
	1.50	106	61	61	62	63	68	1.11	1.11	1.09	1.08	54	0.88	0.88	0.86	0.85	70	1.14	1.14	1.12	1.11
	1.75	144	68	69	71	72	83	1.21	1.21	1.17	1.16	61	0.89	0.88	0.85	0.84	83	1.21	1.20	1.15	1.14
	2.00	188	75	77	78	79	99	1.32	1.29	1.27	1.25	67	0.90	0.88	0.86	0.84	75	1.01	0.98	0.96	0.94
	2.50	293	94	95	93	97	131	1.40	1.38	1.41	1.34	79	0.84	0.83	0.84	0.80	91	0.97	0.95	0.96	0.92
	3.00	422	113	114	113	117	164	1.46	1.44	1.45	1.41	89	0.78	0.78	0.78	0.75	105	0.93	0.92	0.91	0.88
	3.25	496	123	124	124	127	182	1.48	1.47	1.47	1.43	93	0.76	0.75	0.75	0.73	111	0.91	0.90	0.89	0.86
	3.50	575	133	133	134	137	199	1.50	1.50	1.49	1.45	98	0.73	0.73	0.72	0.71	118	0.89	0.89	0.87	0.85
C22 (L_{crd}=800; L_{crl}=110)	1.00	42	39	36	39	36	35	0.90	0.98	0.90	0.98	34	0.86	0.93	0.85	0.93	42	1.06	1.16	1.06	1.16
	1.10	50	43	40	43	40	40	0.94	0.99	0.94	0.99	37	0.87	0.91	0.86	0.91	43	1.02	1.07	1.01	1.07
	1.25	65	47	46	47	47	48	1.01	1.03	1.00	1.02	42	0.88	0.90	0.88	0.89	51	1.08	1.10	1.07	1.09
	1.50	94	55	55	56	56	60	1.10	1.10	1.08	1.07	49	0.88	0.88	0.87	0.86	63	1.15	1.15	1.13	1.12
	1.75	127	62	63	65	65	74	1.18	1.18	1.14	1.13	55	0.88	0.88	0.85	0.85	75	1.20	1.20	1.16	1.15
	2.00	166	68	69	72	71	87	1.28	1.26	1.22	1.22	61	0.89	0.88	0.85	0.85	67	0.98	0.96	0.92	0.93
	2.50	260	84	85	83	88	116	1.38	1.36	1.39	1.32	71	0.85	0.83	0.85	0.81	80	0.95	0.93	0.95	0.90
	3.00	374	101	103	102	105	146	1.44	1.42	1.43	1.39	80	0.79	0.78	0.79	0.76	92	0.91	0.89	0.89	0.87
	3.25	439	110	111	111	114	161	1.46	1.45	1.45	1.41	85	0.77	0.76	0.76	0.74	98	0.89	0.88	0.87	0.85
	3.50	510	119	120	120	123	177	1.49	1.47	1.47	1.44	89	0.74	0.74	0.74	0.72	103	0.87	0.86	0.85	0.83
C23 (L_{crd}=825; L_{crl}=110)	1.00	37	35	32	35	32	31	0.90	0.98	0.89	0.98	30	0.87	0.95	0.85	0.94	37	1.06	1.15	1.04	1.15
	1.10	44	40	36	37	36	35	0.89	0.99	0.95	0.99	33	0.84	0.93	0.88	0.92	39	0.98	1.09	1.04	1.09
	1.25	57	44	41	42	41	42	0.95	1.02	1.00	1.02	37	0.85	0.92	0.89	0.91	46	1.05	1.13	1.09	1.12
	1.50	82	52	49	50	50	53	1.03	1.08	1.07	1.06	44	0.85	0.90	0.88	0.87	58	1.11	1.18	1.15	1.14
	1.75	112	60	56	58	58	65	1.08	1.15	1.12	1.11	50	0.84	0.89	0.85	0.85	68	1.14	1.21	1.17	1.16
	2.00	146	66	62	65	65	77	1.17	1.24	1.18	1.19	55	0.84	0.89	0.84	0.85	79	1.19	1.27	1.19	1.20
	2.50	229	79	76	74	79	102	1.29	1.34	1.37	1.30	65	0.82	0.85	0.86	0.82	70	0.89	0.92	0.93	0.88
	3.00	329	95	92	91	94	128	1.35	1.40	1.41	1.36	73	0.77	0.80	0.80	0.77	80	0.85	0.88	0.88	0.84
	3.25	386	99	100	99	102	142	1.43	1.42	1.44	1.39	77	0.78	0.78	0.78	0.75	85	0.86	0.86	0.86	0.83
	3.50	448	111	107	107	110	155	1.40	1.45	1.45	1.41	81	0.73	0.76	0.75	0.73	90	0.81	0.84	0.83	0.81
C24 (L_{crd}=850; L_{crl}=110)	1.00	32	31	28	31	28	27	0.89	0.98	0.88	0.98	26	0.87	0.95	0.86	0.95	32	1.05	1.15	1.04	1.15
	1.10	39	35	31	33	31	31	0.89	0.99	0.94	0.99	29	0.85	0.94	0.89	0.94	39	1.11	1.24	1.05	1.11
	1.25	50	38	36	37	36	36	0.95	1.02	0.99	1.02	33	0.87	0.93	0.90	0.92	41	1.07	1.15	1.11	1.14
	1.50	72	46	43	44	44	46	1.02	1.07	1.06	1.06	39	0.86	0.91	0.89	0.89	51	1.13	1.19	1.17	1.17
	1.75	98	53	50	51	52	56	1.06	1.13	1,10	1.10	45	0.83	0.89	0.86	0.86	61	1.15	1.23	1.18	1.18
	2.00	128	60	56	58	58	67	1.12	1.20	1.15	1.15	49	0.83	0.88	0.84	0.85	71	1.18	1.26	1.20	1.21
	2.50	199	70	68	67	70	89	1.26	1.31	1.33	1.27	58	0.83	0.86	0.86	0.83	61	0.86	0.90	0.90	0.86
	3.00	287	84	81	80	84	112	1.33	1.37	1.40	1.34	66	0.78	0.81	0.82	0.78	69	0.83	0.85	0.86	0.82
	3.25	337	91	88	87	90	123	1.36	1.40	1.41	1.37	69	0.76	0.79	0.79	0.76	73	0.81	0.83	0.83	0.81
	3.50	391	98	95	95	97	135	1.38	1.42	1.43	1.39	73	0.74	0.76	0.76	0.74	77	0.79	0.81	0.81	0.79
C25 (L_{crd}=875; L_{crl}=110)	1.00	28	27	24	27	24	23	0.88	0.98	0.88	0.98	23	0.87	0.96	0.86	0.96	28	1.04	1.15	1.03	1.15
	1.10	33	30	27	28	27	27	0.89	0.99	0.94	0.99	26	0.86	0.96	0.91	0.95	33	1.12	1.24	1.18	1.24
	1.25	43	33	31	32	31	31	0.95	1.01	0.99	1.02	29	0.88	0.94	0.91	0.94	36	1.09	1.17	1.14	1.17
	1.50	62	39	38	38	38	40	1.02	1.06	1.05	1.05	35	0.88	0.92	0.90	0.91	46	1.16	1.21	1.19	1.20
	1.75	84	47	44	45	45	49	1.04	1.11	1.08	1.08	39	0.84	0.90	0.87	0.87	54	1.16	1.24	1.20	1.20
	2.00	110	53	50	52	51	58	1.09	1.16	1.12	1.13	44	0.82	0.88	0.84	0.85	63	1.18	1.27	1.21	1.22
	2.50	172	62	60	62	62	77	1.23	1.29	1.24	1.25	52	0.83	0.87	0.83	0.83	52	0.83	0.87	0.84	0.84
	3.00	248	74	71	70	74	96	1.31	1.35	1.37	1.31	59	0.79	0.82	0.83	0.79	59	0.79	0.82	0.84	0.80
	3.25	291	80	77	76	80	107	1.34	1.38	1.39	1.34	62	0.77	0.80	0.80	0.77	62	0.77	0.80	0.81	0.78
	3.50	337	84	84	83	86	117	1.39	1.40	1.41	1.37	65	0.77	0.78	0.78	0.75	65	0.77	0.78	0.79	0.76
C26 (L_{crd}=900; L_{crl}=110)	1.00	25	24	22	24	22	21	0.88	0.98	0.88	0.98	21	0.87	0.97	0.86	0.97	25	1.03	1.15	1.03	1.16
	1.10	30	26	24	26	24	24	0.94	0.99	0.94	0.99	23	0.91	0.96	0.91	0.96	30	1.18	1.24	1.18	1.24
	1.25	39	29	28	29	28	29	0.99	1.01	0.99	1.01	27	0.92	0.95	0.92	0.95	33	1.15	1.19	1.15	1.18
	1.50	56	35	34	35	35	36	1.05	1.06	1.04	1.05	32	0.92	0.92	0.91	0.92	42	1.22	1.22	1.20	1.21
	1.75	77	40	40	41	41	44	1.10	1.10	1.07	1.07	36	0.90	0.90	0.88	0.88	50	1.25	1.24	1.21	1.21
	2.00	100	46	46	48	47	53	1.15	1.14	1.10	1.11	40	0.89	0.88	0.84	0.85	58	1.27	1.26	1.21	1.22
	2.50	156	55	55	58	57	70	1.27	1.27	1.21	1.23	48	0.87	0.87	0.82	0.83	48	0.87	0.87	0.82	0.83
	3.00	225	66	66	64	68	88	1.33	1.34	1.36	1.30	54	0.82	0.82	0.84	0.79	54	0.82	0.82	0.84	0.79
	3.25	264	71	71	70	73	97	1.36	1.37	1.38	1.32	57	0.80	0.81	0.81	0.78	57	0.80	0.81	0.81	0.78
	3.50	307	77	77	76	79	106	1.38	1.39	1.40	1.35	60	0.78	0.78	0.78	0.76	60	0.78	0.78	0.78	0.76
C27 (L_{crd}=950; L_{crl}=110)	1.00	20	19	17	19	17	17	0.88	0.98	0,87	0,99	17	0.87	0.98	0.87	0.98	20	1.03	1.15	1.03	1.16
	1.10	24	21	19	20	19	19	0.89	0.99	0,94	0,99	19	0.87	0.97	0.92	0.97	24	1.11	1.24	1.18	1.24
	1.25	31	24	22	23	22	23	0.94	1.01	0,99	1,01	21	0.90	0.96	0.94	0.96	27	1.13	1.21	1.18	1.21
	1.50	44	28	27	28	27	29	1.01	1.05	1,04	1,05	26	0.90	0.94	0.92	0.93	34	1.21	1.25	1.23	1.24
	1.75	60	34	33	33	33	35	1.03	1.07	1,06	1,06	29	0.86	0.90	0.88	0.89	41	1.20	1.26	1.23	1.24
	2.00	79	40	38	*	38	41	1.04	1.10	*	1,08	33	0.82	0.87	*	0.85	47	1.19	1.26	*	1.23
	2.50	123	50	46	*	48	55	1.11	1.19	*	1,15	39	0.78	0.84	*	0.81	39	0.78	0.84	*	0.81
	3.00	177	56	53	*	55	69	1.24	1.29	*	1,25	44	0.79	0.83	*	0.80	44	0.79	0.83	*	0.80
	3.25	208	60	58	61	60	76	1.28	1.32	1,26	1,28	47	0.78	0.81	0.76	0.78	47	0.78	0.81	0.76	0.78
	3.50	241	64	62	66	64	84	1.31	1.35	1,28	1,32	49	0.76	0.79	0.74	0.76	49	0.76	0.79	0.74	0.76

* Due to numerical difficulties, no ultimate strength could be obtained for these columns.

ANNEX C – RACK-SECTION COLUMN RESULTS

Table C1: R columns: SFEA ultimate strengths and corresponding DSM estimates (dimensions in *mm*, stresses in *MPa*) – I

			SFEA	DSM			NDL			MNDL			
	λ_d	f_y	f_u	f_{nl}	f_{nd}	$\frac{f_{nd}}{f_u}$	λ_{dl}	f_{ndl}	$\frac{f_{ndl}}{f_u}$	f_{nl}^*	λ_{dl}^*	f_{mndl}	$\frac{f_{mndl}}{f_u}$
C1 (L_{crd}=600; L_{crl}=170)	1.00	112	93	112	84	0.91	0.99	84	0.91	112	0.99	84	0.91
	1.10	135	104	135	94	0.91	1.09	94	0.91	135	1.09	94	0.91
	1.25	174	124	171	109	0.88	1.23	107	0.87	174	1.24	109	0.88
	1.50	251	161	219	131	0.82	1.39	123	0.76	251	1.49	131	0.82
	1.75	342	177	269	153	0.87	1.54	136	0.77	342	1.74	153	0.87
	2.00	447	195	321	174	0.89	1.69	149	0.76	447	1.99	174	0.89
	2.50	698	242	430	214	0.89	1.95	171	0.71	698	2.48	214	0.89
	3.00	1005	294	543	253	0.86	2.19	191	0.65	1005	2.98	253	0.86
	3.25	1179	319	601	271	0.85	2.31	200	0.63	1179	3.23	271	0.85
	3.50	1368	343	661	289	0.84	2.42	209	0.61	1368	3.48	289	0.84
C2 (L_{crd}=620; L_{crl}=150)	1.00	139	114	139	105	0.92	0.99	105	0.92	139	0.99	105	0.92
	1.10	168	129	168	117	0.91	1.09	117	0.91	168	1.09	117	0.91
	1.25	217	154	203	135	0.88	1.20	130	0.85	216	1.24	135	0.88
	1.50	312	196	259	164	0.84	1.36	149	0.76	311	1.48	163	0.83
	1.75	425	215	318	191	0.89	1.50	165	0.77	422	1.73	190	0.88
	2.00	555	236	379	217	0.92	1.64	181	0.76	549	1.97	216	0.92
	2.50	868	292	506	267	0.92	1.89	208	0.71	856	2.46	265	0.91
	3.00	1250	353	639	315	0.89	2.13	232	0.66	1229	2.95	312	0.89
	3.25	1466	381	707	338	0.89	2.24	243	0.64	1441	3.20	335	0.88
	3.50	1701	409	777	360	0.88	2.35	254	0.62	1670	3.44	358	0.87
C3 (L_{crd}=640; L_{crl}=140)	1.00	129	106	129	98	0.92	0.99	98	0.92	129	0.99	98	0.92
	1.10	156	120	155	109	0.91	1.09	109	0.90	156	1.09	109	0.91
	1.25	202	142	185	126	0.89	1.19	120	0.84	199	1.23	126	0.89
	1.50	291	179	236	152	0.85	1.34	137	0.76	283	1.47	150	0.84
	1.75	396	195	289	178	0.91	1.48	152	0.78	381	1.70	174	0.89
	2.00	517	215	344	202	0.94	1.62	166	0.77	492	1.94	198	0.92
	2.50	808	257	459	249	0.97	1.87	191	0.74	758	2.40	242	0.94
	3.00	1163	322	580	293	0.91	2.10	213	0.66	1080	2.87	283	0.88
	3.25	1365	349	642	314	0.90	2.21	224	0.64	1262	3.10	304	0.87
	3.50	1583	374	705	335	0.90	2.32	234	0.62	1458	3.33	324	0.87
C4 (L_{crd}=1050; L_{crl}=230)	1.00	61	48	61	46	0.96	1.00	46	0.96	61	1.00	46	0.96
	1.10	74	54	71	51	0.96	1.07	50	0.93	73	1.09	51	0.96
	1.25	95	63	84	59	0.94	1.17	55	0.88	94	1.23	59	0.94
	1.50	137	77	108	72	0.93	1.32	63	0.82	133	1.47	71	0.91
	1.75	187	85	132	84	0.99	1.46	70	0.83	179	1.71	82	0.96
	2.00	244	96	157	95	1.00	1.60	77	0.80	232	1.94	93	0.97
	2.50	382	121	209	117	0.97	1.84	88	0.73	357	2.41	114	0.94
	3.00	550	147	264	138	0.94	2.07	99	0.67	509	2.87	133	0.91
	3.25	645	160	292	148	0.93	2.18	104	0.65	595	3.11	143	0.89
	3.50	748	173	321	158	0.91	2.28	108	0.63	688	3.34	152	0.88
C5 (L_{crd}=950; L_{crl}=190)	1.00	85	69	85	64	0.93	0.99	64	0.93	85	0.99	64	0.93
	1.10	103	77	97	72	0.93	1.06	69	0.90	102	1.09	72	0.93
	1.25	134	91	115	83	0.91	1.15	76	0.84	129	1.22	83	0.91
	1.50	192	115	146	100	0.87	1.30	87	0.76	181	1.45	97	0.85
	1.75	262	124	179	117	0.94	1.44	97	0.78	241	1.67	113	0.91
	2.00	342	133	213	133	1.00	1.57	106	0.80	310	1.90	127	0.96
	2.50	534	168	284	164	0.98	1.82	122	0.73	472	2.34	155	0.92
	3.00	769	203	358	193	0.95	2.04	136	0.67	666	2.78	181	0.89
	3.25	903	220	396	207	0.94	2.14	143	0.65	776	3.00	194	0.88
	3.50	1047	236	435	221	0.94	2.25	149	0.63	894	3.22	206	0.87
C6 (L_{crd}=870; L_{crl}=180)	1.00	110	90	107	83	0.93	0.98	82	0.91	110	0.99	83	0.93
	1.10	133	101	122	93	0.92	1.04	88	0.87	131	1.08	93	0.92
	1.25	172	119	145	107	0.90	1.14	97	0.82	167	1.22	107	0.90
	1.50	248	148	184	130	0.88	1.29	111	0.75	235	1.45	126	0.85
	1.75	338	157	225	151	0.96	1.42	124	0.79	314	1.68	146	0.93
	2.00	441	173	268	172	1.00	1.55	135	0.78	405	1.91	165	0.96
	2.50	689	216	357	212	0.98	1.79	156	0.72	620	2.36	202	0.93
	3.00	993	259	450	249	0.96	2.01	174	0.67	880	2.81	236	0.91
	3.25	1165	280	498	268	0.96	2.11	182	0.65	1026	3.03	253	0.90
	3.50	1351	300	546	286	0.95	2.21	190	0.63	1183	3.26	270	0.90
C7 (L_{crd}=890; L_{crl}=170)	1.00	105	85	100	79	0.93	0.97	77	0.91	104	0.99	79	0.93
	1.10	127	95	114	88	0.93	1.04	83	0.87	123	1.08	88	0.93
	1.25	164	113	136	102	0.90	1.13	92	0.81	155	1.21	102	0.90
	1.50	236	138	173	124	0.90	1.28	105	0.76	217	1.43	118	0.86
	1.75	322	145	211	144	0.99	1.41	117	0.80	288	1.65	136	0.94
	2.00	420	160	251	164	1.02	1.54	128	0.80	368	1.86	154	0.96
	2.50	656	203	334	202	0.99	1.77	147	0.72	557	2.29	187	0.92
	3.00	945	240	421	237	0.99	1.99	164	0.68	783	2.72	218	0.91
	3.25	1109	263	466	255	0.97	2.09	172	0.65	910	2.93	234	0.89
	3.50	1286	282	511	272	0.96	2.19	180	0.64	1047	3.14	248	0.88

Table C2: R columns: SFEA ultimate strengths and corresponding DSM estimates (dimensions in *mm*, stresses in *MPa*) – II

			SFEA	DSM			NDL			MNDL			
	λ_d	f_y	f_u	f_{nl}	f_{nd}	$\frac{f_{nd}}{f_u}$	λ_{dl}	f_{ndl}	$\frac{f_{ndl}}{f_u}$	f_{nl}^*	λ_{dl}^*	f_{mndl}	$\frac{f_{mndl}}{f_u}$
C8 (L_{crd}=930; L_{crl}=170)	1.00	96	77	89	72	0.94	0.96	69	0.90	93	0.98	72	0.94
	1.10	116	86	101	81	0.94	1.02	75	0.87	111	1.07	81	0.94
	1.25	150	102	120	93	0.91	1.11	82	0.81	139	1.20	93	0.91
	1.50	216	120	153	113	0.94	1.25	94	0.78	192	1.41	106	0.89
	1.75	294	127	187	132	1.04	1.39	105	0.82	254	1.62	123	097
	2.00	383	143	222	150	1.05	1.51	114	0.80	324	1.83	138	0.97
	2.50	599	180	295	184	1.02	1.74	132	0.73	487	2.24	167	0.93
	3.00	863	215	371	217	1.01	1.96	147	0.69	682	2.65	195	0.91
	3.25	1012	233	410	233	1.00	2.06	155	0.66	791	2.86	209	0.90
	3.50	1174	250	450	248	0.99	2.16	161	0.65	908	3.06	222	0.89
C9 (L_{crd}=980; L_{crl}=170)	1.00	88	70	79	66	0.95	0.94	62	0.89	84	0.97	66	0.95
	1.10	107	78	90	74	0.95	1.00	67	0.86	99	1.05	74	0.95
	1.25	138	91	106	86	0.94	1.09	74	0.82	124	1.18	86	0.94
	1.50	198	104	135	104	1.00	1.23	85	0.82	170	1.38	96	0.92
	1.75	270	113	165	121	1.07	1.36	94	0.84	224	1.58	110	0.98
	2.00	352	127	196	138	1.08	1.48	103	0.81	283	1.78	124	0.98
	2.50	551	160	261	169	1.06	1.71	119	0.74	423	2.18	150	0.94
	3.00	793	193	328	199	1.03	1.92	133	0.69	588	2.57	174	0.90
	3.25	930	208	363	214	1.03	2.02	139	0.67	680	2.76	186	0.89
	3.50	1079	223	398	228	1.02	2.11	146	0.65	779	2.96	198	0.89
C10 (L_{crd}=1050; L_{crl}=170)	1.00	146	117	126	110	0.94	0.92	101	0.86	135	0.95	110	0.94
	1.10	177	127	144	123	0.97	0.98	109	0.86	159	1.03	123	0.97
	1.25	228	144	170	142	0.99	1.07	121	0.84	196	1.15	142	0.99
	1.50	328	163	216	172	1.06	1.20	138	0.85	267	1.34	155	0.95
	1.75	447	175	264	201	1.15	1.33	154	0.88	347	1.53	177	1.01
	2.00	584	198	313	229	1.16	1.45	168	0.85	436	1.71	199	1.00
	2.50	912	248	415	281	1.13	1.67	194	0.78	642	2.08	239	0.96
	3.00	1313	295	522	332	1.12	1.87	217	0.74	883	2.44	277	0.94
	3.25	1541	317	577	356	1.12	1.97	228	0.72	1017	2.61	296	0.93
	3.50	1787	337	633	380	1.13	2.06	238	0.71	1160	2.79	314	0.93

Table C3: R columns: SFEA ultimate strengths and corresponding DSM estimates (dimensions in *mm*, stresses in *MPa*) – III

			SFEA		DSM				NDL			MNDL		
	λ_l	f_y	$f_{u.D}$	$f_{u.L}$	f_{nl}	f_{nd}	$\frac{f_{nl}}{f_{u.D}}$	$\frac{f_{nl}}{f_{u.L}}$	f_{ndl}	$\frac{f_{ndl}}{f_{u.D}}$	$\frac{f_{ndl}}{f_{u.L}}$	f_{mndl}	$\frac{f_{mndl}}{f_{u.D}}$	$\frac{f_{mndl}}{f_{u.L}}$
C11 (L_{crd}=1050; L_{crl}=170)	1.00	138	112	118	117	105	1.05	0.99	95	0.85	0.80	105	0.94	0.89
	1.10	167	122	132	133	118	1.09	1.01	103	0.84	0.78	118	0.96	0.89
	1.25	216	134	145	158	136	1.18	1.09	114	0.85	0.78	136	1.01	0.94
	1.50	310	152	156	200	164	1.32	1.28	130	0.86	0.83	164	1.08	1.05
	1.75	423	163	165	244	192	1.50	1.48	145	0.89	0.88	168	1.03	1.02
	2.00	552	184	175	290	218	1.57	1.66	159	0.86	0.91	189	1.03	1.08
	2.50	862	232	222	384	269	1.66	1.73	183	0.79	0.83	228	0.98	1.02
	3.00	1242	276	269	483	317	1.75	1.80	205	0.74	0.76	264	0.96	0.98
	3.25	1457	295	292	534	340	1.81	1.83	215	0.73	0.74	281	0.95	0.96
	3.50	1690	314	312	586	363	1.87	1.88	225	0.72	0.72	299	0.95	0.96
C12 (L_{crd}=1050; L_{crl}=170)	1.00	130	107	111	110	100	1.03	0.99	90	0.84	0.81	100	0.93	0.90
	1.10	157	118	125	125	112	1.06	1.00	98	0.83	0.78	112	0.95	0.89
	1.25	203	128	139	148	129	1.16	1.07	108	0.84	0.78	129	1.01	0.93
	1.50	292	145	151	188	157	1.30	1.25	124	0.85	0.82	157	1.08	1.04
	1.75	398	156	164	230	183	1.47	1.40	138	0.88	0.84	160	1.03	0.98
	2.00	519	175	182	273	208	1.56	1.50	151	0.86	0.83	180	1.03	0.99
	2.50	811	220	225	362	256	1.64	1.61	174	0.79	0.78	217	0.99	0.96
	3.00	1168	262	266	455	302	1.74	1.71	195	0.74	0.73	251	0.96	0.95
	3.25	1371	281	285	503	324	1.79	1.76	205	0.73	0.72	268	0.95	0.94
	3.50	1590	299	303	552	346	1.84	1.82	214	0.72	0.71	285	0.95	0.94
C13 (L_{crd}=1200; L_{crl}=180)	1.00	157	141	134	133	123	0.95	1.00	111	0.79	0.83	123	0.87	0.92
	1.10	190	156	150	151	138	0.97	1.01	121	0.77	0.80	138	0.89	0.92
	1.25	245	166	164	179	160	1.08	1.09	134	0.81	0.82	160	0.97	0.98
	1.50	353	177	177	228	195	1.29	1.29	154	0.87	0.87	195	1.10	1.10
	1.75	481	189	190	278	228	1.47	1.46	172	0.91	0.90	193	1.02	1.01
	2.00	628	209	206	329	259	1.58	1.60	188	0.90	0.91	215	1.03	1.04
	2.50	981	262	258	437	320	1.67	1.69	217	0.83	0.84	258	0.98	1.00
	3.00	1412	309	308	550	377	1.78	1.79	243	0.79	0.79	297	0.96	0.97
	3.25	1657	330	329	608	405	1.84	1.85	255	0.77	0.78	316	0.96	0.96
	3.50	1922	350	350	667	432	1.91	1.91	267	0.76	0.76	335	0.96	0.96

Table C4: R columns: SFEA ultimate strengths and corresponding DSM estimates (dimensions in *mm*, stresses in *MPa*) – IV

			SFEA		DSM				NDL			MNDL		
	λ_l	f_y	$f_{u.D}$	$f_{u.L}$	f_{nl}	f_{nd}	$\frac{f_{nl}}{f_{u.D}}$	$\frac{f_{nl}}{f_{u.L}}$	f_{ndl}	$\frac{f_{ndl}}{f_{u.D}}$	$\frac{f_{ndl}}{f_{u.L}}$	f_{mndl}	$\frac{f_{mndl}}{f_{u.D}}$	$\frac{f_{mndl}}{f_{u.L}}$
C14 (L_{crd}=1250; L_{crl}=170)	1.00	133	123	114	113	107	0.92	0.99	97	0.78	0.85	107	0.87	0.94
	1.10	161	136	128	129	121	0.95	1.01	105	0.77	0.82	121	0.89	0.94
	1.25	208	146	143	152	140	1.04	1.07	117	0.80	0.81	140	0.96	0.98
	1.50	300	158	157	193	170	1.22	1.23	134	0.85	0.85	170	1.08	1.09
	1.75	408	167	169	236	200	1.41	1.40	150	0.90	0.89	159	0.95	0.94
	2.00	533	181	182	280	228	1.55	1.54	164	0.91	0.90	177	0.98	0.97
	2.50	833	227	224	372	281	1.64	1.66	190	0.84	0.85	209	0.92	0.93
	3.00	1200	269	268	467	331	1.74	1.74	213	0.79	0.80	238	0.88	0.89
	3.25	1408	287	287	517	356	1.80	1.80	224	0.78	0.78	252	0.88	0.88
	3.50	1633	305	305	567	380	1.86	1.86	234	0.77	0.77	266	0.87	0.87
C15 (L_{crd}=1300; L_{crl}=170)	1.00	122	114	105	104	101	0.91	0.99	91	0.79	0.86	101	0.88	0.96
	1.10	148	125	117	118	114	0.94	1.01	99	0.79	0.84	114	0.91	0.97
	1.25	191	137	133	140	132	1.02	1.05	110	0.80	0.83	132	0.96	0.99
	1.50	275	149	148	177	162	1.19	1.20	127	0.85	0.86	162	1.08	1.09
	1.75	374	164	159	216	189	1.32	1.36	142	0.86	0.89	147	0.89	0.92
	2.00	489	180	170	257	216	1.43	1.51	156	0.86	0.92	162	0.90	0.95
	2.50	764	218	207	341	267	1.56	1.65	181	0.83	0.87	190	0.87	0.92
	3.00	1100	255	249	428	316	1.68	1.72	203	0.79	0.81	216	0.85	0.87
	3.25	1291	272	266	474	339	1.74	1.78	213	0.78	0.80	228	0.84	0.86
	3.50	1497	288	283	519	362	1.80	1.84	223	0.77	0.79	240	0.83	0.85
C16 (L_{crd}=840; L_{crl}=110)	1.00	285	273	254	242	240	0.89	0.96	215	0.79	0.85	240	0.88	0.94
	1.10	345	303	292	275	270	0.91	0.94	234	0.77	0.80	270	0.89	0.93
	1.25	446	347	347	326	315	0.94	0.94	261	0.75	0.75	315	0.91	0.91
	1.50	642	383	386	414	386	1.08	1.07	302	0.79	0.78	386	1.01	1.00
	1.75	873	395	404	505	453	1.28	1.25	338	0.86	0.84	351	0.89	0.87
	2.00	1141	425	424	599	518	1.41	1.41	372	0.87	0.88	388	0.91	0.92
	2.50	1783	505	505	795	641	1.57	1.57	432	0.86	0.86	456	0.90	0.90
	3.00	2567	580	580	999	758	1.72	1.72	485	0.84	0.84	518	0.89	0.89
	3.25	3012	615	615	1105	814	1.80	1.80	510	0.83	0.83	547	0.89	0.89
	3.50	3494	645	645	1212	870	1.88	1.88	533	0.83	0.83	576	0.89	0.89
C17 (L_{crd}=850; L_{crl}=110)	1.00	269	258	240	229	229	0.89	0.95	205	0.79	0.85	229	0.89	0.96
	1.10	326	286	276	260	259	0.91	0.94	224	0.78	0.81	259	0.91	0.94
	1.25	420	331	329	308	303	0.93	0.93	250	0.76	0.76	303	0.91	0.92
	1.50	605	369	372	390	372	1.06	1.05	290	0.79	0.78	372	1.01	1.00
	1.75	824	387	392	476	437	1.23	1.21	325	0.84	0.83	437	1.13	1.11
	2.00	1076	441	404	565	500	1.28	1.40	358	0.81	0.89	370	0.84	0.92
	2.50	1682	485	483	750	619	1.55	1.55	416	0.86	0.86	434	0.89	0.90
	3.00	2422	557	546	943	732	1.69	1.73	468	0.84	0.86	492	0.88	0.90
	3.25	2842	589	587	1042	787	1.77	1.78	492	0.83	0.84	519	0.88	0.88
	3.50	3296	619	616	1143	841	1.85	1.86	515	0.83	0.84	546	0.88	0.89
C18 (L_{crd}=880; L_{crl}=110)	1.00	235	228	209	200	202	0.88	0.96	180	0.79	0.86	202	0.89	0.97
	1.10	285	248	242	227	229	0.92	0.94	197	0.80	0.81	229	0.92	0.94
	1.25	367	288	289	269	267	0.93	0.93	221	0.77	0.76	267	0.93	0.92
	1.50	529	324	333	341	328	1.05	1.02	256	0.79	0.77	328	1.01	0.99
	1.75	720	338	348	416	386	1.23	1.20	287	0.85	0.83	386	1.14	1.11
	2.00	941	350	360	494	442	1.41	1.37	316	0.90	0.88	316	0.90	0.88
	2.50	1470	410	406	655	548	1.60	1.61	368	0.90	0.91	368	0.90	0.91
	3.00	2116	473	469	824	648	1.74	1.76	414	0.87	0.88	414	0.87	0.88
	3.25	2484	503	499	911	697	1.81	1.83	435	0.86	0.87	435	0.86	0.87
	3.50	2880	531	527	999	745	1.88	1.90	455	0.86	0.86	455	0.86	0.86
C19 (L_{crd}=870; L_{crl}=110)	1.00	245	236	218	208	214	0.88	0.95	190	0.81	0.87	214	0.91	0.98
	1.10	296	262	251	236	242	0.90	0.94	209	0.80	0.83	242	0.93	0.97
	1.25	382	303	301	280	284	0.92	0.93	234	0.77	0.78	284	0.94	0.94
	1.50	551	346	348	355	349	1.03	1.02	271	0.78	0.78	349	1.01	1.00
	1.75	750	366	368	433	412	1.18	1.18	305	0.83	0.83	412	1.13	1.12
	2.00	979	409	382	514	472	1.26	1.35	336	0.82	0.88	340	0.83	0.89
	2.50	1530	463	449	682	585	1.47	1.52	392	0.85	0.87	398	0.86	0.89
	3.00	2203	518	517	858	693	1.66	1.66	441	0.85	0.85	449	0.87	0.87
	3.25	2586	548	548	948	745	1.73	1.73	464	0.85	0.85	473	0.86	0.86
	3.50	2999	577	576	1040	797	1.80	1.81	486	0.84	0.84	496	0.86	0.86
C20 (L_{crd}=890; L_{crl}=110)	1.00	224	217	200	190	199	0.88	0.95	177	0.81	0.88	199	0.92	0.99
	1.10	271	240	230	216	226	0.90	0.94	194	0.81	0.84	226	0.94	0.98
	1.25	350	280	276	256	265	0.91	0.93	218	0.78	0.79	265	0.95	0.96
	1.50	504	322	325	325	328	1.01	1.00	254	0.79	0.78	328	1.02	1.01
	1.75	686	332	346	396	387	1.19	1.15	286	0.86	0.83	387	1.16	1.12
	2.00	896	351	367	470	443	1.34	1.28	315	0.90	0.86	315	0.90	0.86
	2.50	1399	414	418	624	551	1.51	1.49	368	0.89	0.88	368	0.89	0.88
	3.00	2015	477	482	785	653	1.64	1.63	415	0.87	0.86	415	0.87	0.86
	3.25	2365	509	512	867	703	1.70	1.69	436	0.86	0.85	436	0.86	0.85
	3.50	2743	538	539	951	751	1.77	1.76	457	0.85	0.85	457	0.85	0.85

Table C5: R columns: SFEA ultimate strengths and corresponding DSM estimates (dimensions in *mm*, stresses in *MPa*) – V

			SFEA		DSM				NDL			MNDL		
	λ_l	f_y	$f_{u.D}$	$f_{u.L}$	f_{nl}	f_{nd}	$\frac{f_{nl}}{f_{u.D}}$	$\frac{f_{nl}}{f_{u.L}}$	f_{ndl}	$\frac{f_{ndl}}{f_{u.D}}$	$\frac{f_{ndl}}{f_{u.L}}$	f_{mndl}	$\frac{f_{mndl}}{f_{u.D}}$	$\frac{f_{mndl}}{f_{u.L}}$
C21 (L_{crd}=900; L_{crl}=110)	1.00	213	207	190	181	213	0.87	0.95	169	0.82	0.89	213	1.03	1.12
	1.10	257	225	219	205	217	0.91	0.94	186	0.83	0.85	217	0.97	0.99
	1.25	332	266	263	243	256	0.91	0.93	209	0.79	0.80	256	0.96	0.97
	1.50	478	311	313	308	316	0.99	0.99	244	0.78	0.78	316	1.02	1.01
	1.75	651	333	334	376	374	1.13	1.13	275	0.83	0.83	374	1.12	1.12
	2.00	851	351	354	446	429	1.27	1.26	304	0.87	0.86	304	0.87	0.86
	2.50	1329	402	401	593	533	1.47	1.48	355	0.88	0.89	355	0.88	0.89
	3.00	1914	464	464	745	632	1.61	1.61	401	0.86	0.86	401	0.86	0.86
	3.25	2246	492	492	824	680	1.67	1.67	422	0.86	0.86	422	0.86	0.86
	3.50	2605	519	520	904	728	1.74	1.74	442	0.85	0.85	442	0.85	0.85
C22 (L_{crd}=920; L_{crl}=110)	1.00	195	191	175	166	195	0.87	0.95	158	0.82	0.90	195	1.02	1.12
	1.10	236	214	201	189	203	0.88	0.94	173	0.81	0.86	203	0.95	1.01
	1.25	305	251	241	223	240	0.89	0.93	196	0.78	0.81	240	0.96	0.99
	1.50	439	298	291	283	297	0.95	0.97	229	0.77	0.79	297	1.00	1.02
	1.75	598	321	315	346	352	1.08	1.10	259	0.81	0.82	352	1.10	1.12
	2.00	781	333	333	410	405	1.23	1.23	286	0.86	0.86	286	0.86	0.86
	2.50	1220	367	371	544	504	1.48	1.47	335	0.91	0.90	335	0.91	0.90
	3.00	1757	424	434	684	598	1.61	1.58	378	0.89	0.87	378	0.89	0.87
	3.25	2063	452	461	756	644	1.67	1.64	398	0.88	0.86	398	0.88	0.86
	3.50	2392	479	486	830	689	1.73	1.71	417	0.87	0.86	417	0.87	0.86
C23 (L_{crd}=940; L_{crl}=110)	1.00	181	177	162	154	181	0.87	0.95	147	0.83	0.91	181	1.02	1.12
	1.10	219	194	186	174	191	0.90	0.94	163	0.84	0.87	191	0.99	1.03
	1.25	282	228	224	207	226	0.91	0.92	184	0.81	0.82	226	0.99	1.01
	1.50	406	273	272	262	281	0.96	0.96	216	0.79	0.79	281	1.03	1.03
	1.75	553	292	298	320	334	1.09	1.07	244	0.84	0.82	334	1.14	1.12
	2.00	723	315	315	379	384	1.20	1.21	270	0.86	0.86	384	1.22	1.22
	2.50	1129	353	353	503	479	1.43	1.43	317	0.90	0.90	317	0.90	0.90
	3.00	1626	409	408	633	569	1.55	1.55	358	0.88	0.88	358	0.88	0.88
	3.25	1908	434	434	700	613	1.61	1.61	377	0.87	0.87	377	0.87	0.87
	3.50	2213	459	458	768	655	1.67	1.68	396	0.86	0.86	396	0.86	0.86
C24 (L_{crd}=970; L_{crl}=110)	1.00	161	157	144	137	161	0.87	0.95	133	0.85	0.93	161	1.02	1.12
	1.10	195	170	166	155	174	0.91	0.93	147	0.87	0.89	174	1.02	1.05
	1.25	251	202	199	184	207	0.91	0.92	167	0.83	0.84	207	1.02	1.04
	1.50	362	245	245	233	258	0.95	0.95	197	0.80	0.81	258	1.05	1.06
	1.75	492	273	274	284	307	1.04	1.04	224	0.82	0.82	307	1.13	1.12
	2.00	643	288	290	337	354	1.17	1.16	248	0.86	0.86	354	1.23	1.22
	2.50	1005	313	333	448	443	1.43	1.35	292	0.93	0.88	292	0.93	0.88
	3.00	1447	354	384	563	527	1.59	1.47	330	0.93	0.86	330	0.93	0.86
	3.25	1698	378	408	623	567	1.65	1.53	348	0.92	0.85	348	0.92	0.85
	3.50	1969	402	431	683	607	1.70	1.58	365	0.91	0.85	365	0.91	0.85
C25 (L_{crd}=990; L_{crl}=110)	1.00	144	141	128	122	144	0.87	0.95	120	0.85	0.94	144	1.02	1.12
	1.10	174	159	148	139	174	0.87	0.94	134	0.84	0.90	174	1.09	1.18
	1.25	225	194	177	164	189	0.85	0.93	152	0.78	0.86	189	0.98	1.07
	1.50	324	237	220	209	238	0.88	0.95	180	0.76	0.82	238	1.00	1.08
	1.75	440	256	251	254	284	0.99	1.01	205	0.80	0.82	284	1.11	1.13
	2.00	575	276	269	302	327	1.09	1.12	228	0.83	0.85	327	1.19	1.22
	2.50	899	316	305	401	410	1.27	1.31	269	0.85	0.88	269	0.85	0.88
	3.00	1294	362	351	504	489	1.39	1.44	305	0.84	0.87	305	0.84	0.87
	3.25	1519	383	374	557	527	1.45	1.49	322	0.84	0.86	322	0.84	0.86
	3.50	1762	404	395	611	564	1.51	1.55	338	0.84	0.86	338	0.84	0.86
C26 (L_{crd}=1000; L_{crl}=110)	1.00	135	132	120	115	135	0.87	0.95	113	0.86	0.94	135	1.02	1.12
	1.10	163	145	139	130	163	0.90	0.94	126	0.87	0.91	163	1.12	1.17
	1.25	211	170	167	154	180	0.91	0.92	144	0.85	0.86	180	1.06	1.08
	1.50	303	210	207	195	226	0.93	0.94	171	0.81	0.83	226	1.08	1.09
	1.75	413	235	238	239	270	1.02	1.00	195	0.83	0.82	270	1.15	1.13
	2.00	539	251	257	283	312	1.13	1.10	217	0.86	0.84	312	1.24	1.21
	2.50	842	291	290	376	391	1.29	1.30	256	0.88	0.88	256	0.88	0.88
	3.00	1213	335	334	472	467	1.41	1.41	291	0.87	0.87	291	0.87	0.87
	3.25	1424	357	356	522	503	1.46	1.47	307	0.86	0.86	307	0.86	0.86
	3.50	1651	377	376	573	539	1.52	1.52	322	0.85	0.86	322	0.85	0.86
C27 (L_{crd}=1050; L_{crl}=110)	1.00	121	119	108	103	121	0.86	095	102	0.86	0.95	121	1.02	1.12
	1.10	146	133	125	117	146	0.88	0.93	114	0.86	0.92	146	1.10	1.17
	1.25	189	156	150	138	165	0.89	0.92	131	0.84	0.87	165	1.06	1.10
	1.50	272	189	187	175	208	0.93	0.94	156	0.83	0.84	208	1.10	1.11
	1.75	370	221	217	214	249	0.97	0.99	179	0.81	0.83	249	1.13	1.15
	2.00	484	242	238	254	289	1.05	1.07	200	0.82	0.84	289	1.19	1.21
	2.50	756	273	267	337	363	1.23	1.26	236	0.87	0.89	236	0.87	0.89
	3.00	1089	311	308	424	434	1.36	1.38	269	0.86	0.87	269	0.86	0.87
	3.25	1278	331	327	469	468	1.42	1.43	284	0.86	0.87	284	0.86	0.87
	3.50	1482	350	346	514	501	1.47	1.49	298	0.85	0.86	298	0.85	0.86